Titre: Title:	Performance, Erosivity and Mechanical Properties of Plasticized Nitrocellulose and the Performance of Azidodeoxycellulose as a Propellant Additive
Auteur: Author:	Étienne Comtois
Date:	2020
Type:	Mémoire ou thèse / Dissertation or Thesis
Référence: Citation:	Comtois, É. (2020). Performance, Erosivity and Mechanical Properties of Plasticized Nitrocellulose and the Performance of Azidodeoxycellulose as a Propellant Additive [Ph.D. thesis, Polytechnique Montréal]. PolyPublie. https://publications.polymtl.ca/5372/

POLYTECHNIQUE MONTRÉAL

affiliée à l'Université de Montréal

Performance, erosivity and mechanical properties of plasticized nitrocellulose and the performance of azidodeoxycellulose as a propellant additive

ÉTIENNE COMTOIS

Département de génie chimique

Thèse présentée en vue de l'obtention du diplôme de *Philiosophiæ Doctor*

Génie chimique

Août 2020

POLYTECHNIQUE MONTRÉAL

affiliée à l'Université de Montréal

Cette thèse intitulée :

Performance, erosivity and mechanical properties of plasticized nitrocellulose and the performance of azidodeoxycellulose as a propellant additive

présentée par **Étienne COMTOIS**

en vue de l'obtention du diplôme de *Philiosophiæ Doctor*

a été dûment acceptée par le jury d'examen constitué de :

Pierre CARREAU, président
Charles DUBOIS, membre et directeur recherche
Basil FAVIS, membre et codirecteur de recherche
Nick VIRGILIO, membre
Shanti SINGH, membre externe

DEDICATION

À ma femme, ma famille, mes collègues et futur bébé.

ACKNOWLEDGEMENTS

First and foremost, I would like to thank my advisors Charles Dubois and Basil D. Favis for supporting me throughout this endeavour.

I would also like to thank Mr. Pierre-Yves Paradis, Mr. Marc Boileau and Mr. Daniel Lepage from General Dynamics Ordnance and Tactical System Canada Valleyfield (GD OTS) for providing me with the time, the materials, the funding and the equipment needed for this project.

Thanks to Mr. Florin Petre, Mr. Patrick Brousseau, Mr. Charles Nicole and Mr. Pascal Béland from Defence Research and Development Canada Valcartier Research Center for providing me the time, the equipment and materials needed for the preliminary analysis of my formulation.

Thanks to Mrs. Sophie Balaguer and Mr. Denis Sens from Rayonier Advanced Material and to Mr. Claude Guillaume from Manuco for providing the cellulose needed for this work.

Thanks to Mr. Alain Gagnon and Mrs. Caroline Sauvé from GD OTS pilot plant for providing me with the support needed.

Thanks to Mr. Simon Durant, Mr. Jean-Christophe St-Charles, Morganne Massard and Marion Combe for their help and support.

Thanks to Mr. Louis-Landry Ishii from Mecaquip and Mr. Sébastien Fournier from GDOTS for their help and providing me with the tooling needed for this work.

Thanks to Mr. Yvon Gagné and Mr. Pierre Lavigne from GD OTS for their support in evaluating the two-roll mill safety guard.

Thanks to Mrs. Fanny Charest, Mr. Ian Levac, Mrs. Rachelle Lavigueur and Mr. Daniel Pelletier and all the laboratory technicians from the analytical chemistry laboratory at GD OTS for their help in running various analyses and teaching me how to use various equipment.

Thanks to Mrs. Annie Fergusson, Mr. Denis Paquin, Mr. Guillaume Côté, Mr. Richard Beaulieu, Mr. Jean-Maxime Chatigny and Mr. Mathieu Lafleur for their work on the closed vessel without whom it would not have been possible to complete this work.

Thanks to Mr. Mathieu Lévesque for his help in adapting the figures in this document.

Finally, I would like to thank my family, friends and colleagues who supported me during the course of my studies.

RÉSUMÉ

La fabrication de propulsif à faible érosion ainsi que l'innovation dans le secteur des contenants combustibles thermoplastiques sont limitées par de multiples facteurs : l'absence de matériel thermoplastique capable de se consumer sans laisser de résidus et l'usure prématurée des systèmes d'armes causée par l'érosion associée à la haute température de combustion des propulsifs. Ces deux facteurs ont été adressés dans cet ouvrage.

Des mélanges de nitrocellulose (NC) plastifiés par la nitroglycérine (NG) et le polyazoture de glycidyl (GAP) ont été caractérisés afin d'obtenir les propriétés thermomécaniques, les propriétés de combustion et l'érosivité relative des mélanges.

Le GAP n'a pas démontré qu'il pouvait efficacement plastifier la nitrocellulose à cause de son incapacité à se situer entre les chaînes de NC. Cependant, de bonnes propriétés plastifiantes ont été obtenues en utilisant un mélange composé de NG et de GAP. Cette plastification accrue est expliquée par la capacité de la NG de distancer les chaînes de NC permettant ainsi au GAP d'agir comme un bon plastifiant. Les mélanges obtenus présentent des transitions vitreuses en dessous de la température de décomposition de la NC et similaires à celles mesurées pour d'autres matériaux thermoplastique dérivés de la cellulose. Les propriétés de combustion étudiées dans cette thèse permettent une meilleure compréhension des mélanges de NC, NG et GAP et faciliteront le développement de nouvelles formulations et applications dans le domaine des matériaux énergétiques.

Finalement, l'azidodeoxycellulose (AC) a été évaluée comme candidat potentiel à titre de remplaçant à la NC dans les systèmes de propulsion. L'évaluation de la combustion de l'AC démontre que celle-ci est efficace d'un point de vue balistique. Cependant, son incapacité à se dissoudre dans les solvants normalement utilisés dans le procédé des propulsifs extrudés la rend plus adaptée comme charge solide.

ABSTRACT

The manufacturing of improved propellant formulations and thermoformable combustible containers is limited by multiple factors. This thesis addresses two of them: the lack of clean-burning thermoplastic binders and the premature wear of components due to the high erosivity associated with increased propellant temperature.

In order to address the lack of clean-burning thermoplastic binders, the thermo-mechanical properties, combustion properties, and relative erosivity of nitrocellulose (NC) plasticized using a system of plasticizer comprised of low-molecular weight nitrate ester and low-molecular weight azido polymer were investigated.

Glycidyl azide polymer (GAP) did not prove to be an efficient plasticizer due to its inability to situate between NC chains. Good plasticization was obtained when using a plasticizer system comprised of both nitroglycerine (NG) and GAP. This increased plasticization is explained by the ability of NG to situate itself between NC chains, separating them and thus allowing GAP to act as an effective plasticizer. Glass transition temperatures below the onset of decomposition of NCs and similar to what is observed in the thermoforming of other cellulose-base thermoplastic material were obtained. The combustion properties documented in this study provide a better understanding of the combustion properties of NC, NG and GAP formulations, which are useful for the future development of novel energetics and applications.

In addition, azidodeoxycellulose (AC) was evaluated as a potential replacement for NCs in propellant formulations to prevent the premature wear of gun components. Replacement of the nitro group by the azide group was expected to reduce erosivity due to the lower flame temperature associated with the azide moieties. The combustion evaluation of AC proved that it is indeed quite effective as a nitrogen-rich material, although its inability to dissolve in common organic solvents used in the extruded propellant process makes it more suitable as a solid filler.

TABLE OF CONTENTS

LIST OF TABLES

LIST OF FIGURES

LIST OF SYMBOLS AND ABBREVIATIONS

AC Azidodeoxycellulose

AGU Anhydroglucose unit

BTA 5,5'-bis-(1H-tetrazolyl)-amine

BTTN Butanetriol trinitrate

CAB Carboxy acetate butyrate

CA Cellulose acetate

CV Closed vessels

DBP Dibutyl phthalate

DEGDN Diethylene glycol dinitrate

DMA Dynamic mechanical analysis

DMF Dimethylformamide

DS Degree of substitution

ECH Epichlorohydrin

EM Energetic material

Et_3N Triethyl amine

EVV Erosivity vented vessel

FtIR Fourrier transformed infrared spectroscopy

GAP Glycidyl azide polymer

GD OTS General Dynamics Ordnance and Tactical System[1]

---

[1] Unless otherwise specified GD OTS is refering to the Valleyfield propellant plant.

HTPB Hydroxy terminated poly butadiene

HV High viscosity

LBR Linear burning rate

LiCl Lithium chloride

LV Low viscosity

%N Nitrogen content

NC Nitrocellulose

NaN_3 Sodium azide

M_n Number average molecular weight

M_w Average gas molecular weight

NC Nitrocellulose

NG Nitroglycerine

OB Oxygen balance

PECH Polyepichlorohydrin

PDI Polydispersity index

polyGLYN Poly(glycidyl nitrate)

polyBAMO Poly(3,3-Bis-Azidomethyl Oxetane)

RDX 1,3,5-trinitro-1,3,5-triazacyclohexane

SEM Scanning electron microscope

TA Triacetine

TEGDN triethylene glycol dinitrate

TMETN trimetylol ethane trinitrate

TsCell Tosylated cellulose

TsCl Toluenedulfonyl chloride

LIST OF APPENDICES

CHAPTER 1 INTRODUCTION

Energetic materials (EMs) are chemical substances that undergo a rapid chemical decomposition under stimuli generating large quantity of hot gases and are used in a wide variety of applications and industries [1]. The automotive industry uses EMs in airbags, the mining industry uses them in blasting charges, the aerospace industry uses EMs as a solid propellant for rockets and the military uses EMs in propellant, pyrotechnics and other applications [2].

EMs can be granular solids, liquids or polymers. Often, to be transformed into useful products, EMs must be given a shape. In order to do so, binders comprised of polymers and plasticizers are used [3].

One military application making use of such binders is in the manufacturing of combustible containers. They are manufactured with thermoformable sheets of celluloid using low-nitration level nitrocellulose (NC) and an inert plasticizer. This combination of low nitration and inert plasticizers leads to the formation of residues, which is a safety issue [4].

By comparison, in the propellant industry, binders are often comprised of plasticized NC using low-molecular weight nitrate esters [5]. Nitrate esters are toxic for the workers manufacturing the EMs, for the users and for the environment. They also generate a high-combustion flame temperature, which is one of the main causes of gun-barrel erosivity, the phenomena by which the barrel is enlarged trough successive firing resulting in the combustion gases leaking around the projectile leading to a loss of muzzle velocity, reduced range and increased dispersion of the rounds at the target [6]. Nitrate esters are also prone to migration, which affects ballistic performance over time [7].

In order to reduce flame temperatures, toxicity and migration issues, it is proposed to replace nitrate ester plasticizers with a low-molecular weight nitrogen-rich polymeric plasticizer. Such polymers are readily available and have been evaluated in rocket propulsion and in some measure in gun propulsion, but always as part of a cured formulation or highly filled binder, never as a neat plasticizer or as part of a mixture of plasticizers.

Azido-based high-molecular weight polymers are also a way of reducing flame temperatures while providing the mechanical properties needed in solid propellant formulations. Syntheses of

polymers, such as azidodeoxycellulose (AC) and 1-azido-2-hydroxypropyl cellulose ether, are covered in the scientific literature, yet there is no evaluation of their combustion properties [8].

The reduced erosivity of nitrogen rich formulation and the lack of information on the influence of azido plasticizer on NC, from a thermomechanical property or a combustion standpoint, illustrates the need to evaluate azido-based plasticizers and binders in comparison to nitrate ester-based plasticizers and binders.

The main goals of this research thesis are to quantify the effects of azido-based plasticizers on the plasticization of NC, as well as to compare azido-modified cellulose against its nitrated version.

The results of the research are reported according to the following actions plan:

- Quantify the impact of energetic plasticizers on thermo-mechanical properties
- Quantify the impact of energetic plasticizers on the combustion of a binder formulation
- Quantify the impact of energetic plasticizers on the erosivity of a binder formulation
- Quantify the impact of an azido-based polymer on the combustion of a binder formulation

The research seeks to provide a path toward the development of a clean, combustible thermoplastic material and a nitrogen-rich binder for reduced erosion application.

CHAPTER 2 LITERATURE REVIEW

The literature review covers the fundamental concepts relevant to this research. This section is organized in three parts. The first provides the reader with an overview of the definitions, classification, properties and method of characterisation of EMs. The second section addresses plasticization of materials and the last section provides an introduction to combustible containers, their usage and the problems associated with them.

2.1 Energetic material

Energetic materials (EMs) are chemical substances that undergo a rapid chemical decomposition under stimuli such as friction, impact, shock, heat or the application of an energy pulse that induces hot spot in the material. This decomposition generates a large quantity of heat and gas [1]. The rapid increase in pressure generated by the expansion of these hot gases is defined as an explosion. The rate at which gas generation occurs is a key factor in the classification of these materials and how they can be used.

The first EM to be discovered was black powder. Ancient Chinese scriptures from A.D. 1110, narrate the demonstration as opening with “a thunder like noise” and continuing with fireworks exploding in the sky [9].

Nowadays, EMs are used in many fields such as construction, defense and aerospace. Table 2-1 provides a brief overview of current fields of applications and examples of how EMs are used.

The next section will present the classification of EMs and provide a more in-depth understanding of the chemical reactions that take place in EMs.

2.1.1 Chemical functionality of energetic materials

Multiple approaches are utilized in the manufacturing of EMs in order to achieve combustion and the release of energy. One method is to have chemical functionality that permits the oxidizer and fuel to be next to one other on the same molecule.

Table 2-1 Examples of current applications of EMs in various fields [2, 10-12].

Field	**Application**	**Example**
Military	-Propulsion of small-, medium- and large-caliber guns -Missile propulsion -Explosive warhead -Demolition charge -Shaped charge -Flare -Pyrotechnic grenades	Name: Composition C4 Usage: Demolition charge Composition: -RDX -Polyisobutylene -Dioctyl adipate -Lubricating oil
Aerospace	-Rocket propulsion for atmospheric research -Space shuttle booster -Explosives bolt	Name: EAP P241 Usage: Solid rocket engine Ariane 5 Composition: -Ammonium perchlorate - Aluminum -Cured hydroxy-terminated polybutadiene
Industrial	-Explosive cladding -Mining explosives	Name: Centra Control ANE Usage: Emulsion component to blend with ANFO to produce explosive products on mining or construction sites. Composition: -Ammonium nitrate -Petroleum distillates (naphtha) -Glass, oxide
Civilian	-Fireworks and other pyrotechnics -Firearms for hunting or sport shooting -Airbags	Name: Road Emergency Flare Usage: Emergency signaling Composition: - Strontium nitrate - Sulphur -Potassium nitrate -Paraffinic oil -Potassium chlorate -Waxy sawdust -Polyvinyl chloride -Shellac -Charcoal

Often, the organic backbone of the molecule, composed primarily of carbon and hydrogen, will present oxygen-rich functionality such as the nitro group (-NO_2) or nitramine (-N-NO_2) groups. Bonds like N-N or N-O have atoms covalently bonded with non-bonding electrons present in p-orbital. The induced electrostatic repulsion between these atoms allows reduction reactions to occur when these bonds break, forming gaseous products like CO, H_2O, H_2, CO_2 and N_2. The energy release from the decomposition of products leads to the formation of more stable compounds coupled to the gas formation, allowing EMs to produce work [13]. NC, nitroglycerine (NG) and 1,3,5-trinitro-1,3,5-triazacyclohexane (RDX) are types of material containing both the oxidizer and fuel at the molecular level.

A second method is to increase the nitrogen content of composition by adding nitrogen-rich molecules. The addition of nitrogen in a formulation increases the concentration of N_2 generated when undergoing combustion. This increase in N_2 lowers the overall molecular weight of the gas, leading to greater moles of gas for the same mass, which in turn translates into more work being produced for the same mass of propellant. In addition, nitrogen-rich molecules can also form triazole and tetrazole rings, which decompose with increased energy [14-16]. 5,5'-bis-(1H-tetrazolyl)-amine (BTA) is an example of a high-nitrogen compound.

A third method is to form a rigid, cage-like structure at the molecular level. Such molecules contain energy from the strain in the covalent bonds that are established between atoms at angles different from the normal coordination topology. When enough energy is applied to the material, the cage structure breaks releasing energy. Such EMs are designated as structural bond energy release materials or SBER. SBERs can also be combined with the first proposed method by having the cage structure bearing oxidizer group such as octanitrocubane [15, 17].

NC, BTA and octanitrocubane are presented in Figure 2-1 as an example of how the energy is stored in the molecule.

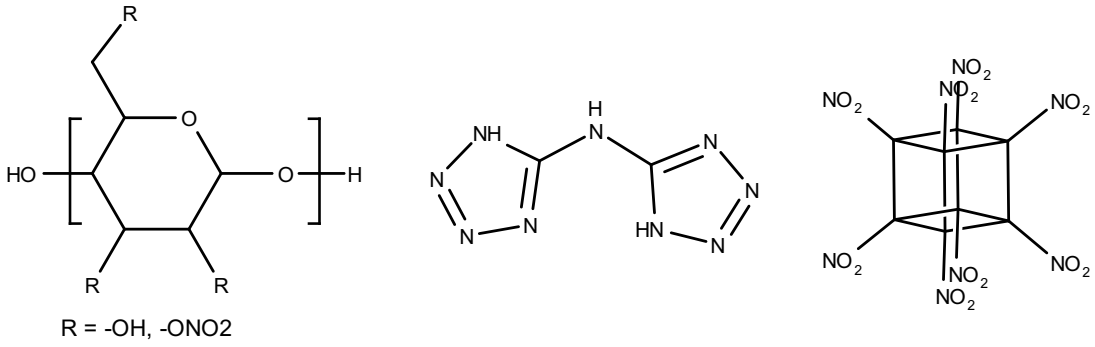

Figure 2-1 NC (left), BTA (middle) and octanitrocubate (right) [1, 18].

In order to classify EMs, Plets [19] looked at their chemical group. Plets, demonstrated that EMs contain explosophoric groups from the following families:

1. $–NO_2$ and $–ONO_2$, in organic and inorganic molecules
2. –N=N- et –N=N=N- in organic and inorganic azides
3. $–NX_2$, such as NCl_3 (-X being a halogen)
4. -N=C- present in fulminates and cyanogen
5. $–OClO_2$ et $–OClO_3$ in organic and inorganic chlorates and perchlorates
6. –O-O- et –O-O-O- in organic and inorganic peroxides and ozonides
7. -C≡C- in acetylene and metal acetylides
8. -M-C- metal bonded with carbon in some organometallic compounds

The presence of these groups increases the internal energy of the formulation [20].

2.1.2 Properties of energetic materials

As presented above, the role of both oxygen and nitrogen is key in the effectiveness of EMs; oxygen is the main driving force behind the combustion of carbon and hydrogen into CO_2 and H_2O, while nitrogen leads to low molecular weight gas. The quantity of O_2 and N_2 are not indicative of the speed at which they will combust. For a better understanding of EMs, the four following parameters will be explained: the oxygen balance (OB) and nitrogen content (%N), the heat of formation (ΔH_f^o), the linear burning rate (LBR) and lastly the influence on barrel erosion.

2.1.2.1 Oxygen balance and nitrogen content

The OB indicates whether an EM has enough oxygen to oxidize its molecular structure into CO_2 and H_2O. Each carbon atom is oxidized to carbon dioxide, hydrogen to water and metal to metal oxides. As the vast majority of energetic binders are organic molecules and do not have metal in their structures, a general formula can be used to calculate OB [5].

$$OB = \frac{[d - (2a) - (b/2)] \times 1600}{M} \quad (2.1)$$

In this formula, OB is given in percentages a, b, c and d, and are, respectively, the amounts of molecules of carbon, hydrogen, nitrogen and oxygen in the molecular formula ($C_aH_bN_cO_d$) and M is the molecular weight in g mol^{-1} of the EM. Nitrogen leading to the formation of the gaseous species N_2, it does not affect the OB and is not represented in (2.1).

If $OB = 0$, then the EM has enough oxygen within itself to completely oxidize its molecular structure into CO_2 and H_2O. If $OB > 0$, not only does it have enough oxygen to completely oxidize its structure, it actually contains an excess of oxygen. This is detrimental as the excess oxygen does not participate in the combustion of the EMs and will lead to the formation of O_2. Finally, if $OB < 0$, then the material lacks the oxygen concentration needed to completely oxidize into CO_2 and H_2O and will lead to the formation of CO and H_2.

The nitrogen content ($\%N$) is the percentage by mass (%wt) of nitrogen present in the EM formulation. Table 2-2 presents OB and %N for various EMs covered in this thesis. It should be noted NCs $\%N$ will vary depending on the application and as an example 11%N, 12.6%N and 13.4%N are presented in Table 2-2. AC presented in Table 2-2 is completely substituted and GAP has a hydroxyl functionality of two and is comprised of eight GA repeating unit.

Table 2-2 Example of current application of energetic materials in various fields [1, 8].

Name	Formula	OB [%]	%N
NG	$C_3H_5N_3O_9$	3.5	18.5
NC (11.0%N)	$(C_6H_{8.02}N_{1.98}O_{8.98})_n$	-44.9	11.0
NC (12.6%N)	$(C_6H_{7.54}N_{2.46}O_{9.92})_n$	-34.3	12.6
NC (13.4%N)	$(C_6H_{7.27}N_{2.73}O_{10.46})_n$	-29.1	13.4
AC	$(C_6H_7N_9O_2)_n$	-91.1	53.2
GAP-diol	$C_{24}H_{42}N_{24}O_9$	-118.5	41.5

2.1.2.2 Heat of formation

The heat of formation (ΔH_f^o) is a key parameter of EMs, as it is an evaluation of their explosive properties [13, 16]. When a chemical species is formed, it can either absorb heat in an endothermic reaction or release heat in an exothermic reaction. For EMs, the ideal net amount of heat liberated during an explosion is the sum of ΔH_f^o of the products of explosion minus the ΔH_f^o of the combustion gases (2.2).

$$\Delta H^o = \sum \Delta H^o_{f,products} - \sum \Delta H^o_{f,reactants} \qquad (2.2)$$

ΔH_f^o of EMs can be extracted from calorimetric data obtained using calorimetric bomb results in an excess of oxygen if the chemical composition is known. As stated above, most EMs are organic compounds comprised of carbon, hydrogen, nitrogen and oxygen. When burning in the presence of excess oxygen, they form the following gaseous species: CO_2, H_2O, N_2 (2.3).

$$C_aH_bN_cO_d + O_2 = aCO_2 + \frac{b}{2} H_2O + N_2 + O_2 \qquad (2.3)$$

From calorimetric data in excess of oxygen, the heat of combustion (ΔH_c^o) is obtained. CO_2, H_2O, N_2 values of ΔH_f^o are known from the literature. Therefore, from equation (2.2) one can calculate ΔH_f^o for an EM (2.4).

$$\Delta H^o_{f,EMs} = \Delta H^o_c + \sum \Delta H^o_{f,reactants} \qquad (2.4)$$

In order to simulate EMs properties, thermochemical software such as CHEETAH can be used. To perform simulation on a novel EM compound, the software requires the following parameters: ΔH_f^o, density and chemical composition of an EM formulation or chemical compound. From the chemical composition, the software calculates the gaseous species concentration which will vary depending on the type of simulation chosen (rocket, combustion or detonation). The gaseous species are well documented in the literature and their ΔH_f^o are known. The heat generated during the combustion can then be calculated from the difference between the ΔH_f^o of the EMs and the product. Having the gaseous species concentration and the heat generated from the chemical reactions, the behaviour of an EM can be predicted and used in simulation models.

2.1.2.3 Closed vessel and linear burning rate

It is known that a combustion reaction is a function of the available surface of the combustible material. A good example of this is that one kg of kindling and one kg of a hard wood log are not going to burn in the same time-lapse, even though they have the same OB, %N and ΔH_f^o.

Typical geometries found in gun propellant applications are, shown in Figure 2-2, spherical, sheet, strip, cord, cylindrical (unperforated, single perforated or multi perforated) and rosette. All of these geometries affect the rate at which the propellant burns in the gun tube and is dictated by the gun system parameters such as the maximum pressure, allowable case volume, barrel length, projectile weight etc.

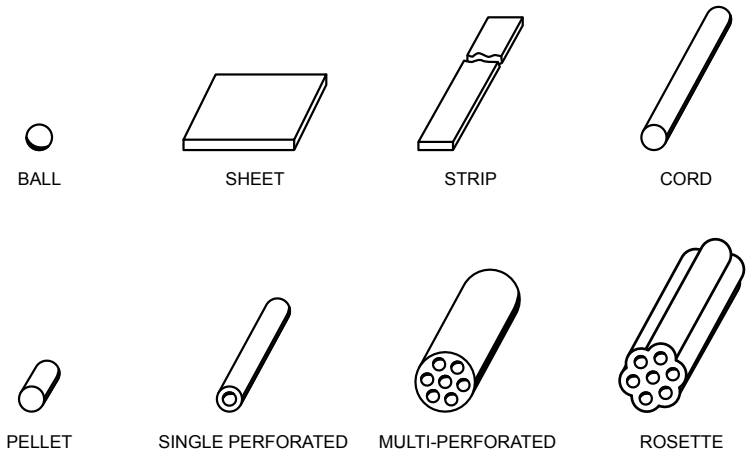

Figure 2-2 Typical shapes used in propellant.

As an example, for a artillery gun system, the 10.8 kg propellant charge is comprised of thousands multi-perforated cylindrical propellant grains weighing individually only a few grams (Figure 2-3).

Figure 2-3 Large caliber propellant grains; provided by GD OTS.

To be able to engineer EMs into useful products, it is necessary to tailor the speed of the combustion reaction to match the desired application. For this reason, the rate at which an EM burns independently of its geometry is crucial.

To obtain this value, closed vessels (CV) are used. A CV is a sealed high-pressure vessel equipped with a pressure transducer and an ignition electrode (Figure 2-4), which permits the combustion of propellant geometry and the following of the pressure-time curve throughout combustion.

A typical pressure-time curve is presented in Figure 2-5. From the kindling example above, it is evident how geometry affects the pressure-time curve in a closed vessel. Assuming adiabatic combustion in the closed vessel, the same quantity of the same formulation, but with different

geometry, would generate the same amount of gas but at a different rate. For this reason, the pressure-time curves cannot be used to provide relevant information on the burning behaviour of the propellant, but rather is used to compare two propellants in terms of the pressure generated that is, the "force" of the propellant.

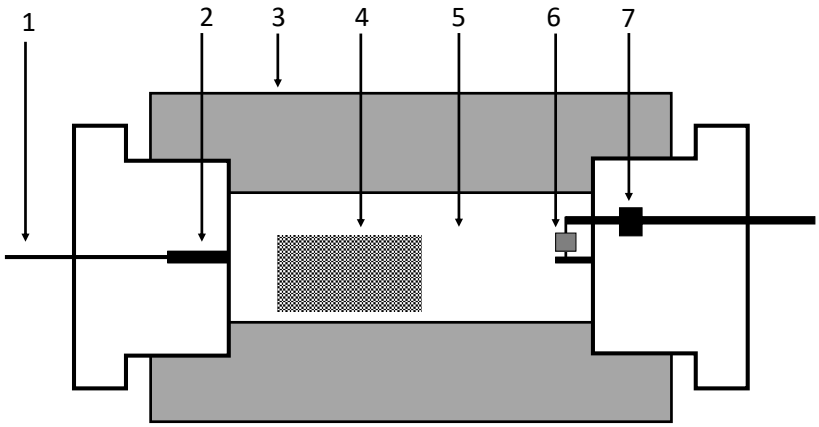

Figure 2-4 CV diagram, coaxial cable (1), pressure transducer (2), jacketed wall (3), propellant (4), combustion chamber (5), ignition grain (6) and ignition fixture (7); adapted from [21].

Mathematical transformations are performed on this curve in order to obtain the combustion rate of the material, as shown in Figure 2-5. First, the dP/dT is traced as a function of time (T) giving the rise in pressure as a function of time. Depending on the geometry, as time varies dP/dT as a function of T is, again, a poor measure of a property of the material. From the pressure-time curve, one can associate a pressure for each time and plot dP/dT as a function of pressure (P); this is called the "quickness" of the propellant [22]. Assuming two propellants burn at the same pressure, one can use this value to compare both propellants. This is especially useful when comparing two propellant of similar formulation and similar geometry in a quality-control setting since the similar rise of pressure and similar pressure will indicate the similar interior ballistic. By dividing the quickness by the maximum pressure, the "vivacity" is obtained. Vivacity is a value that is used to compare two different formulations. It is independent of the pressure generated by the propellant, meaning that a propellant that generates less gas or with a lower flame temperature can be compared with a propellant generating more gas or with a higher flame temperature.

Vivacity, although very useful, is still insufficient to define the combustion property of an EMs formulation, as the form function is still taken into account. In the same kindling example used above, one could measure the vivacity and find that the kindling exhibits a higher vivacity than the log. Again, both are comprised of the same formulation and would likely have a single parameter to describe the burning behavior of the material.

In order to remove the form function, the following hypothesis is developed. All propellant in the vessel ignites at the same moment, has a known geometry, the geometry is equivalent for each grain of propellant and the formulation is homogeneous. One can then assume that the pressure is directly linked to the percentage of mass burned in the vessel, or by the volume of propellant burned if divided by the density of the propellant.

As an example, let us assume that the propellant in Figure 2-5 is comprised of a single cylinder having a radius of 0.1 cm and a length of 2.54 cm. From the pressure-time curve, the volume of propellant grain as a function of time can be traced (Figure 2-6). Knowing that all surfaces burn at the same rate, the length of the grain will be reduced to 2.52 cm by the time the radius is completely consumed. From this, one can plot the radius of the grain as a function of the volume. This is the form function of our propellant grain. From the form function, one can plot the radius as a function of time and, consequently, the change in radius — or in fact the advancement of the combustion front (in cm s^{-1}) — as a function of time. Similar to quickness, one can then plot the advancement of the combustion front as a function of pressure (Figure 2-7). This is known as Vieille's law [23], which stipulates that the propellant linear burning rate will increase exponentially as a function of pressure as per (2.5) where r is the linear burning rate in cm s^{-1}, β is the linear burn rate coefficient in cm s^{-1}, P is the pressure in MPa and α is the pressure exponent. In the present example $\beta = 0.0898$ cm s^{-1} and $\alpha = 1.0161$.

The above example is only for demonstration purposes and is in not the actual way in which the burning rate is calculated by computer software such as BRLCB. The computer software performs surface regressions and takes into account the heat capacity of gaseous species and the density of the propellant, as well as compensates for the heat loss that occurs in the CV.

Values of α greater than one indicate that a propellant is highly influenced by the increase in pressure, compared to a propellant with a pressure exponent of less than one.

To understand this variation, it is necessary to look at the burning mechanism of solid propellant.

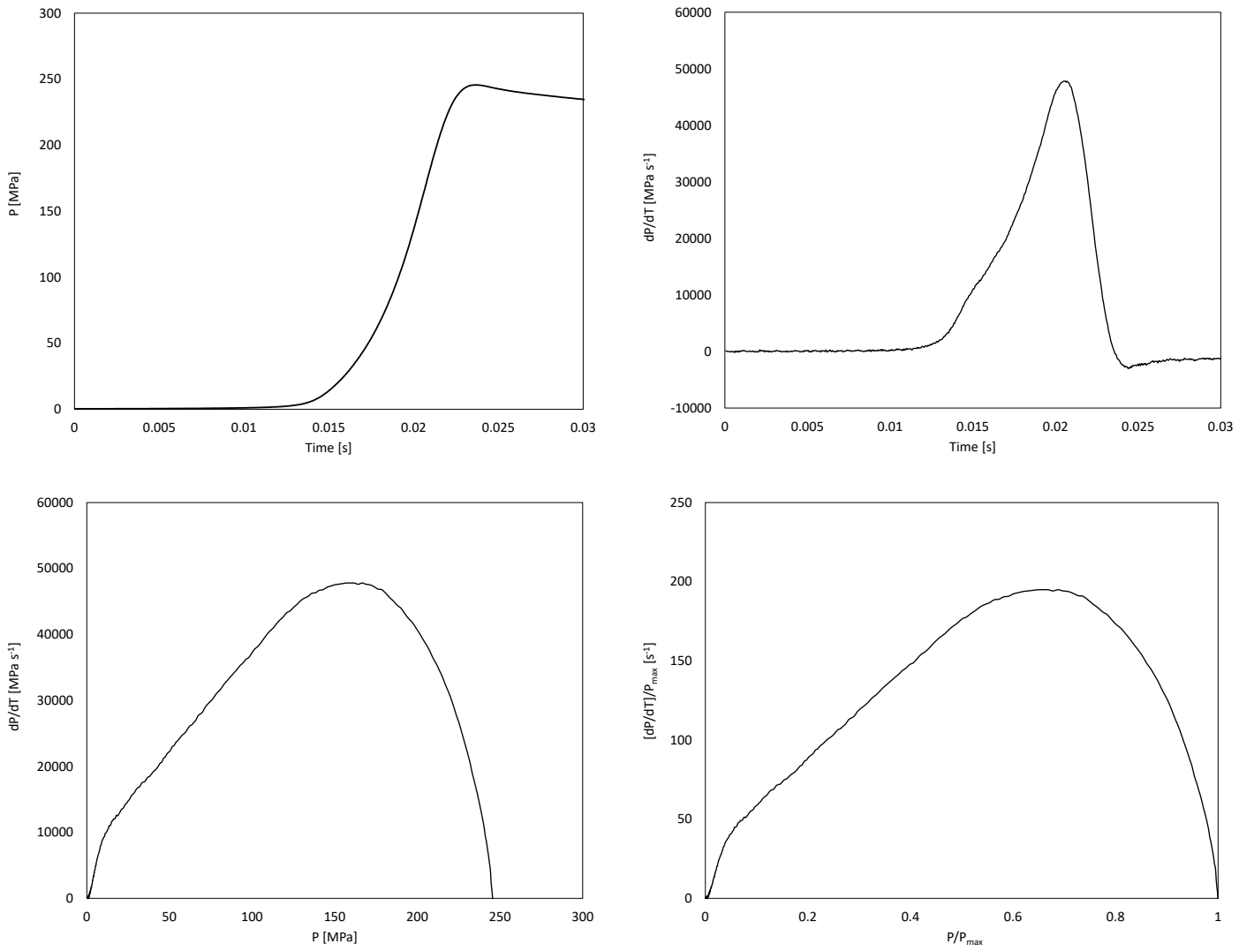

Figure 2-5 Typical pressure-time curve (top left), dP/dT as a function of time (top right), dP/dT as a function of pressure (bottom left) and $(dP/dT)/P_{max}$ as a function of P/P_{max} (bottom right).

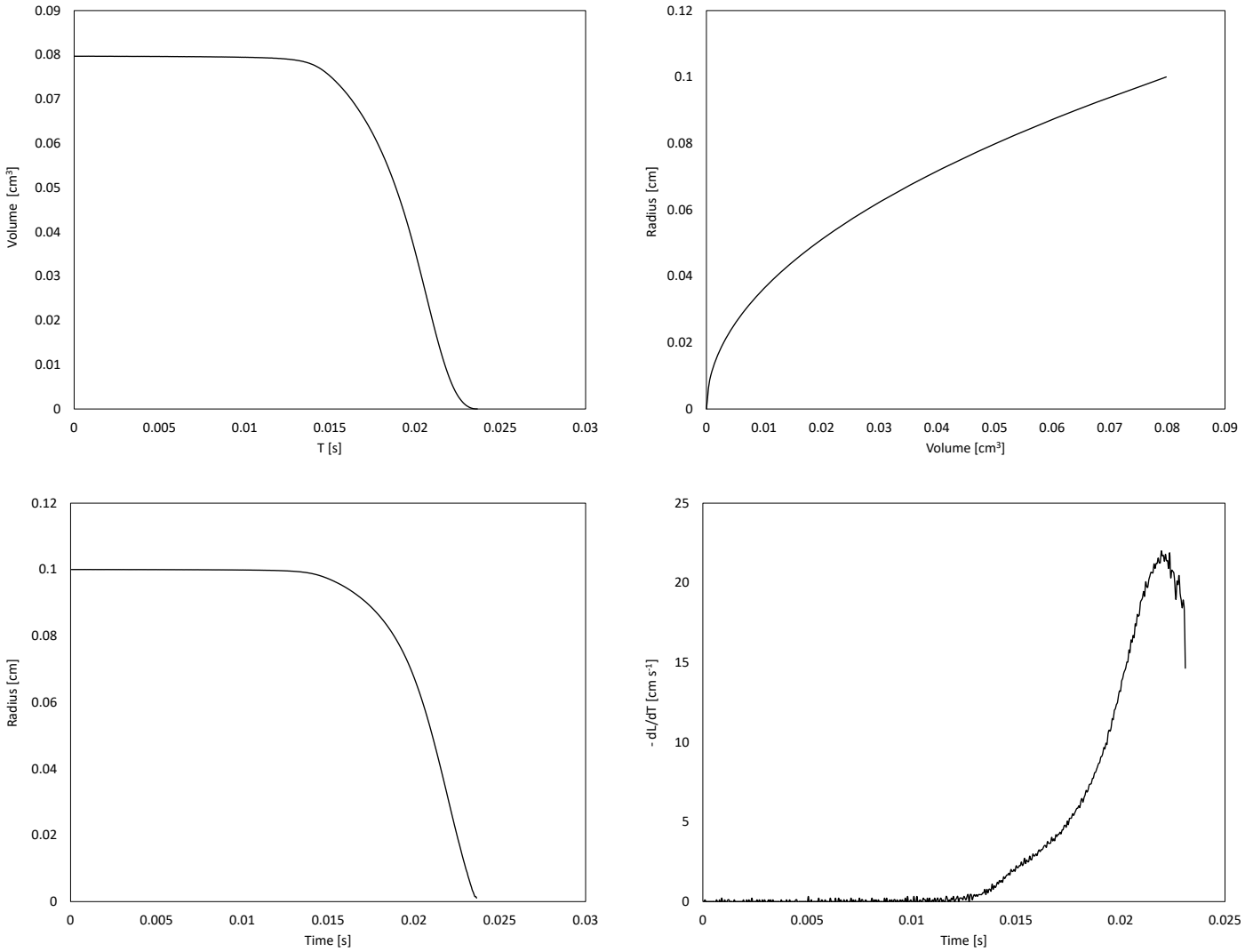

Figure 2-6 Volume of propellant grain (top left), form function (top right), radius as function of time (bottom left) and radius change as a function of time (bottom right).

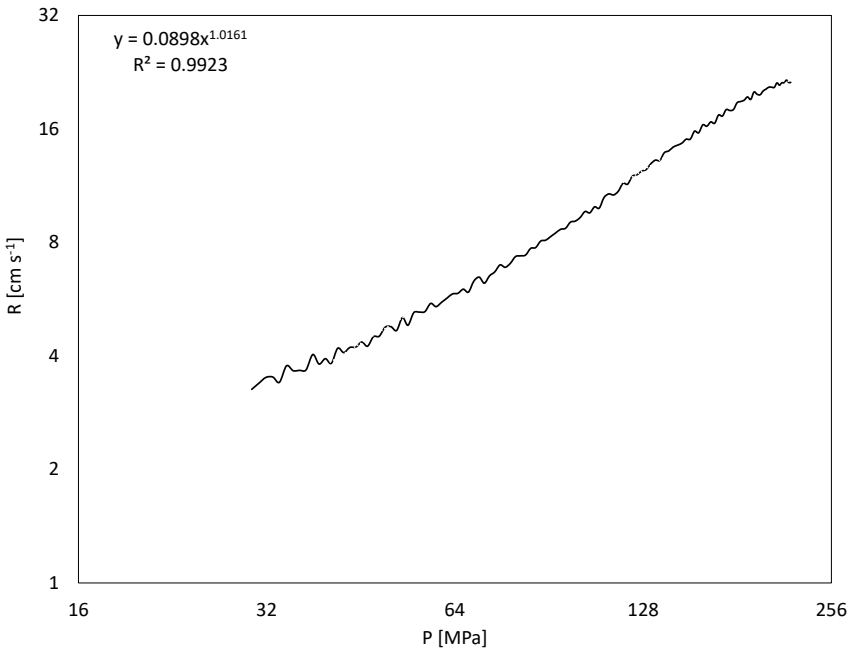

Figure 2-7 Vielle's Law.

$$r = \beta P^{\alpha} \quad (2.5)$$

2.1.2.4 Combustion wave structure

A combustion wave of propellant is composed of five different zones [13]: (I) the heat conduction zone, (II) the solid-phase reaction zone, (III) the fizz zone, (IV) the dark zone and (V) the flame zone as seen in Figure 2-8.

In the heat conduction zone, no chemical reactions occur. The temperature increase is due to heat conduction from the initial temperature in the bulk of the propellant (T_o) to the temperature of the solid-phase reaction zone (T_u), as can be seen in Figure 2.7. In the solid-phase reaction zone, thermal degradation of the surface leads to the formation of nitrogen dioxide and aldehydes at the interface of the solid phase and the burning surface. This interface is composed of solid/gas and/or solid/liquid/gas, depending on whether the propellant species are decomposing, melting or evaporating. This layer is so thin that its temperature is equal to that of the burning surface of the

propellant (T_s). The fizz zone is the region where nitrogen dioxide, aldehydes and other species react to produce NO, CO, H_2, H_2O and other carbon compounds in what are quick chemical reactions. In the dark zone, residual oxidation occurs to produce N_2, CO_2 and H_2O. Compared to the fizz zone, the kinetics of gas formation here is slow due to an induction period, but is affected by the pressure and the temperature at which the propellant is burning. Once the induction period has ended, the gas from the dark zone produces the flame zone, where the final gas composition is obtained and the temperature is that of the adiabatic flame temperature (T_f).

Figure 2-9 shows the influence of pressure on the fizz zone and the dark zone. As mentioned previously, the thickness of the fizz zone is dependent on the chemical kinetics of the gaseous species and how it evolved at the interface of the solid phase and the combustion phase. As pressure increases, the thickness of the fizz zone decreases, leading to an increase in the temperature gradient between the fizz zone and the bulk of the propellant. This augmentation in heat transfer by conduction to the solid phase increases the LBR. Similarly, the length of the dark zone is reduced as pressure increases bring the luminous flame front closer to the solid phase, which in turn increases heat transfer. For this reason, as pressure increases, so does the burning rate [24].

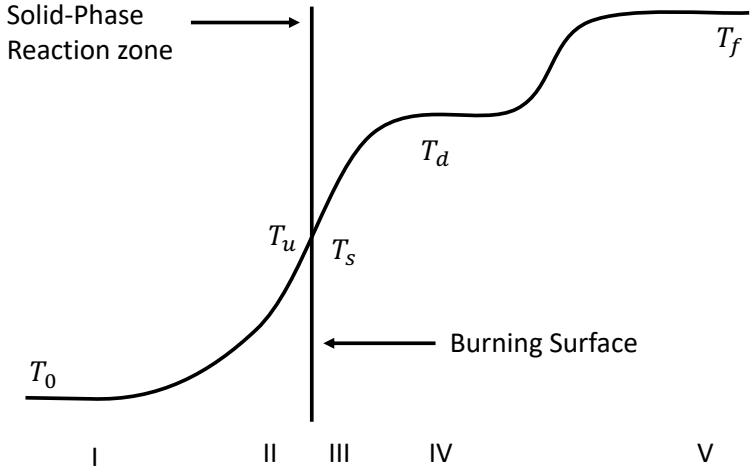

Figure 2-8 Combustion wave structure of propellant; adapted from [13].

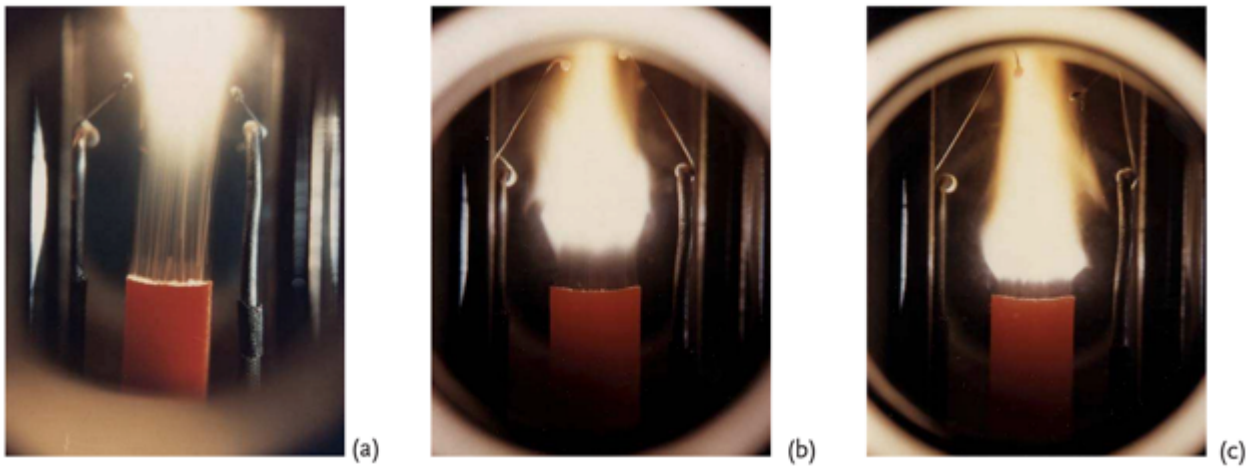

Figure 2-9 Typical flame from a propellant at 1 MPa (a), 2 MPa (b) and 3 MPa (c) [13].

2.1.2.5 Erosivity in gun

The ballistic cycle is comprised of the following sequence: ignition of the primer composition, ignition of the intermediate charge (optional) followed by the ignition of main propellant charge. As the main propellant charge is burning, hot gases push on the seated projectile, increasing breach pressure and accelerating the projectile until it has left the barrel or that the propellant is completely burned. Pressure can reach up to 600 MPa and the bore temperature can reach as high as 1200 K in milliseconds [25]. The flow of gas, the high temperature and the abrasion between the projectile and the barrel wall cause wear on the barrel, increasing the bore diameter (Figure 2-10). This allows gas to be vented around the projectile, which affects the ballistic performance of the weapon. It can also lead to failure of the gun barrel due to fatigue and crack propagation.

Erosion is classified into three categories: chemical, thermal and mechanical.

Chemical erosion is caused by the nature of the gas species. Propellant gases are mainly comprised of CO, CO_2, N_2, H_2 and H_2O [26]. At high temperature and pressure, a chemical reaction between the barrel wall and the gaseous species occurs. The literature refers to four types of reactions: carburization, oxidation, hydrogen embrittlement and nitride formation. Carburization takes place when CO and CO_2 react with steel to form atomic carbon [27, 28].

$$2CO = C + CO_2, \text{ and} \qquad (2.6)$$

$$CO = C + O \quad (2.7)$$

The atomic carbon is free to diffuse in the gun barrel and at high temperatures forms a solution with the steel. As the temperature cools down, carbon precipitates out of the solution and reacts with the iron to form carbide such as cementite (Fe_3C) [29].

$$3Fe + 2CO = Fe_3C + CO_2 \quad (2.8)$$

The cementite lowers the bore surface melting point by 50-400 K, which reduces the barrel wall resistance to thermal and mechanical aggression.

Oxygen can also diffuse in the metal surface, forming various oxides depending on the barrel alloy trough reaction such as the formation of iron oxide (2.9) [30].

$$3Fe + CO_2 = FeO + CO \quad (2.9)$$

This brittle oxide layer allows for increased cracking and erosion as well as reduces the melting point of the barrel layer by 100-200 K, leading to increased thermal erosion [29].

While it is shown that CO, CO_2, H_2O, O_2 and H_2 have proven to increase gun erosivity, it is accepted that nitrogen contribution to erosivity is not only minimal, but can even have a protective effect on the barrel. Research by Hirvonen, Conroy and Leveritt [27, 31] found that a high nitrogen content propellant increases the residual nitrogen near the surface of the barrel wall and is linked to a reduced erosivity. They argued that this was a result of the reduced flame temperature of the nitrogen rich propellant and by the counteraction of the formation of carbide species by reacting with iron forming nitride species. Compared to carbide, the melting point of nitride is higher than that of the steel, and would thus protect the steel from thermal erosion.

Thermal erosion is caused by the high-flame temperature of the combustion gases. The T_f of propellant can be as high as 3800 K when measured using thermochemical software such as CHEETAH V2.0. The heat of the combustion gases is transferred to the surface of the wall and can increase the temperature up to 1500 K, which is very close to the melting temperature of gun steel (1720 K) [30]. The softening of the steel reduces its mechanical property, leading to erosion.

When using low-flame temperature propellant, thermal and chemical erosion are minimal and the dominant form of erosion is through abrasion from the projectile. Throughout its use, a gun barrel experiences cracking, degradation and a softening of part of the bore by thermal aggression. These regions are susceptible to wear between the projectile and the material wall.

Three semi-empirical correlations are proposed to evaluate the erosivity of gun propellant. Lawton proposed two models: one based on the flame temperature (2.10) and another based on the chemical composition of the gaseous species (2.11) [25]. Jaramaz also presented a model based on chemical composition (2.12) [6].

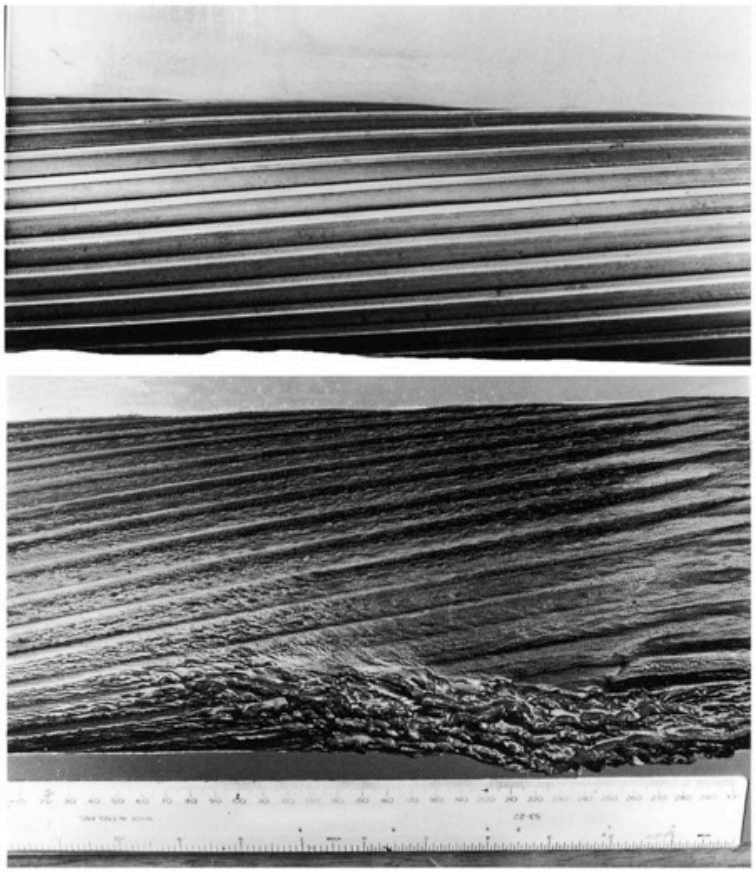

Figure 2-10 Gun erosion at the beginning of the riffling. Unworn surface (top) and abnormal wear due to melt erosion (bottom) [25].

$$w = A \exp\left(bT_{max}\right) \qquad (2.10)$$

$$A = 114 \exp\{0.027[2.4\ \mathrm{f}_{H2} + 0.27\mathrm{f}_{CO} - 0.5\mathrm{f}_{N2} - 3.30.27\mathrm{f}_{CO2} - 3.60.27\mathrm{f}_{H2O}]\} \quad (2.11)$$

$$\ln(\mathrm{Ax}10^{3}) = 1.003\ \mathrm{f}_{R} + 0.348\ \mathrm{f}_{H2O} + 0.079 - 0.273\ \mathrm{f}_{CO2} - 0.141\ \mathrm{f}_{H2} - 0.019\ \mathrm{f}_{N2} \quad (2.12)$$

Where w is the erosivity per round, A is the erosivity parameter of the propellant, T_{max} the maximum temperature in the gun, b is the hardness of the barrel and f_x is the fraction of gas concentration. For Lawton and Jaramaz, the influence of chemical composition on erosivity is, respectively, $H_2 > CO > N_2 > CO_2 > H_2O$ and Residual Gas > H_2O > CO > N_2 > H_2 > CO_2.

Two models predict erosivity as a function of flame temperature and the average molecular weight of the combustion gases. The Kimura model holds that a linear relation takes place between the natural logarithm of the erosion and the square root of the isochronic flame temperature divided by the average gas molecular weight ($\left(T_f/M_w\right)^{0,5}$) [32]. In the Arisawa-Kimura model, a linear relation takes place between the natural logarithm of the erosion and the isochronic flame temperature divided by the square root of the average gas molecular weight ($T_f/M_w^{0,5}$) [33]. In both models, the erosivity contribution is as follows: $CO_2 > CO > H_2O > H_2 > O > N_2$.

While these theories conflict with one another, they are in agreement that CO and H_2 will lead to increased erosivity and that N_2 will prolong the life of the barrel.

Due to the protective effect of N_2 and the negative effect of CO_2, the ratio of N_2/CO has been used as an approximation to evaluate gun erosivity, as well as the ratio of CO/CO_2.

The erosion can be measured in two ways: by performing numerous firings in a single barrel and measuring the increase in bore diameter or by firing in a subsystem called an erosivity vented vessel (EVV). The EVV is comprised of the following parts: a combustion chamber, a pressure transducer, an ignition system, a rupture disc (optional) and an erosivity grain (Figure 2-11).

To evaluate erosivity, propellant is placed in the combustion chamber, which may or may not be scaled with a rupture disc (model dependent). Assuming a rupture disc is present, as the propellant is burned, pressure increases until it reaches the bursting point. Upon failure of the rupture disc, hot gases from the propellant formulation are channelled through the erosion grain resulting in chemical, thermal and mechanical erosion. Multiple firings can be done in a single grain to amplify the signal. Erosion is measured by the weight loss of the erosion grain.

The erosivity of a formulation is a complex phenomenon. High-flame temperatures and oxygen-rich propellant will tend to lead to the formation of CO_2 and H_2O. Gaseous products are favourable in terms of erosivity, but the flame temperature will become a factor. Low-flame temperatures and oxygen-poor propellant will lead to the formation of CO and H_2, which chemically affects the steel barrel. It will also lead to a lowered flame temperature, reducing thermal erosivity. The use of a low-flame temperature formulation containing high nitrogen concentration is a way to provide high impetus formulation with low erosivity values.

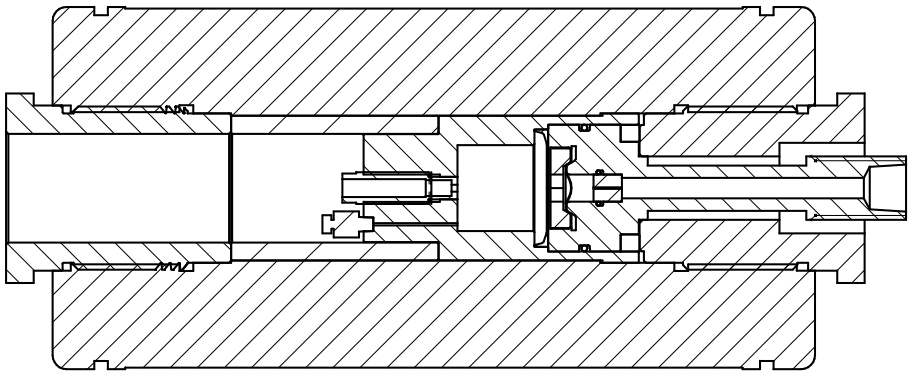

Figure 2-11 Erosivity vented vessel cross-sectional representation.

2.1.3 Energetic polymers and binders

When working with EMs, the geometry and shape of the compositions must be adapted to suit the targeted application. As an example, the propellants found in hunting carbine and in large artillery gun systems, although very similar in composition, have different geometry in order to accommodate the specific ballistic parameter of the system, such as chamber volume, maximum allowable pressure, barrel length, projectile weight, etc. [23].

The previous section defined EMs as molecules presenting explosophoric moieties. Molecules such as RDX and BTA are crystalline solid, while NG is a liquid. In order to shape them into useful applications, EMs are compounded using binders and various plasticizers.

Binders and plasticizers can be inert or may contain explosophoric groups which allows them to take part in the combustion cycle actively.

Carboxy acetate butyrate (CAB), hydroxyl-terminated polybutadiene (HTBP) and polyisbutylene are examples of such binders, which are used, in applications such as RDX-based gun-propellant formulations, rocket propellant and polymer-bonded explosives [34-36]. Inert plasticizers such as dibutyl phthalate (DBP) and triacetin (TA) are commonly used in guns and rockets propellants [16]. These are all examples of inert binders and plasticizers common in the manufacture of EMs.

Inert binders and plasticizers concentration must be kept to a minimum in high-energy applications as they require large amounts of oxidizers to complete their combustion, thus reducing the impetus of the formulation.

The use of energetic binders and plasticizers is, therefore, a better option when it comes to high-energy applications. Many energetic binders are available or have been synthesized, including NC, GAP, poly(3,3-bis-azidomethyl oxetane) (polyBAMO) and poly(glycidyl nitrate) (polyGLYN). Energetic plasticizers are also very common and are of two main types: nitrate ester plasticizer and azido plasticizer. NG, trimetylol ethane trinitrate (TMETN) and triethylene glycol dinitrate (TEGDN) are examples of nitrate ester plasticizer, while pentaerythritol tetrakis (azidoacetate) and low-molecular weight GAP are examples of azido-based plasticizer.

The following section will focus on the energetic binders NC and AC and on the plasticizers GAP and NG.

2.1.4 Nitrocellulose

NC was first synthesized in 1845 by Cristian Friedrich Schonbein and Rudolf Christian Bottger [37]. It is formed by nitrating cellulose with mixtures of sulphuric and nitric acid.

Cellulose, found in nature, is a key constituent of the cellular wall of plants, trees, cotton and bacteria. Cotton and wood-pulp fibres are highly structured and are comprised of distinct macroscopic layers. Cotton, for example, is made up of the cuticle, the primary wall, the winding layer, the secondary wall and the lumen (Figure 2-12) [38]. All these parts consist primarily of cellulose, resulting in a 95 % cellulose concentration in the case of cotton fibre. When arranging itself, cellulose organises in successions of amorphous and crystalline domains, as shown in

Figure 2-13.

Chemically, cellulose is a homopolysacharide comprised of repeating anhydroglucose units (AGU) with alternating AGUs rotated 180º with respect to its neighbour (Figure 2-14). Three-hydroxyl groups are on each AGU. These hydroxyl are available for chemical modification and are in order of reactivity C6 > C3 ≈ C2 [39].

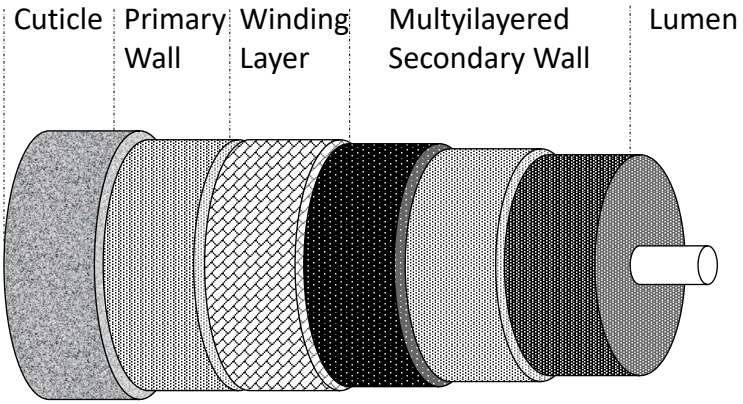

Figure 2-12 Structure of cotton fibre; adapted from [38].

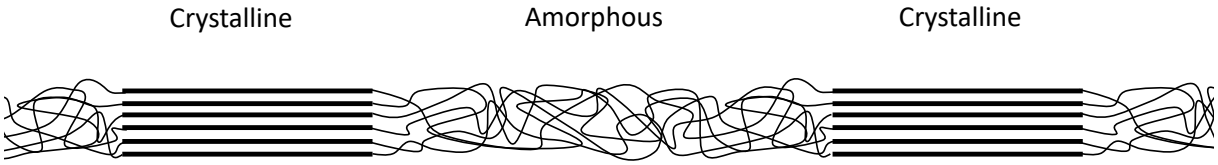

Figure 2-13 Molecular structure of cellulose amorphous and crystalline regions.

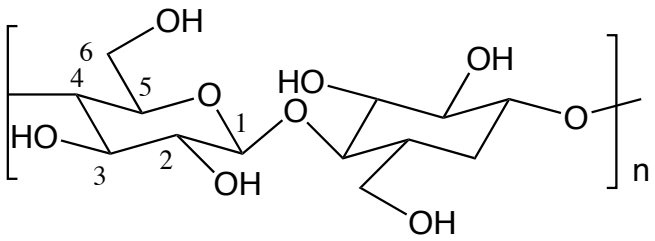

Figure 2-14 Cellulose molecular backbone [40].

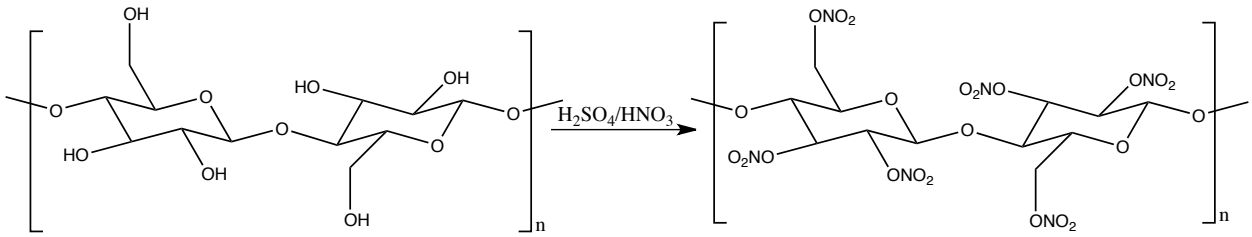

Figure 2-15 NC synthesis from cellulose using mixed acid condition [40].

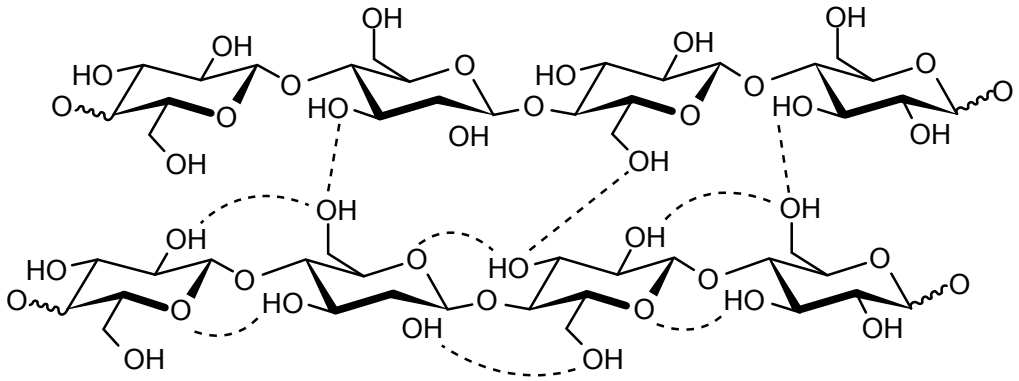

Figure 2-16 Intra and intermolecular bonds within cellulose; adapted from [41].

Nitration of the hydroxyl side group is performed using a mix of concentrated nitric acid and sulphuric acid in a ratio of 1:1 and up to 1:3 [42].

The degree of nitration of NC is commonly described as the percentage by weight of nitrogen over the total mass of the NC. Although in theory a fully substituted NC could achieve a degree of nitration would yield 14.14%N, it is found that the maximum achievable %N value is 13.9 %N [40]. The higher the %N, the more energetic is the NC.

The nitration of cellulose does not change the morphology of the fibres. In order to use NC as a binder for EMs, the fibrous structure must first be broken down. Solvents and mechanical energy are used to swell the NC fibres, which allows solvent to enter in between the polymer chains. This softens the material into a cohesive mass, allowing its use as a binder. However, not all NC presents the same affinity with solvent, as the degree of nitration greatly affects NC's solubility.

At 0 %N (DS = 0), cellulose is insoluble in water and in most non-polar organic solvents. While the presence of a hydroxyl group on the chain explains the lack of interaction with non-polar

solvents, it is expected that cellulose has a good affinity with polar solvents such as starch. It is accepted that the lack of solubility with polar solvents is a result of its ability to form intra-molecular hydrogen bonds between each AGU (Figure 2-16) [41].

As %N increases from 0 to 11.2 NC (DS = 2.20 – 2.32), the reduced intra-molecular forces allow for NC to be soluble in low-molecular weight alcohol, esters and ketone. As %N increases to 11.8 to 12.2, the reduced hydroxyl group on NC diminishes its affinity with low-molecular weight alcohol, but keeps its affinity with esters, ketones and mixtures of ether-alcohol. Above 12.6 %N (DS = 2.45 – 2.87), NC is only soluble in esters and ketones [43].

Due to its rigid molecular structure, NC has a very high glass transition (T_g) overlapping its decomposition temperature. T_g value for NC containing 12.6 %N has been reported to be 195 °C in the literature and its decomposition temperature (T_d) ranges between 197 and 199 °C, depending on the nitration level [44, 45], with an activation energy of 196 kJ mol^{-1} [13]. For this reason, it is usually blended not only with solvents, but also with plasticizers to reduce both its glass transition and brittleness.

NC, is used in many applications, including lacquer, propellant, explosives binders and in thermoplastic binders as discovered by Alexander Parkes.

In 1862, Alexander Parkes realized that a mixture of NC and solvent had thermoforming ability. Unfortunately, the lack of plasticizer in the formulation resulted in a material that would crack over time, making high-scale production impossible. A few years later, John Wesley Hyatt discovered that camphor is a good plasticizer for NC, making the material the first thermoplastic manufactured on an industrial scale. The product was named “celluloid” and is still in use to this day [46, 47]. A DMA analysis of celluloid sheet indicate a T_g of 96 and 108°C respectively for the maxima of E’’ or the maxima of Tan δ (Figure 2-17).

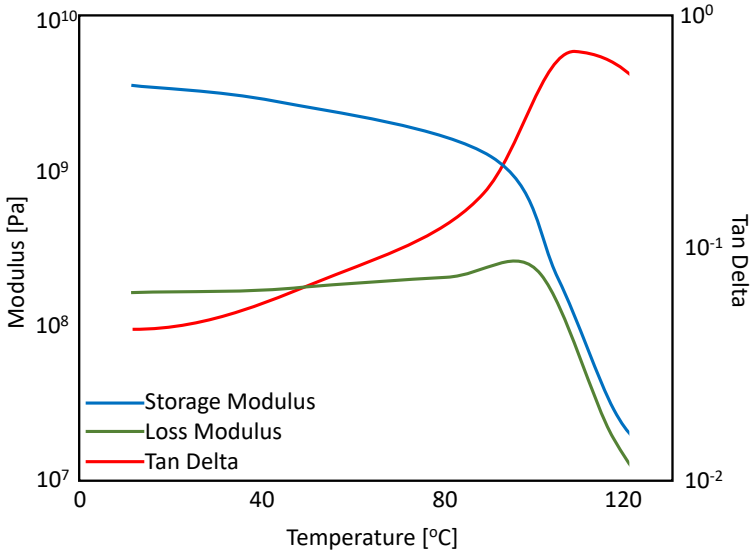

Figure 2-17 DMA analysis of 0.6 mm thick celluloid sheets; provided by GD OTS.

2.1.5 Azidodeoxycellulose

AC, much like NC, is a derivative of cellulose whereby the hydroxyl group is replaced with azide moieties. It is currently being investigated as a means to manufacture membranes on which click chemistry can occur with the azide moieties on the AC chain [48].

It is synthesized in four steps. First, the cellulose is boiled in dimethylacetamide (DMA) to drive off any residual water. Second, lithium chloride (LiCl) is added to allow the dissolution of the cellulose. Third, tosylation of the hydroxyl group is performed using 4-Toluenesulfonyl chloride (TsCl) in the presence of triethylamine (Et_3N) to form tosylated cellulose (TsCell) and triethylamine hydrochloride [49]. Degrees of tosylation (DSTs) found in the literature are presented in Table 2-3.

Once purified, TsCell is dissolved in dimethylformamide (DMF) at 100 °C under nitrogen flow in the presence of sodium azide (NaN_3). This forms AC and sodium p-toluenesulfonate by nucleophilic displacement (S_N), giving a final substitution degree in azide moieties (DS_{N3}) of 0.82 and a residual DS_{Ts} of 0.05 as obtained from Schmidt et al. [8]. Chemical reactions and conditions are presented in Figure 2-18.

The stability of AC as a energetic material has been evaluated by DSC and proved to be similar to that of NC [50, 51]. This is of interest as it is expected that AC with a DS_{N3} of 1, 2 and 3 would, respectively, have a nitrogen content (%N) of 22.3, 39.8 and 53.2, making this material very interesting from a high-nitrogen energetic binder standpoint. To this day, no information are available on the combustion properties of AC.

Table 2-3 DS_{Ts} present in the literature.

DS_{Ts}	Ref.
0.40 – 0.68	[52]
0.43 – 0.95	[8]
0.38 – 2.30	[49]
0.74 – 1.29	[53]

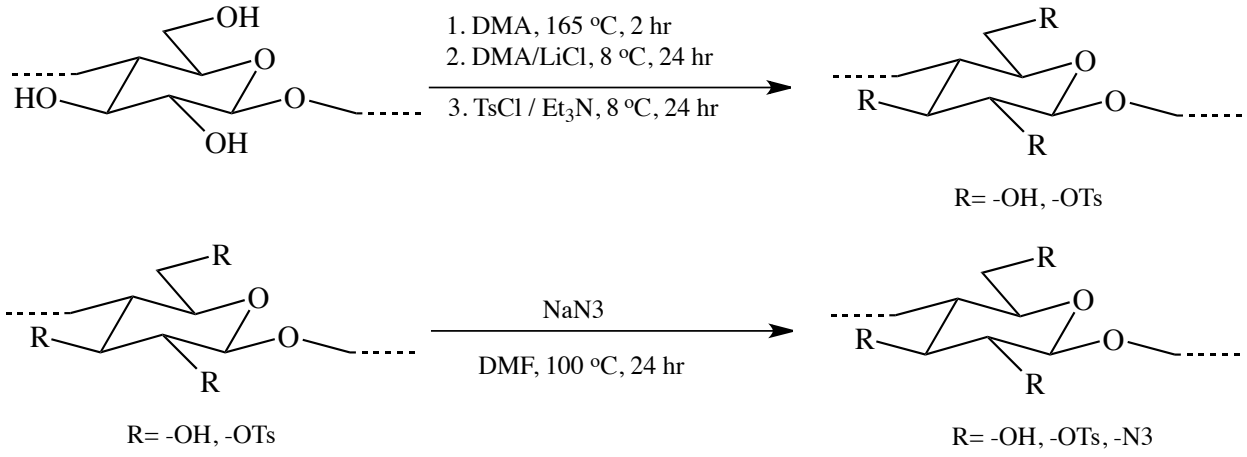

Figure 2-18 Synthesis pathways of cellulose to TsC (top) and from TsC to AC (bottom) [8, 49].

2.1.6 Nitroglycerine

Nitroglycerine (NG), or more specifically trinitroglycerine, was developed by Italian chemist Ascanio Sobrero in 1847 by adding glycerol to a mixture of concentrated nitric and sulphuric acids [54]. It is a dense, oily and colorless liquid, as well as a powerful explosive. It is used primarily in the manufacturing of dynamite and in gun propellant as a plasticizer for NC. It is also used in medicine as a vasodilator and can be toxic to humans at high dosages [1, 16]. It has a density of

1.6 g cm^{-3}, a melting point of 14 ºC and a vapour pressure of 0.03 Pa at 20 ºC [55]. The decomposition activation energy of NG is 109 kJ mol^{-1} [13].

The properties of NC plasticized with NG will be discussed in the section on plasticization.

2.1.7 Glycidyl azide polymer

Glycidyl azide polymer (GAP) was first manufactured by Rocketdyne USA in 1976 in order to produce hydroxyl-terminated azido polymers to replace inert binders in rocket formulations [3].The first proposed method of synthesis was to react epichlorohydrin (ECH) and NaN_3 in hydrazoic acid to produce 1-azido-3-chloro-2-propanol. It was then cyclicized by the addition of a base to form the monomer glycidyl azide (GA). Unfortunately, the low reactivity of GA prevented it from polymerizing. The azide tended to react as a pseudo-halogen, making the procedure unsuccessful. A new synthesis was proposed in which ECH was first polymerized to polyepichlorohydrin (PECH) and then reacted with NaN_3 to obtain GAP, as shown in Figure 2-20

3M has commercialized GAP under two names: GAP-5527 Polyol, a hydroxyl terminated polymer with a hydroxyl functionality between 2.5 and 3 and a viscosity of 12 000 cps at 25 ºC and GAP0700 Plasticizer, a non-functional plasticizer with a viscosity of 140 cps at 25 ºC. For GAP0700, an extra synthesis step is performed to convert the residual hydroxyl group into azide, allowing GAP0700 to be used as plasticizer for a cured GAP binder.

GAP0700 and GAP-5527 have a reported T_g of -64.4 ºC and -59.9 ºC and of -56ºC and -45ºC, depending on the literature [56, 57]. The activation energy of GAP degradation is 174 kJ mol^{-1} [58].

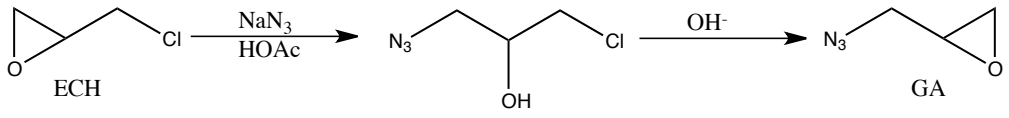

Figure 2-19 GA synthesis from ECH [59].

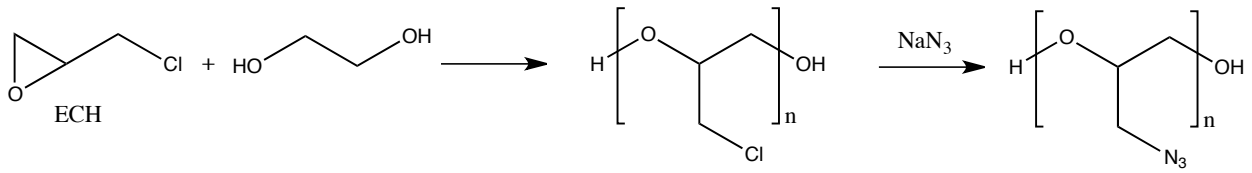

Figure 2-20 Preparation of GAP-diol from ECH, ethylene glycol and NaN_3 [56].

2.2 Plasticization of nitrocellulose

The nitration of NC does not change its fibrous morphology, as previously discussed. For this reason, solvents and plasticizers are added to NC formulation in order to swell or completely dissolve the fibre.

The literature makes many references to the influence of plasticizers, including [60]:

- Low molecular weight material added to polymeric materials such as paints, plastics or adhesives to improve their flexibility.
- Plasticizer interacts with the polymer chains at the molecular level so as to speed up its viscoelastic response or increase its chain mobility.
- Plasticizer lowers the glass transition temperature (T_g) and makes material more flexible.
- Polymeric plasticizer has sufficiently high-molecular weight (usually M_n greater than 5,000). An increase in molecular weight contributes to its permanence due to a low vapour pressure and a low diffusion rate.

There are multiple theories to explain the mechanism of plasticization. The lubricity, the gel and the viscosity theory — all developed in the 1940s — have been replaced by the free volume theory.

Free volume is defined as the difference between the volume measured for the material and the volume measured at absolute zero.

$$v_f = v_T - v_0 \qquad (2.13)$$

Although this definition is impractical due to the difficulty of measuring v_0, the variation in v_f as a function of temperature is attributed to the variation of space between the polymer chains. Above

T_g, the internal energy of the molecules allows them to move, bend and rotate. Multiple degrees of freedom are available for the polymer. As the temperature reaches T_g, less degrees of freedom are available to the polymer chain diminishes due to reducing free volume. At T_g, the segments are so densely packed that the mobility in the polymer chain is negligible. Below this temperature, no chain movements are allowed and the structure is "frozen" in its final shape.

From the free volume theory, the introduction of plasticizer in a polymer system greatly increases the free volume in the system by "wedging" the small molecule of the plasticizer in between the polymer chains (Figure 2-21).

The main criticism of this theory is that there is no influence on the chemical compatibility of the polymer-plasticizer system and that the polymer is considered as a homogeneous amorphous phase without the presence of a crystalline phase.

A simple method of correlating the free volume theory and T_g in the material, also known as the Fox equation (2.4.2), can be used to estimate the glass transition of a plasticized system.

$$\frac{1}{T_g} = \frac{w_1}{T_{g1}} - \frac{w_2}{T_{g2}} \qquad (2.14)$$

Where T_g, T_{g1} and T_{g2} are the glass transitions of the mixture, the polymer and the plasticizer w_1 and w_2 are the weight fraction of the polymer and plasticizer.

Another model correlating the T_g of a material is proposed based on the Gordon-Taylor equation [61], where K is the fitting parameter.

$$T_{g,mix} = \frac{\left[w_1\, T_{g1} + K\, w_2 T_{g2}\right]}{\left[w_1 + K\, w_2\right]} \qquad (2.15)$$

Natural polymers such as cellulose, its derivatives and starch have multiple advantages. They are available in large quantities, are cheap, come from renewable resources and are usually biodegradable. Some drawbacks of natural polymers are their source, the time required to harvest and their tendency to absorb moisture, which changes their properties. They are also thermally unstable, given that they are prone to decomposition.

Cellulose and starch are composed of hundreds of D-glucopyranoside units linked by acetal bonds between the two cyclic monomers. The ring on the main chain and the presence of hydrogen bonding among the hydroxyl group make the processing of these polymers difficult in traditional equipment due to the rigid intramolecular structure of the polymer.

Compared to starch and other polysaccharides, cellulose molecular chains are very long and made up of a single repeating unit [62] containing both amorphous and crystalline phase.

As was discussed previously, energetic plasticizers are defined as liquid materials having a positive heat of formation and bearing explosophore groups [1]. Examples of energetic plasticizers are NG, butanetriol trinitrate (BTTN), diethyleneglycol dinitrate (DEGDN) and TMETN.

DMA results for NC plasticized with DEGDN or triacetine showed multiple transitions in the material (Figure 2-22). One takes place at around -20 ^{o}C (β relaxation), which does not shift, and another one (α relaxation) shifting as a function of gelatinization levels at around 60-80 ^{o}C. According to the research, the relaxation at 60-80 ^{o}C is associated with the glass transition in the material, while the relaxation at -20 ^{o}C is attributed to the motion of the NC molecule side groups and with NG [63, 64]. Similar results were observed by Baker and Privett [65].

When plasticized, NC exhibited multiple relaxations. The α relaxation, the first of the two main transitions, appears above 50 ^{o}C and indicates the beginning of a segmental movement of the NC main chain. The β relaxation occurs below 10 ^{o}C, and its significance is the subject of debate.

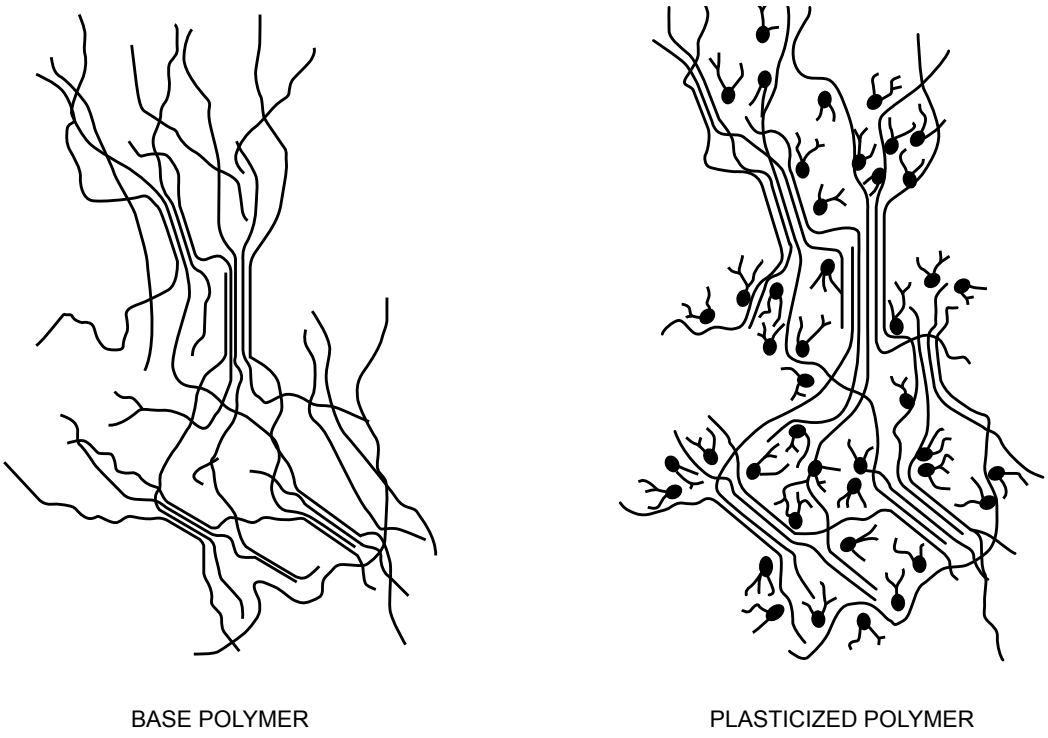

Figure 2-21 Concept of plasticization of semi- crystalline polymer; adapted from [60].

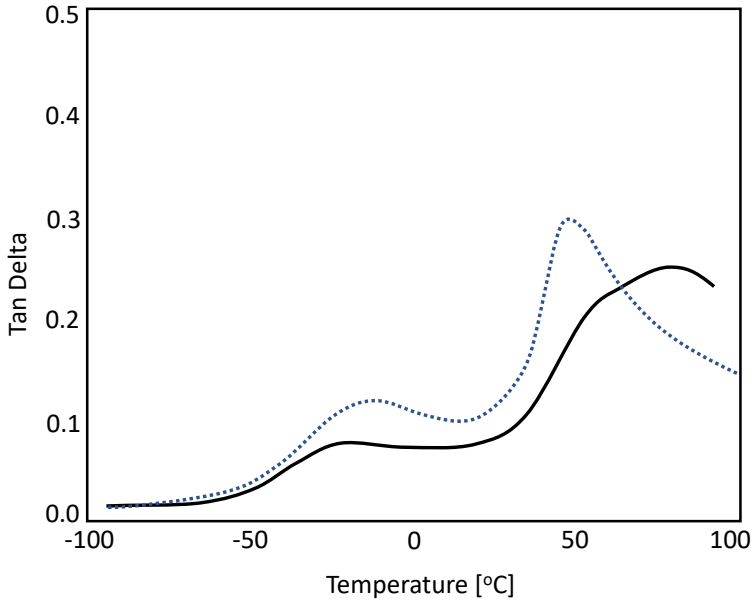

Figure 2-22 Dynamical mechanical analysis (DMA) study of NC plasticized with 35% DEGDN (solid) and 20% triacetine (dotted); adapted from [63].

In order to explain the presence of multiple relaxations, various hypotheses are proposed.

The results of the study of the plasticization of cellulose derivatives (cellulose acetate (CA), benzylated cellulose and starch) are presented in Figure 2-23. The β-transition is present in all the samples, although the intensity and localization of the peak can vary depending on the mixing conditions. ϒ-transition is only detected in a low plasticized CA prepared sample. It was also found that the α-transition was associated with the T_g of the material. The similarity in the spectra demonstrates that the modes of relaxation in natural polymers are very similar to one another and that the intensity and shifts of the ϒ and β transitions seem to be more influenced than the α-transition. The authors associate this observation with the movement of small units in the polymer. Therefore, the intensity and temperature at which these transitions occur are more influenced by the type of modification and chemical modification than by the α-transition, which is associated with the movement of the glucose ring in the polymer.

It may also be associated with the movement of the plasticizers in regard to the NC side groups [66], of smaller structure units in the main chain such as the glucose ring in the case of cellulose acetate [44], or otherwise, to the presence of a plasticizer-rich phase as proposed by work on thermoplastic starch. Starch-glycerol films are partially miscible systems, giving rise to a polymer-rich phase and a plasticizer-rich phase at concentrations higher than 30 wt% in glycerol [67-70].

One of the advantages of using high-molecular weight polymeric energetic plasticizers is that the migration of plasticizers is diminished and weight loss is better controlled. Figure 2-24 shows the polyGLYN losing less than 1.5 wt% in a 0.2 mm Hg vacuum compared to 4.5 wt% in the case of BTTN over a period of 42 and 34 days.

Polymers such as GAP have been used in the literature to plasticize NC. In the work of Wu et al., NC is compounded to GAP and NG to manufacture crosslinked double-base propellants (XLDB) [71]. In the work of Niehaus, NC plasticized with a mixture of GAP and other plasticizers is added to an RDX-based propellant so as to examine the influence of the compression mechanical properties of the propellant [72]. In the work of Wang, NC is added to an energetic thermoplastic elastomer (ETPE) in order to improve the mechanical properties of the elastomeric blend [73].

Never has GAP been used solely for its plasticization property of nitrocellulose or evaluated as part of a binary plasticizer system comprised of GAP and NG.

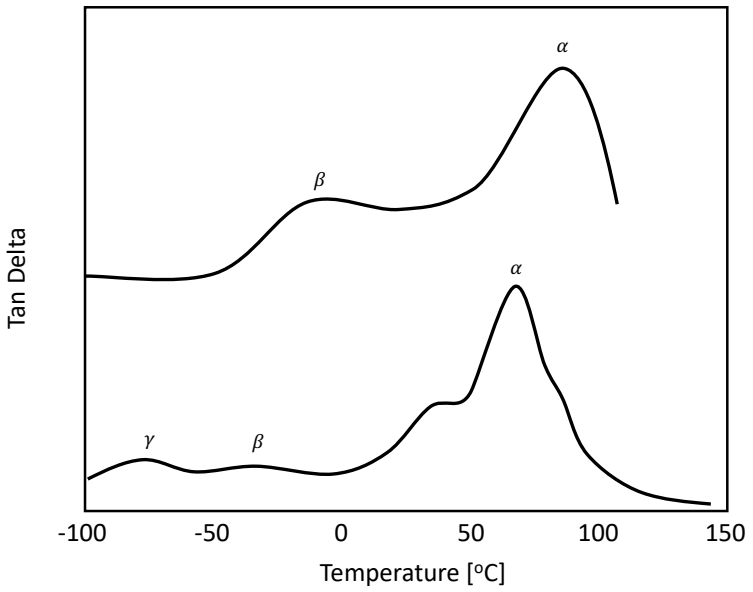

Figure 2-23 Characteristic DMTA spectra of various plasticized natural polymers and their derivatives: (bottom) CA (mixed in internal mixer at180 °C for 20 min with 35 wt % CL), (top) CA (mixed in internal mixer at 180 °C for 20 min with 45% CL); adapted from [74].

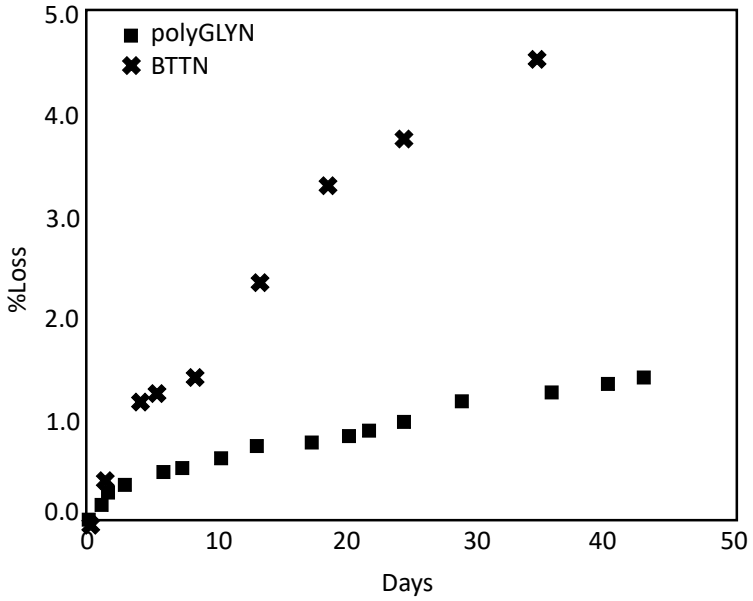

Figure 2-24 Loss of plasticizer under vacuum of 0.2 mm Hg; adapted from [75].

2.3 Combustible containers

As previously discussed, EMs are used in a vast array of applications. One such application is as a combustible container in indirect fire systems such as large calibre artillery systems and mortar, as well as in direct fire systems in tank ammunitions.

Many technologies are available, including impregnated containers, NC-felted material, and celluloid.

The impregnated container is a technology in which propellant powders are placed inside rigid combustible cases obtained by the impregnation of NC paper with trinitrotoluene. Paint, lacquers and chemicals are used to protect the impregnated NC paper from water. Due to the acute deleterious effects of trinitrotoluene on humans, it is used only in legacy applications and current applications use the NC-felted fibres technology.

NC felted material, also known as NC felted fibres, is produced when NC and kraft pulp are dispersed in a liquid medium and polymer fibres are then added to the mixture. The slurry is pressed into a mold that removes the water and takes the shape of the container.

The manufacturing process of dispersing the slurry and filling the mold cavity induces large variations in the final thickness and in the density of the product's wall. For this reason, multiple inspection steps are needed to ensure that the mechanical properties, geometric dimensions and burning properties all meet specifications.

The high reject rate, the multistep manufacturing process, the certification requirements and the lack of competition within the industrial base, result in the felted fibre technology being increasingly expensive. In reaction, the U.S. Army Combat Capabilities Development Command Armaments Center is actively seeking substitute material due to the prohibitive cost of felted fibres. Felted fibres casings are currently used in mortar, artillery and tank applications.

Celluloid is used as a combustible container in mortar systems. To be used as a container, a sheet of celluloid is thermoformed into a cavity shaped like a horseshoe. Two halves are then welded together, filled with the propellant and assembled on the mortar ammunition. During the ballistic cycle, the igniter of the mortar round ignites both the propellant and the casing, thus propelling the munitions out of the barrel (Figure 2-25 and Figure 2-26).

As mentioned previously, celluloid is manufactured using NC with a nitration level of 11 %N and an inert plasticizer, making it a thermoplastic binder.

In comparison, the nitration level of propellant-grade NC ranges between 12.5 to 13.55 %N, and is typically plasticized using low-molecular weight nitrate ester such as NG, DEGDN and TMETN.

This combination of low-nitration NC and inert plasticizer reduces the total energy of the container, lowers its oxygen balance and leads to unclean combustion of the material, which generates fouling.

This fouling may lead to hangfire or to the ammunition getting stuck partway down the tube while the weapon is loaded. Both are critical issues of the weapon system, as they increase the chance of double loading the weapon if the operators do not follow standard operating procedures. Double loading the weapon is a weapon malfunction, in which a second round is inserted into the gun tube while a first round has already been chambered. Although this is an uncommon type of weapon malfunction in gun, artillery and tank, such a malfunction is more likely in mortars, since the ammunition is fed from the top of mortar tube. Upon ignition of the first ammunition, the obstruction caused by the second one can have tragic consequences, as demonstrated by the incident that took place at Camp Lejeune, N.C. on March 18, 2013 in which seven Marines were killed and eight wounded [76].

Another issue that stems from unclean combustion of the container is that bits of smouldering material can be found down the tube, causing the next round to ignite leading to the unintentional discharge of the weapon. Smouldering materials and unburned material can also interfere with the firing mechanism, causing a weapon malfunction.

To reduce fouling, work has been done to modify the celluloid sheet and to improve the quickness at which it burns by foaming the material [4].

Another way to mitigate the fouling problem is to develop new formulations to improve combustion while preserving the desirable thermoplastic properties.

This can be achieved by either increasing the energetic content of the base polymer or by replacing the initial inert plasticizer with an energetic one.

The ideal plasticizer should have the following qualities: be non-volatile, be completely miscible with a solvent, remain stable throughout processing, have good affinity with the polymer and demonstrate explosophoric properties [77].

Figure 2-25 Empty celluloid combustible container; provided by GD OTS.

Figure 2-26 various mortar rounds (top) [2], Unites States soldier firing a 60 mm mortar in Afghanistan (bottom) [3].

---

[2] Released by Alex Borland under Public Domain license
https://www.publicdomainpictures.net/pictures/140000/velka/army-mortar-bombs.jpg

[3] DoD photo by Staff Sgt. Adam Mancini, U.S. Army. (Released)

https://commons.wikimedia.org/wiki/File:60mm_mortar_round_being_launch.JPG

This file has been identified as being free of known restrictions under copyright law, including all related and neighboring rights.

CHAPTER 3 GLOBAL APPROACH AND METHODOLOGY

Two issues were presented in Chapters 1 and 2: the lack of clean-burning thermoplastic binders, and the lack of nitrogen-rich polymeric binders allowing for reduced erosion. This chapter presents the methodological approach and decision-making process related to the choice of materials required to evaluate the plasticization properties of energetic binders and the methods for manufacturing novel nitrogen-rich binders.

General Dynamics Ordnance and Tactical Systems - Canada Valleyfield (GD OTS) funded this project because the development of thermoformable casings with clean-burning properties and innovation in nitrogen-rich binders are part of their core business.

3.1 Thermoplastic binders

In order to manufacture clean-burning materials with thermoplastic properties, it is necessary to either develop a brand-new thermoplastic material or examine existing, available binders and plasticizers to formulate the proper material.

The material must have the following properties:

- A glass transition temperature below its decomposition temperature
- A linear burning rate allowing the material to burn completely during the ballistic cycle
- A thermochemistry allowing for enough oxygen to burn cleanly without the presence of residues

The glass transition must be low enough to allow for safe processing of the material without running into the autocatalytic decomposition reaction. For example, the celluloid decomposition temperature is that of NC (180 ºC) and the T_g is around from 102 ºC measured DMA.

The linear burning rate must allow for the material to completely burn within the thermal cycle as seen from the pressure-time curves presented in the last chapter. This is a complex calculation, as this pressure-time curve is itself a function of the specific weapon system and other conditions such as the amount of propellant used and the temperature at which the propellant is fired.

Finally, the material must be able to sustain its own combustion without generating residues.

In the case of celluloid, for example, when fired in a 100 cm^{-3} CV at a loading density of 0.1 g cm^{-3} (meaning that a charge weight of 10 g is used), 1.6 g of solid carbon residues (16wt%) are generated. When performing thermochemical calculations with CHEETAH V2, it is expected that 11 wt% of solid carbon is generated. Although there is a significant difference between both results, the presence of solid carbon residues can be used when calculating thermodynamically with CHEETAH as a way to predict incomplete combustion.

3.1.1 Material selection

In order to select the materials to be investigated as energetic binders, the following criteria were used for the base polymer and its plasticizer:

- Base polymer
    - Presence of an explosophoric group
    - Availability of the materials
- Plasticizer
    - Presence of an explosophoric group
    - Availability of the materials
    - Small-molecular or low-molecular weight polymer

NC is a key component in many industries (i.e., propellant, lacquer, thermoplastic films). It is readily available in many ranges of viscosity and nitrogen content, is inexpensive, and is proven to have affinities with various plasticizers.

For these reasons, NC is the polymer of choice.

In selecting plasticizers, Chapter 2 defines the ideal plasticizer as having:

- Good compatibility with the base polymer
- Capacity to reduce T_g of the base polymer
- Capacity to increase elongation at break
- Capacity to reduce tensile modulus

- Low migration behaviour
- Presence of explosophoric groups

Nitroglycerine is a well-known plasticizer for NC. It is a low-molecular weight molecule presenting toxicity and migration issues, but its high OB makes it an ideal energetic plasticizer. It retails around USD 6 per kg and is readily available in Canada. However, transportation of nitroglycerine is complex due to its hazard transport classification. It can either be transported as a Class 4.1 (UN 3319) when desensitized in a solid with 2 wt% < NG < 10 wt%, or as a Class 3 (UN 3343 or UN 3357) when desensitized in liquid with no more than 30 wt% NG.

GAP is a low molecular weight azido polymer. It has been evaluated as part of a binder formulation in propellant and rocket propulsion when compounded with NC, but never as a sole plasticizer for a thermoplastic binder. Although it has a poor OB due to the sole presence of the ether group, the %N of GAP makes it interesting as a low-molecular weight polymeric plasticizer. The main drawback of GAP is its cost; it is a niche product that retails at close to USD 600 per kg. Transportation must also be considered as it is a Class 1.3C explosive material.

3.1.2 Sample preparation and characterisations

To mitigate transportation issues, it was decided that the samples would be manufactured at GD OTS. GD OTS is a gun propellant manufacturer specialised in the manufacturing of single-, double- and multiple-based extruded propellants. NC, NG and GAP are readily available and can be safely transported on site for the manufacturing of plasticized samples. GD OTS is also equipped with an analytical laboratory allowing for the characterisation of the samples.

Samples were prepared using the cast-film method in concentrations of up to 40 wt% in NG, GAP and mixtures of GAP and NG to evaluate the influence of plasticizer concentration on phase behaviour, glass transition and mechanical properties. Phase behaviour was evaluated using SEM, glass transition using DMA and mechanical properties using tensile testing. Sample preparation, characterisation and results are covered in Chapter 4

3.1.3 Evaluation of combustion

The film-casting method for the preparation of samples is not appropriate to evaluate the LBR of plasticized NC with GAP, NG or a mixture of both plasticizers. As previously mentioned, LBR is

measured in CV using a pressure-time curve, the geometrical measurement and the thermodynamic data of the tested formulation. When ignition occurs, it is assumed that all the grains ignite and burn simultaneously. This, however, is not the case, as some grains will ignite sooner than others. Following this logic, the best possible condition would be to have a single grain burning at a time in the closed vessel. Nevertheless, this is impractical, because a 100 cm^{-3} CV loading density of 0.2 g cm^{-3} would require a 20 g of propellant. The propellants density is approximately 1.5 g cm^{-3} and the inner diameter dimension of a 100 cm^{-3} CV at GD OTS is 6.3 cm, requiring that the grain be no less than 1.7 cm in diameter. In order for the fibrous structure of NC to be used as a binder, it must first be altered using solvent, converting it into a usable binder. It is typical to extrude between 12 and 50 wt% of solvent in the formulation, depending on the concentration of plasticizer in the propellant formulation. For this reason, a large propellant grain would require a long drying time and uneven geometrical measurements would be obtained because of the shrink associated to the solvent evaporation. Although not ideal, smaller cylindrical formulations are a good avenue to evaluate LBR in CV.

Prior work at the Valcartier Research Center of Defence Research and Development Canada showed that combining GAP and NC using the solvent extrusion process failed to produce the desired results due to the highly viscoelastic nature of the material. Although a heated die would have solved that problem, this capacity was unavailable at the time of the experiment.

GD OTS was equipped with similar equipment but lacked the capacity to manufacture small quantities of test propellant. The smallest sigma blade mixer available was suited to handle 8 kg of material. At USD 600, a 40 wt% GAP batch would have cost nearly USD 2,000 in raw materials alone. For this reason, it was decided to develop the capacity to manufacture small quantities of GAP/NC blends.

Rather than use a smaller sigma blade mixer, a two-roll mill similar to that utilized in the solvent-less propellant process was used. The roll mill was built in China and arrived at the Valleyfield plant in early 2017. Prior to using the equipment, it was first necessary to perform a safety analysis and assess the CSA electrical requirements.

The safety analysis required the construction of a specialised enclosure to protect the operator in the event of a fire. A model of the twin-roll mill was built out of sheet metal and equipped with a polycarbonate shield and protective transparent rubber layer (Figure 3-1).

The guard was placed in a controlled enclosure at the GD OTS burning ground and wired with ignition pellets. A sample was tested with 100, 330, 575 and 800 g of celluloid and double-base propellant. The celluloid formulation was 75 wt% of 11%N NC and 25 wt% of camphor. The double-base formulation was 60 wt% 13.0%N NC and 40 wt% NG. The test was conducted remotely under the supervision of the fire brigade supervisor. The guard reacted as expected, containing the flames in the enclosure (Figure 3-3).

From this investigation, it was concluded that the roll mill would be safe to use with quantities no higher than 100 g of EMs, when equipped with a guard similar to that used in the tested.

The two-roll mill mixer was commissioned on April 4, 2018 (Figure 3-2).

The material preparation using the two-roll mill and cylindrical extruded grains is described in Chapter 5

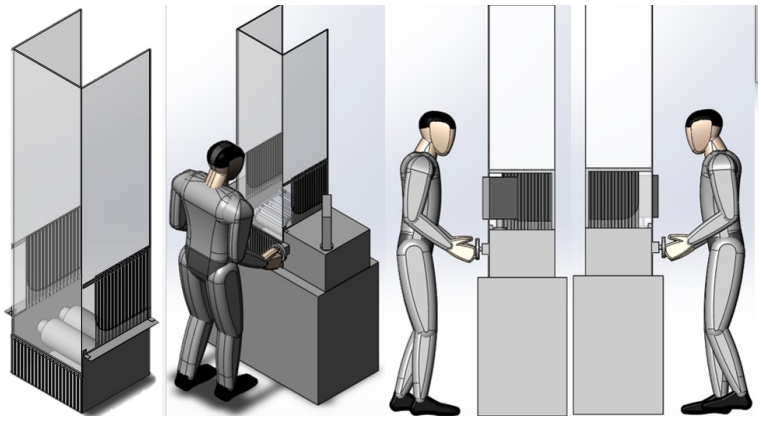

Figure 3-1 From left to right: proposed roll-mill model equipped with safety guard, isometric, right and left view of the roll mill equipped with safety guard.

Figure 3-2 Two-roll mills equipped with a security guard (center), power supply (left) and recirculatory heater (right).

Figure 3-3 Installation of a sheet of double-base propellant and the electrical ignite (top), front (bottom left) and lateral view (bottom right) of the model guard with 100 g of double-base propellant.

3.2 Development of novel azido-based energetic binder

Cellulose can be chemically modified to increase its solubility, thus allowing it to be a useful polymer in binder applications. **Error! Reference source not found.** covered two chemical treatments, nitration and azidation, making cellulose an explosophoric material.

When fully substituted, AC is expected to have a 53.2 %N. This would make it an ideal nitrogen-rich binder, permitting the formation of lower average molecular weight gases comprising mainly N_2, CO and H_2 compared to CO_2, H_2O and N_2 when complete oxidization is obtained. As discussed in Chapter 2, CO and H_2 are erosive gas species in comparison to CO_2 and H_2O, although the low flame temperature and the increase in N_2 allow for reduced flame temperature and reduced gun barrel wear.

For this reason, it was decided that AC would be synthesized in an amount sufficient to conduct a thermochemical analysis of the product and its ballistic characterization in a closed vessel to obtain its LBR contribution when compounded in a typical formulation. AC synthesis, characterisation, compounding in formulation and analysis in CV are presented in Chapter 6.

3.3 Other safety and economic considerations

Other energetic plasticizers and polymers could have been assessed, including TMETN, DEGDN, polyBAMO and polyGLYN. Most of these are not readily available, however, requiring that they be purchased and shipped or synthesized on site.

Transportation regulations for controlled substances are intricate, lengthy, and thereby costly. For instance, it took more than a year to move a 1 kg sample of GAP-5527 from GD OTS Le Gardeur to GD OTS Valleyfield, in order to comply with safety regulations and have the material safely transported. The alternative of synthesizing the material on site was debated, yet this idea was abandoned as performing the synthesis and work up in an industrial, as opposed to a research, setting would have taken months to carry out.

Accordingly, it was decided to concentrate on readily available materials.

3.4 Scientific contribution and resulting articles

This research has led to three scientific articles that have been published or submitted for publication.

The first article, presented in Chapter 4, focuses on the phase transition and the mechanical properties of NC plasticized by GAP and NG. This article is published in *Polymer Engineering and Science*.

The second article, presented in Chapter 5, focuses on the combustion behavior and erosivity properties of NC plasticized by GAP and NG. This article is submitted in *Propellant Explosives and Pyrotechnics*.

The third article, presented in Chapter 6, is devoted to the synthesis of AC and its influence on the combustion properties of a nitrocellulose nitroglycerine-based binders. This article is submitted in *Journal of Energetic Materials*.

CHAPTER 4 ARTICLE 1: PHASE TRANSITIONS AND MECHANICAL PROPERTIES OF NITROCELLULOSE PLASTICIZED BY GLYCIDYL AZIDE POLYMER AND NITROGLYCERINE

Étienne Comtois, Charles Dubois and Basil D. Favis

Published in *Polymer Engineering and Science.*

The aim of this article was to evaluate how a mixture of plasticizers comprised of glycidyl azide (GAP) polymer and nitroglycerine (NG) will affect the thermo mechanical properties of nitrocellulose with a view to manufacture a casing material with thermoplastic properties in a range acceptable for safe processing with lower toxicity.

The scientific contribution of this work is threefold. Firstly, it is demonstrated that GAP will coaless into in spherical droplets when compounded using the solvent casting method. Secondly, using dynamical mechanical analysis, it is found that GAP, as a sole plasticizer, is not capable of perfectly inserting itself between NC polymer chains and therefore does not act as a plasticizer until a high enough concentration is added. A small molecular weight plasticizer, such as NG, has sufficient mobility to situate between and separate the NC chains, allowing GAP to then be inserted and act as a plasticizer. From these findings, a mechanism on the plasticisation of NC with GAP and NG in the presence of solvent was established. Finally, mechanical properties in tensile showed that replacing a significant portion of NG with GAP in the combined GAP-NG plasticizer approach demonstrate that excellent plasticization of NC can be achieved at significantly lower levels of NG while maintaining good mechanical properties.

The supporting information mentioned in this article is presented in Appendix A.

4.1 Abstract

Films of nitrocellulose (NC), glycidyl azide polymer (GAP) and nitroglycerine (NG) have been evaluated using scanning electron microscopy, FTIR, dynamic mechanical analysis and tensile testing. The SEM micrographs demonstrate that, even at low GAP concentration, a portion of GAP will coalesce into spherical domains due to a saturation effect. This is related to the inability of higher molecular weight GAP to effectively situate itself between NC polymer chains. The addition of a small fraction of lower molecular weight NG completely changes this behaviour. DMA

confirms that two transitions are present and can be attributed to a plasticizer rich plase (β), a polymer rich phase (α) and that NC plasticized with GAP is in accordance with the Gordon-Taylor equation. Tensile results show that the addition of a small fraction of NG to a NC/GAP based formulation-increases elongation at break to values similar to that of the NC/NG base formulation. The combination of these two plasticizers, GAP and NG, allows the plasticization of NC at significantly lower environmental and human toxicity levels.

4.2 Introduction

Thermoplastic materials based on nitrocellulose (NC) are used in a number of applications such as combustible containers and as a part of pyrotechnical igniters.

One of these, celluloid, the first thermoplastic material invented by mankind, is manufactured using NC with a nitration level of 11 %N and an inert plasticizer [78]. In comparison, the nitration level of propellant-grade NC ranges between 12.5 and 13.55 %N, and is typically plasticized using low molecular weight nitrate esters such as nitroglycerine (NG), diethylene glycol dinitrate and trimethylolethane trinitrate.

The combination of low nitration NC and inert plasticizer reduces the total energy of the container, lowers its oxygen balance and leads to unclean combustion of the material generating fouling. To mitigate the fouling issue, work has been reported on modifying the celluloid and improving the rapidity at which it burns by foaming the material [79].

Another way to approach the problem is to develop new formulations to improve combustion while preserving the desirable thermoplastic properties.

To do so one can either increase the energetic content of the NC or replace the initial inert plasticizer by an energetic one. The ideal plasticizer should have the following qualities: non-volatile, completely miscible with a solvent, remain stable throughout processing, have good affinity with NC and demonstrate explosophoric properties [77].

As mentioned previously, low molecular weight nitrate esters are commonly used with NC in propulsion applications. Nitrate esters like nitroglycerine (NG) are effective but they also possess many drawbacks such as high migration and stability issues throughout the life cycle of the propellant. Also, NG is toxic to the users and the environment [79-81]. It is therefore important to investigate novel energetic plasticizers for NC.

Recent developments have considered glycidyl azide polymer (GAP) as a potential replacement for nitrate esters in propellant formulations and other solid propulsion applications [72, 82-87]. Work performed in propellant applications was often performed using a curing agent such as di-isocyanate. GAP has also been investigated as a replacement in rocket propellant formulation [59, 88-90]. Work on rocket propulsion have included NC in their formulations, but only at low NC concentration [73].

GAP is synthesized by the direct azidation of polyepichlorohydrin and, akin to the nitro group in nitrate esters, confers to GAP its explosophoric properties.

The plasticization of NC and cellulose derivatives such as cellulose acetate has been extensively covered [63-65, 74, 91-96]. These works show that multiple relaxations are occurring in the material. The reasons for these relaxations are explained differently by various authors and while it is accepted that the α relaxation is dictated by the main polymer chains, the β relaxation origin is debated. It may be associated with the movement of the plasticizers with regards to the NC side groups, of smaller structure units in the main chain such as glucose ring in the case of cellulose acetate, or to the presence of a plasticizer rich phase [67, 74, 92, 93, 97-99].

The objective of this research is to evaluate how a mixture of plasticizers comprised of GAP and NG will affect the thermo mechanical properties of NC with a view to manufacture a material with thermoplastic properties in a range acceptable for safe processing with lower toxicity.

In this work the SEM, DMA and tensile properties of NC plasticized films will be evaluated as a function of the following variables: NC molecular weight, GAP molecular weight, nitrogen content of the nitrocellulose and the addition of a low molecular weight nitrate ester plasticiser (NG).

Nitrocellulose, nitroglycerine and glycidyl azide polymer chemical structures are available in supporting information Figure S1.

4.3 Experimental

4.3.1 Materials

Low viscosity, low nitrogen content NC (“NC11%N-LV”, 11.19%N, Mw = 75 kDa, PDI = 2.78) was purchased from Synthesia (Semtin, Czech Republic). High viscosity, low nitrogen content NC (“NC11%-HV”, 11.16 %N, Mw = 203 kDa, PDI = 3.44) was purchased from Sichuan Nitroellulose

Corporation (Luzhou, China). Grade A high viscosity NC ("NC12.5%N-HV", 12.5 %N, Mw = 150 kDa, PDI = 3.57) was purchased from Eurenco (Bergerac, France). Low molecular weight GAP plasticizer ("GAP0700", Mw = 1.1 kDa, PDI = 1.2, OHvalue = 1.27) was purchased from 3M. GAP polyol ("GAP5527", Mw = 5.9 kDa, PDI = 1.2, OHvalue = 2.5-3) was provided by DRDC-RDDC Valcartier and originally produced by 3M (USA). NG was manufactured onsite by General Dynamics Ordnance and Tactical Systems Canada (Salaberry-de-Valleyfield, Canada) using the Biazzi process.

All NCs were received water wet and had to be dehydrated prior to processing. The excess water was removed by rinsing the slurry with a continuous flow of ethanol in a dehydration press. The excess ethanol was removed by applying pressure forming a consolidated block of nitrocellulose. The ethanol-wet NC was broken up in a sigma blade mixer to expose the fibers. The loose NC fibers were placed in a conductive tray and air dried until total volatiles were less than 1 wt% when measured using gas chromatography and Karl Fisher titration.

GAP0700 and GAP5527 were used without further processing.

NG was desensitized in ethyl acetate at a concentration of 30 wt% for safe handling.

4.3.2 Preparation of NC/GAP/NG film

Dry NC was weighed and added to a hermetic container. GAP and desensitized NG solution were weighed and added to a separate beaker. A quantity of ethyl acetate was added to the plasticizer solution and then agitated using a magnetic stirrer. The solution was then added to the dry NC fibers and the container was hermetically sealed. The total concentration of polymer and plasticizer in the solution was set at 5 wt% The container was stored at 60 °C for no less than 7 days and was agitated as often as possible to ensure the good dissolution of the NC fibers.

The solution was cooled to ambient temperature and then cast on large microscopic slides (178 x 127 x 1.2 mm) held in a Teflon mold. The mold was covered to limit evaporation of the solvent and to avoid film warpage. After 7 days the film was firm enough and was removed from the glass slide using a scalpel to delicately peel it off. The film was cut into 10 mm ribbons and then placed in a convection oven set at 73 °C to dry off the solvent. An example of the film is presented in supporting information Figure S2.

For this work the formulation nomenclature of the films is as follows: the nitrogen content of the NC followed by the letter HV and LV for high and low viscosity NC respectively; then the plasticizer type followed by its concentration in parenthesis. As an example "NC12.5%N-HV / NG(10%) / GAP700(10%)" indicates a 12.5%N content of high viscosity NC plasticized with 10 wt% of NG and 10 wt% of GAP700 respectively.

In order to achieve the mechanical properties suitable for applications with structural strength requirements, the plasticizer concentration must be kept below a certain concentration. This concentration was evaluated by mixing a formulation of NC11%N-LV with up to 50 wt% GAP0700. At the highest GAP concentration formulations the material showed signs of exudation. For this reason, a maximum of 40 wt% GAP was evaluated. Unless otherwise specified, all concentrations are given by weight.

4.3.3 Molecular weight determination using gel permeation chromatography

Molecular weight determination of NC11%N-LV, NC11%N-HV, NC12.5%N-HV, GAP0700 and GAP5527 was obtained using a VE 2001 GPCmax from Viscotek. The columns were from Tosoh Bioscience (TSKgel α-2500, TSKgel α-3000, TSKgel α-5000). Detection was performed using a right angle light scattering detector, a low angle light scattering detector and a refractive index (Malvern 270 Dual Detector and Viscotek VE3580). The operating temperature was 40 ^{o}C, sample concentration was 5 mg mL^{-1}, flow rate was 0.8 mL min^{-1} and injection volume was 100 uL. For NCs and GAP5527, the mobile phase was dimethyl formamide (0.01 M LiBr) and the system was calibrated using broad and narrow polymethyl methacrylate standards in multi-detector mode. For GAP0700, the mobile phase was tetrahydrofuran and the system was calibrated with a polystyrene standard using the refractive index signal. Weight average molecular weight and polydispersity index for NCs and GAPs are presented in Table 4-1.

4.3.4 Scanning electron microscopy and image analysis

A 1 cm^2 sample was cast in EpoFix resin and microtomed at ambient temperature using a Leica RM2155 to expose the fresh surface of the sample. The sample was then suspended in dichloromethane at ambient temperature for one hour to leach out any GAP phase if present. Before SEM observation, all the samples were sputter coated with an Au/Pd layer using a Quorum SC7620 Sputter Coater to reduce thermal damage and improve the secondary electron signal to detect

morphology. SEM analysis was performed on a Hitachi TM3000 Tabletop SEM at an accelerating voltage of 15 kV. The dimensions of the leached out phase were obtained using image analysis software (ImageJ) where the SEM micrographs were enhanced using a bandpass filter. The diameter of the leached phase was measured manually using the freehand line tool to obtain the diameter of each feature.

4.3.5 Fourier transform infrared spectroscopy (FTIR)

The FTIR spectrum was obtained using a FTLA2000-104-T from ABB. A few drops of the leached solution was placed on a KBr rectangular window and allowed to evaporate. The spectra were taken in transmission and were used to confirm the chemical composition of the leached phase.

4.3.6 Dynamic mechanical analysis

Samples were cut to a length of 25 mm and mounted in a TA Instrument DMA 850 equipped with film grip. The test was performed from -90 °C to 130 °C to avoid decomposition of the samples and at a heating rate of 3 °C min-1. The amplitude of deformations was kept constant at 0.3 % and at a frequency of 1 Hz. thus staying within the linear viscoelastic region for the samples.

4.3.7 Tensile properties

Tensile testing was carried out using a Instron 6800 equipped with a 2 kN load cell and film grips as per ASTM D882-18 with the exception that the strain rate was set at 0.1 min-1 for all samples. The measurements were performed at ambient temperature (23 ± 2 ºC) and the samples were allowed to condition in a desiccator for no less than 48 hours. The values reported were averaged from five specimens or more.

4.4 Results and Discussion

4.4.1 SEM of NC/GAP/NG film

The SEM micrographs of NC11%N-LV, NC11%N-HV and NC12.5%N-HV plasticized with GAP0700 as well as NC12.5%N-HV plasticized with GAP5527 and with a mixture of GAP-700 and NG are presented in Figure 4-1. The total leached surface, as a percentage of total surface, is tabulated in Table 4-2.

The SEM micrographs show that discrete spherical phases are leached out from the material. The FTIR spectrum confirms that they are comprised of pure GAP as the leached solution does not present an NC associated absorption band at 1650 cm^{-1}, but presents a strong absorption band at 2100 cm^{-1} associated with the azide functionality of GAP. The FTIR spectrum is given in supporting information Figure S3.

4.4.1.1 Influence of GAP concentration

The results in Table 4-2 show that an increase in the concentration of GAP0700 in NC11%N-LV leads to an increase in the presence of GAP0700 droplets in the solvent cast film. Leached out plasticizer droplets are present even at concentrations below 20 wt% with a total surface occupied being 0.6 % of the total surface covered at 10 wt% in GAP0700. Beyond 20 wt% the leached surface area increases significantly and it follows an exponential progression with a total surface occupied of 0.9, 2.3 and 6.5 % for 20, 30 and 40 wt% respectively in GAP0700. A graphical representation of the increase in surface area is available in supporting information Figure S4.

Assuming that the spheres are uniformly dispersed in the material, the leached surface should have a relationship to the volume fraction of GAP phase in the material. This is to be used later in this work when explaining DMA results.

4.4.1.2 Influence of NC, GAP Mw and %N

From Table 4-2 it can be seen that NC plasticized at 40 wt% shows similar values in total leached surface for all NCs, indicating that for all of them, GAP is leaching out. A graphical representation of the leached surface for NC11%N-LV, NC11%N-HV, NC12.5%N-HV plasticized with GAP0700 and GAP5527 is given in supporting information Figure S5. This is an indication that GAP is a poor plasticizer for nitrocellulose and does not insert itself between the NC chains. Therefore, the plasticizer mobility is high resulting in a tendency to exude out of the samples. This also explains the smaller leached surface obtained by GAP5527. Because it is of higher molecular weight (see Table 1), its mobility is reduced and will coalesce in smaller domains.

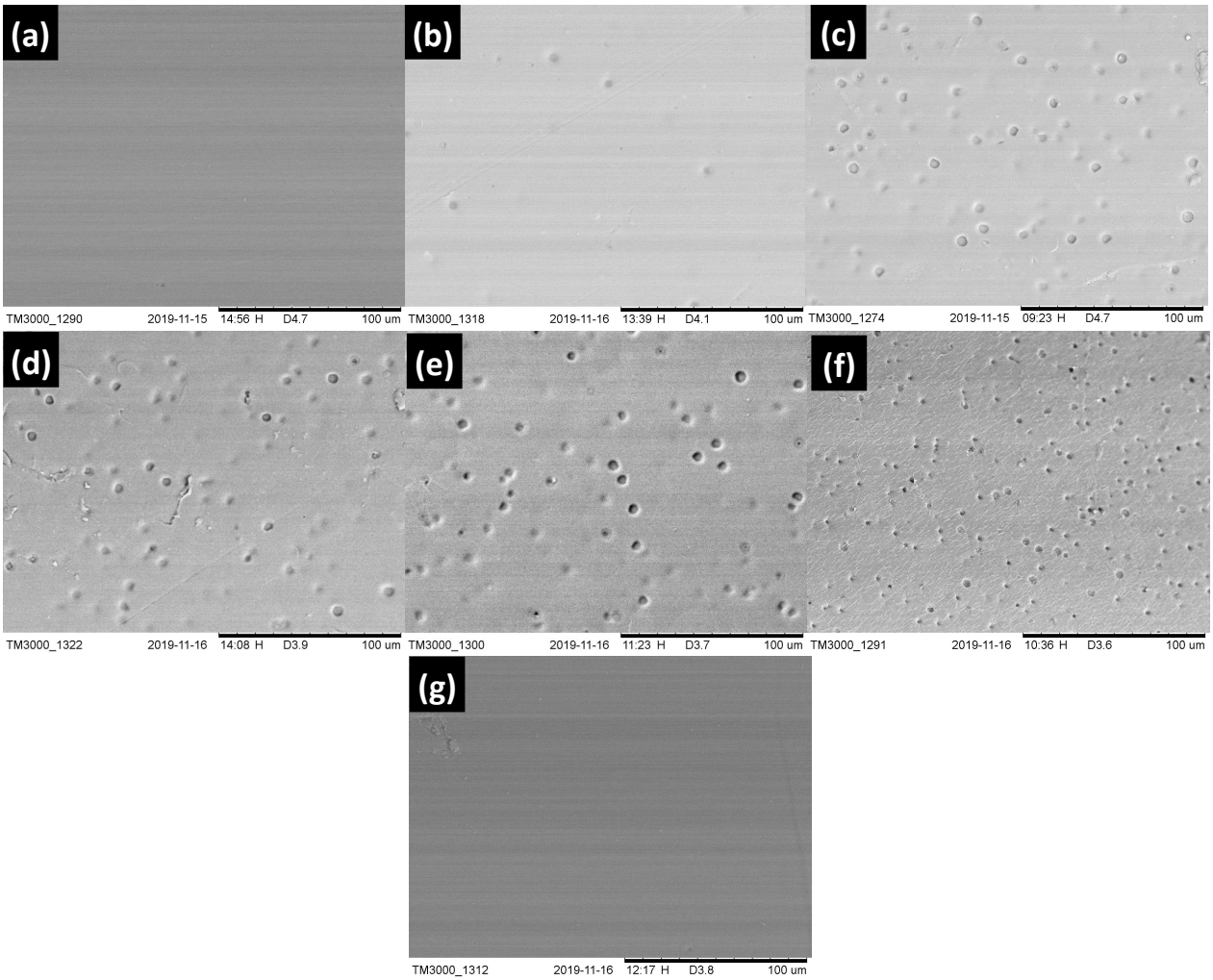

Figure 4-1 SEM micrographs of NC11 %N-LV unplasticized (a), NC11%N-LV/GAP0700(20%) (b), NC11%N-LV/GAP0700(40%) (c), NC11%N-HV/GAP0700(40%) (d), NC11%N-HV/GAP400(40%) (e), NC12.5%N-HV/GAP5527 (40%) (f) and NC12.5%N-HV/NG(10%)/GAP0700(30%) (g). The black bar in each micrographs represents a distance of 100 μm.

Table 4-1 Mw and polydispersity index (PDI) of NCs and GAPs measured by GPC. NG is from literature [1].

ID	Mw [kDa]	PDI
NC11%N-LV	75	2.78
NC11%N-HV	203	3.44
NC12.5%N-HV	150	3.57
GAP5527	5.9	1.24
GAP0700	1.1	1.20
NG	0.23	1.00

Table 4-2 Average surface of leached GAP phase as a percentage of total surface.

ID	% Surf.
NC11%N-LV / GAP0700 (0%)	0
NC11%N-LV / GAP0700 (10%)	0.6
NC11%N-LV / GAP0700 (20%)	0.9
NC11%N-LV / GAP0700 (30%)	2.3
NC11%N-LV / GAP0700 (40%)	6.5
NC11%N-HV / GAP700 (40%)	5.8
NC12.5%N-HV / GAP700 (40%)	6.8
NC12.5%N-HV / GAP5527 (40%)	5.3
NC12.5%N-HV / NG (10%) /GAP0700 (30%)	0

4.4.1.3 Influence of the addition of NG

A key point to notice is that no droplets of GAP are observed by SEM when a portion of NG is present in addition to GAP. In order to explain this phenomenon, the plasticization mechanism must be explained.

Two plasticization mechanisms have been proposed for the plasticization of NC in the literature. One mechanism can be applied for fibrous NC in the presence of a plasticizer and the other where both NC and the plasticizer are mixed in a solvent.

The plasticization of NC as fibrous material considers that plasticizers such as NG and dibutyl phthalate (DBP) are absorbed onto the microfibrilar/microcrystalline sites on the NC into layers. As concentration increases, the addition of these layers leads to a liquid interface between the micro fibrils thus allowing motion within the polymer [91].

The plasticization of NC and DBP in a solvent states that the hydroxyl group of NC can form hydrogen bonding with the carbonyl group of DBP [100]. It also shows that the presence of a solvent acts as a compatibilizer and allows for the mobility of various plasticizers in the material [101]. NG, in comparison to DBP does not have the capability to form hydrogen bonds with the NC hydroxyl group [100, 102]. Thus, it an be assumed that the plasticization property of NG is caused by Vander Waal's forces or weak chemisorption [65].

For GAP, although it can form hydrogen bonds with the hydroxyl group of NC, the steric hindrance cause by the azide and the large molecular weight of the plasticizer will likely stop such interaction. This hypothesis is in line with the SEM observations as no significant difference can be observed between the total leached surface of all sample as a function of NC%N.

From this hypothesis, a mechanism for our NC/GAP/NG system can be explained as follows. At high concentration of ethyl acetate, the viscosity of the solution is such that the polymer and plasticizers are allowed to move freely with regard to each another. In the absence of NG, as solvent evaporates, the distance between the polymer chain and the plasticizer decreases and repulsive interactions begin to form allowing for a discrete liquid GAP phase to coalesce forming a spherical pure GAP domain. In the presence of NG, the low molecular weight plasticizer allows GAP to insert itself between NC polymer chains and allows GAP to interact with it without the presence of leaching.

Similar results have been observed with cellulose acetate and polyvinyl alcohol when compatibilized with glycerol and triacetine [66].

4.4.2 DMA Analysis

In Figure 4-2 the E', E'' and Tan δ are measured at a frequency of 1 Hz, as a function of temperature, for non-plasticized and plasticized 11%N-HV at 0, 10, 20, 30 and 40 wt% with GAP0700. The data shows that two relaxations occur in the material.

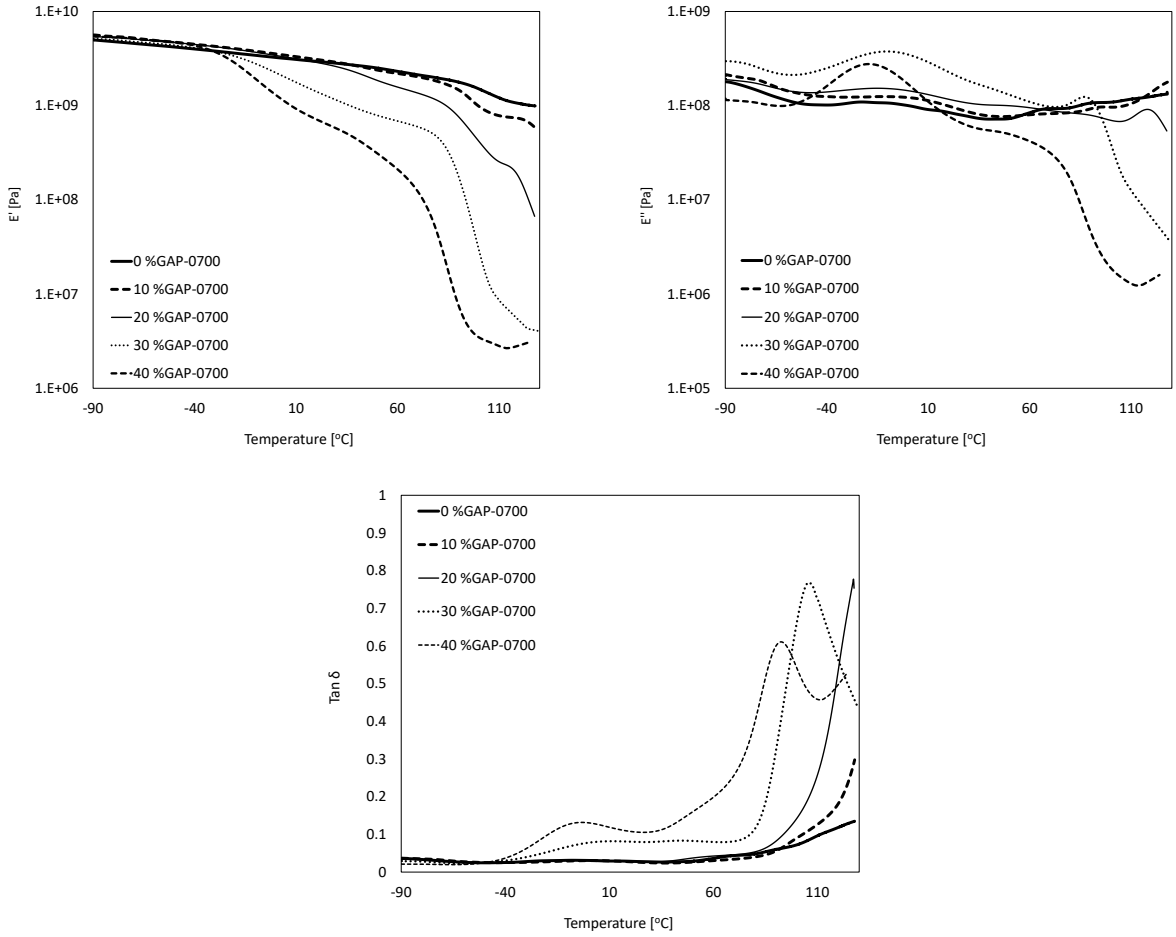

Figure 4-2 Influence of GAP0700 concentration on E' (top left), E'' (top right) and Tan δ (bottom) for NC11%N-HV.

Nitrocellulose consists of rigid chains presenting a single T_g close to its decomposition temperature of 180 ºC [44]. When plasticized, it presents multiple relaxations [63, 64, 94]. The α relaxation, first of two main transitions, appears above 50 ºC and it indicates the beginning of segmental movement of the NC main chain. The β relaxation occurs below 10 ºC and its significance is debated. It may be associated with the movement of the plasticizers with regards to NC sidegroups, of smaller structural units in the main chain such as the glucose ring in the case of cellulose acetate, or with the presence of a plasticizer-rich phase as proposed by work on thermoplastic starch [63, 74, 95, 103]. Starch-glycerol films are partially miscible systems giving rise to a polymer-rich phase and plasticizer-rich phase at concentrations higher than 30 wt% in glycerol [67-70].

From Figure 4-2, the β relaxation is only present beyond 20 %. of GAP0700. The α relaxation is present for 30 and 40 wt%, but could not be obtained from Tan δ at 0 and 10 wt% due to safety concerns (the transition phase is very close to the onset of thermal decomposition).

Using Figure 4-2 and literature values, it is observed that the T_g of a mixture of NC and GAP is in agreement with the Gordon-Taylor equation (4.1). The results are presented in supporting information Figure S6 [3, 44].

$$T_{g,mix} \approx \frac{\left(w_1 T_{g1} + K w_2 T_{g2}\right)}{\left(w_1 + K w_2\right)} \qquad (4.1)$$

Where w_1, w_2, T_{g1}, T_{g2} and K are respectively the weight fraction of the polymer of interest, their glass transition and the adjustable parameter (K = 0.56).

The fact that the mixture is in agreement with the Gordon-Taylor equation would appear to indicate that the system is showing good miscibility between the two polymers. The leach out is caused by an excess of GAP and is expelled as solvent is evaporated.

It should be noted that the observed droplets were found to be pure GAP by FTIR analysis and have a reported T_g of -45 ºC and -56 ºC respectively for GAP5527 and GAP0700 [57]. As shown in Figure 4-2, no transition was observed below -40 °C indicating that the GAP droplets do not affect the macroscopic thermo mechanical behaviour of the material.

Different NCs plasticized under different conditions were studied to confirm the origin of the relaxation.

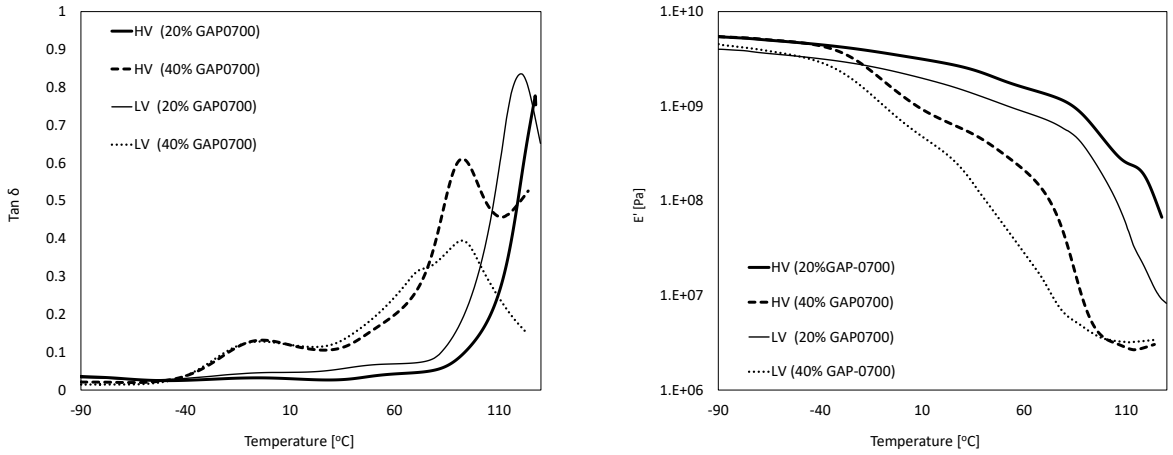

Figure 4-3 Influence of NC Mw and GAP0700 concentration on Tan δ (left) and E' (right) for NC11%N-LV and NC11%N-HV.

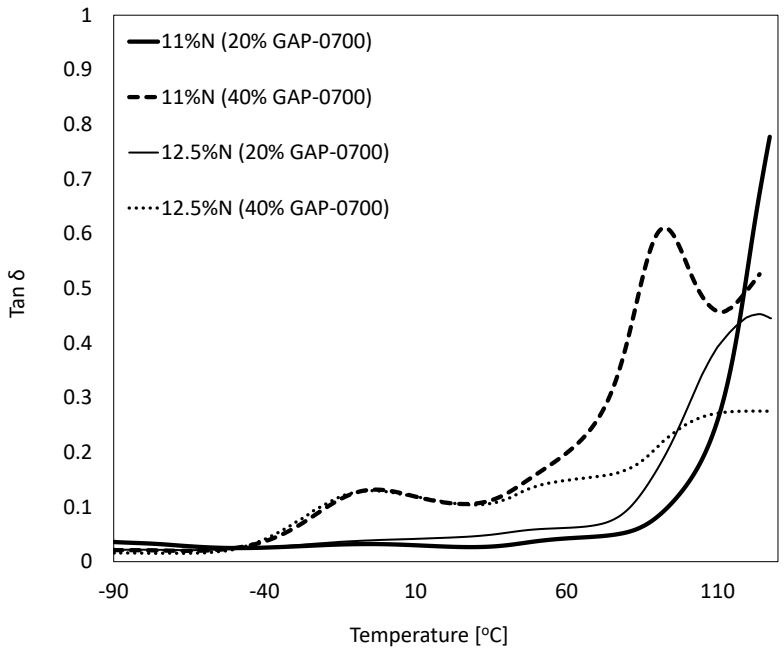

Figure 4-4 Influence of %N and GAP0700 concentration on Tan δ for NC11%N-HV and NC12.5%N-HV.

From Figure 4-3, Tan δ is obtained for two NC samples (NC11%N-LV and NC11%N-HV) with identical nitrogen content but different molecular weight, both plasticized at 20 and 40 wt% of GAP0700. The α relaxation peak temperature is lowered at low GAP concentration meaning that the NC viscosity dictates the overall motion of the chain and that no distinct phases are present below 20 wt% At high concentration, the β relaxation is not affected by the molecular weight of the NC as both curves nearly overlap, an indication that the β relaxation is caused by the plasticizer-rich phase. The α relaxation is lower and is explained by the low molecular weight of the NC as seen in the E' curve (Figure 4-3) and the absence of a rubbery plateau. Also one can see that, when compared at 20 wt% GAP the low molecular weight NC appears to be better plasticized with GAP as the α relaxation is shifted 10 ^{o}C lower than the high molecular weigh NC, indicating that the GAP capacity to insert itself between the NC chains is increased.

From Figure 4-4 the Tan δ is obtained for two high viscosity NC, having different nitrogen contents: NC11%N-HV and NC12.5%N-HV. Both are plasticized at 20 wt% and 40 wt% with GAP0700.

At low GAP concentration, the temperature at the onset of the α relaxation is observed at a lower temperature for the high nitrogen content NC when compared to the low nitrogen content NC. This indicates that the overall chain of NC has more mobility and can initiate large amplitude motions at a lower energy level.

One explanation is that on average every anhydroglucose unit (AGU) nitrated at a nitrogen value of 11 %N will retain 1 hydroxyl group compared to 0.57 when nitrated to 12.5 %N. This reduces the formation of hydrogen bonds within the molecule reducing the energy needed to initiate large chain deformation.

At high GAP concentration, the β relaxations are unchanged and overlapping, showing that the plasticizer-rich phase is present and is not influenced by the %N. A shoulder (β') between the β and α relaxation appears for the low nitrogen content NC. This shoulder is associated with an overlap between the plasticizer rich β relaxation and the main α relaxation associated with polymer rich phase [104].

From Figure 4-5 the Tan δ is obtained for NC11%N-HV plasticized at 20 wt% and 40 wt% with GAP0700 and GAP5527.

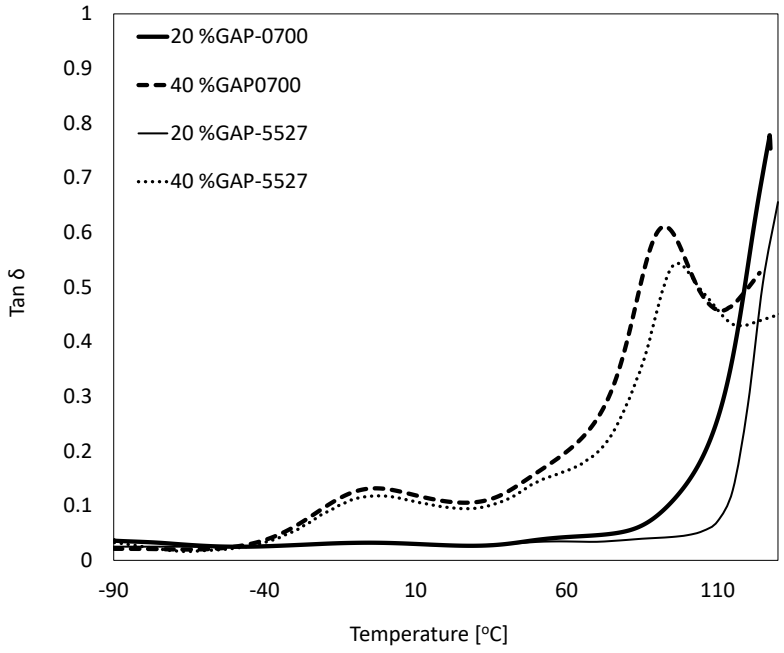

Figure 4-5 Influence of GAP Mw and GAP concentration on Tan δ for NC11%N-HV.

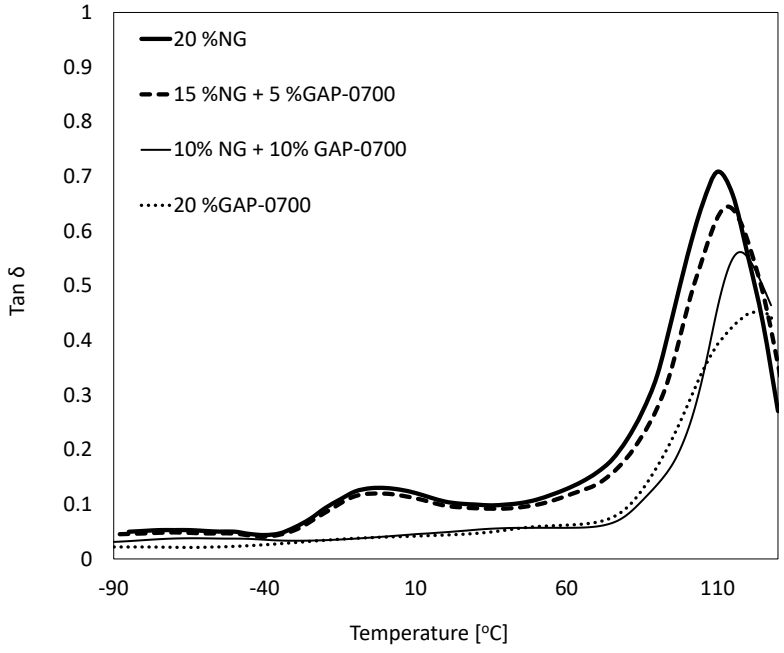

Figure 4-6 Influence of NG and GAP0700 concentration on Tan δ for NC12.5%N-HV.

At low GAP concentration, the Tan δ peaks associated to the α relaxation are both above 130 ºC and could not be recorded, but the earlier onset for the GAP0700 (Mw = 1.1 kDa) indicates that the relaxation occurs sooner than for high molecular weight GAP5527 (Mw = 5.9 kDa). These results indicate that the GAP molecular weight plays a role on the onset of motion of long chains in the polymer.

At high GAP concentration, the associated α relaxation increases by 5ºC for GAP5527 and the height of the peak is lowered. The β relaxation is slightly lower for GAP5527, while it does not show changes as a function of NC Mw and NC %N. This demonstrates that the β relaxation associated plasticizer-rich phase is affected by the plasticizer type and formulation and confirms that this relaxation is associated with the plasticizer–rich phase.

From Figure 4-6 the Tan δ is obtained for NC12.5%N-HV plasticized at a constant concentration of 20 wt% with increasing concentration of NG (0, 5, 10 and 20 wt%) and it is observed that the α relaxation is shifted towards the lower temperature linearly as NG concentration increases. This is expected as NG is known to be an effective plasticizer for NC (Figure 4-7).

No β relaxation is observable before the addition of 15 wt% of NG showing that the material is comprised of a single phase. At 15 and 20 wt% of NG the β relaxation is observed indicating the presence of a plasticizer-rich and polymer-rich phase.

The influence of a low molecular weight plasticizer demonstrates that the β relaxation is caused by the plasticizer-rich phase in the material.

The DMA results for GAP in NC show that it respects the Gordon-Taylor equation. By itself, this could be interpreted as indicating that GAP has a good affinity with NC and could be considered to be acting as a good plasticizer. However, signs to the contrary are also seen. In order to obtain plasticization, 30 and 40 wt% of GAP must be added as compared to 20 wt% of NG. One can also see the influence of GAP and NC molecular weight on the α and β relaxation and furthermore exudation of pure spherical GAP phase occurs at all concentrations. Taken together, this indicates that GAP is not effectively plasticizing NC polymer chains.

To understand these conflicting observations, it needs to be emphasized that a T_g measurement by DMA is sensitive to a certain limit in scale and that ultimately it is a measure of dispersion and not a measure of true miscibility at the individual molecular chain level as demonstrated in the work

of Schultz & Young when studying the influence of annealing of polystyrene and polymethyl methacrylate blends [105]. It is most likely, in the context of NC plasticized with GAP, that this high molecular weight plasticizer has difficulty inserting itself between the NC chains, but forms domains small enough that a single transition is observed in DMA. This is corroborated by the observations in Figure 4-3 and Figure 4-4, where it can be seen that a higher molecular weight NC proves to be more difficult to plasticize and that a higher molecular weight GAP is less apt at plasticizing NC.

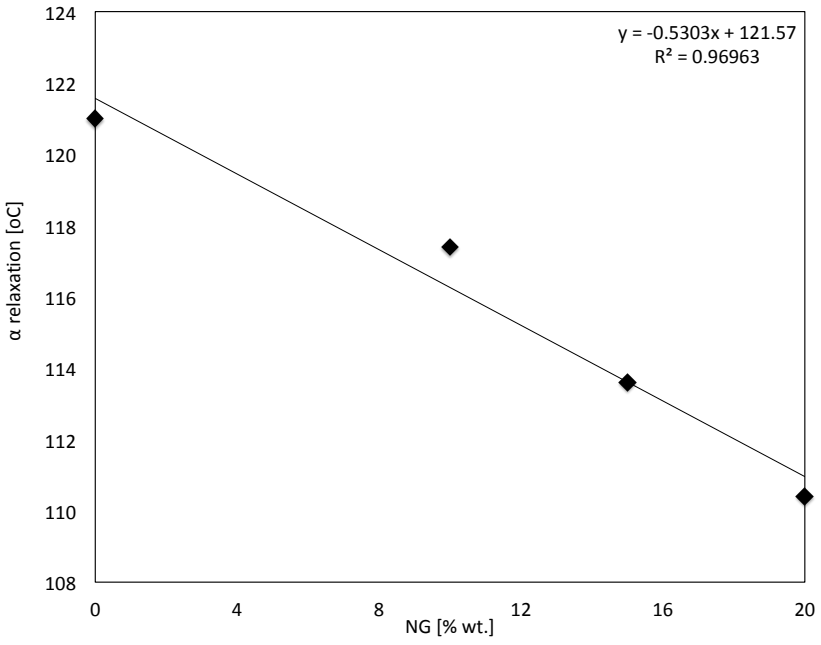

Figure 4-7 Tan δ maxima associated with the α relaxation as a function of NG concentration at constant plasticizer concentration (NG + GAP = 20 wt%).

Importantly, from DMA results, a mixture of GAP and NG show signs that good plasticization can be obtained by replacing a portion of GAP with NG as seen in Figure 4-6. This is a good indication again that the higher molecular weight GAP alone lacks the ability to insert itself perfectly between polymer chains when compared to the small molecular weight NG plasticizer (see Table 1). This improvement in plasticization, through the combined use of GAP and NG, is caused by the ability of lower molecular weight NG initially to separate the NC chains which then allows for an

increased capacity of GAP to insert itself in-between the NC polymer chains. This now allows GAP to act as a good plasticizer as confirmed in the DMA results and from the absence of any plasticizer exudation.

4.4.3 Tensile properties of NC/GAP/NG film

Films prepared by solvent casting were evaluated by tensile testing in order to obtain the tensile modulus, maximum stress, elongation at break and toughness of different NC plasticized with GAP. Film samples plasticized with NG were also evaluated as well as film plasticized with a mixture of GAP and NG to obtain a comparison between an efficient, a non-efficient plasticizer and a mixture of plasticizers. For this work, the lower molecular weight GAP0700 is chosen as it is expected to be a better plasticizer.

For this work, toughness is defined as the area under the stress-strain curve.

From Figure 4-8, one interesting point is that the toughness of NC11%-LV plasticized at 30 wt% is superior to that of 20 wt% and 40 wt% This is evidenced by the increase in elongation at break of the material since at that concentration both high and low nitrogen content NC exhibit the same lower elongation at break and ultimate stress.

When comparing NC12.5%N-HV plasticized at 0, 10, 20, 30 and 40 wt% of GAP0700 or NG, it can be seen that NG acts as a good plasticizer from 0 to 20% by reducing the tensile modulus and improving elongation at break as typically expected (Figure 4-9). For this reason it was decided to mix the two plasticizers so that the total concentration of plasticizer by weight is equal to 20 or 40 wt% and where NG is added by increments of 10 wt% Similar results have been obtained in compression on propellant formulations where binders comprised of NC12.6%N and cellulose acetate are plasticized with a triacetine and GAP at various concentrations [83].

From Figure 4-10 it is seen that replacing a portion of GAP with NG allows for increased mechanical properties. At 20 wt% the addition of NG allows for the β relaxation to occur which reduces tensile modulus, increases elongation at break and consequently increases toughness. At 40 wt%, the β relaxation is already present for both the GAP and NG plasticizer system and therefore no change is observed in the modulus.

When comparing NC plasticized with 20 wt% NG (Figure 4-9) and NC plasticized with a mixture of 10 wt% of GAP0700 and 10 wt% of NG (Figure 4-10), it can be seen that both formulations exhibit similar mechanical properties.

From the combined tensile and DMA results, one can confirm that GAP alone is not a good plasticizer for NC. To obtain a plasticization effect, 30 and 40 wt% of GAP must be added to the formulation, which coincides with the presence of the β relaxation observed in DMA. From the SEM micrographs shown in Figure 4-1, it is shown that at those concentrations GAP is exuding from the material. Tensile, DMA and SEM results show that the addition of NG to GAP improves the ability of GAP to efficiently plasticize NC. This confirms the understanding that higher molecular weight GAP (1.1 and 5.9 kDa), as a sole plasticizer, is not capable of perfectly inserting itself between NC polymer chains and therefore does not act as a plasticizer until a high enough concentration is added. A small molecular weight plasticizer, such as NG (0.2 kDa), has sufficient mobility to situate between and separate the NC chains, allowing GAP to then be inserted and act as a plasticizer.

This capability of replacing a significant portion of NG with GAP in the combined GAP-NG plasticizer approach is an excellent outcome and appears to demonstrate that excellent plasticization of NC can be achieved at significantly lower levels of NG while maintaining good mechanical properties. Since NG has a number of serious environmental/toxicity consequences this approach, which could reduce NG concentration by half and still achieve equivalent levels of plasticization, could have significant potential for NC plasticization.

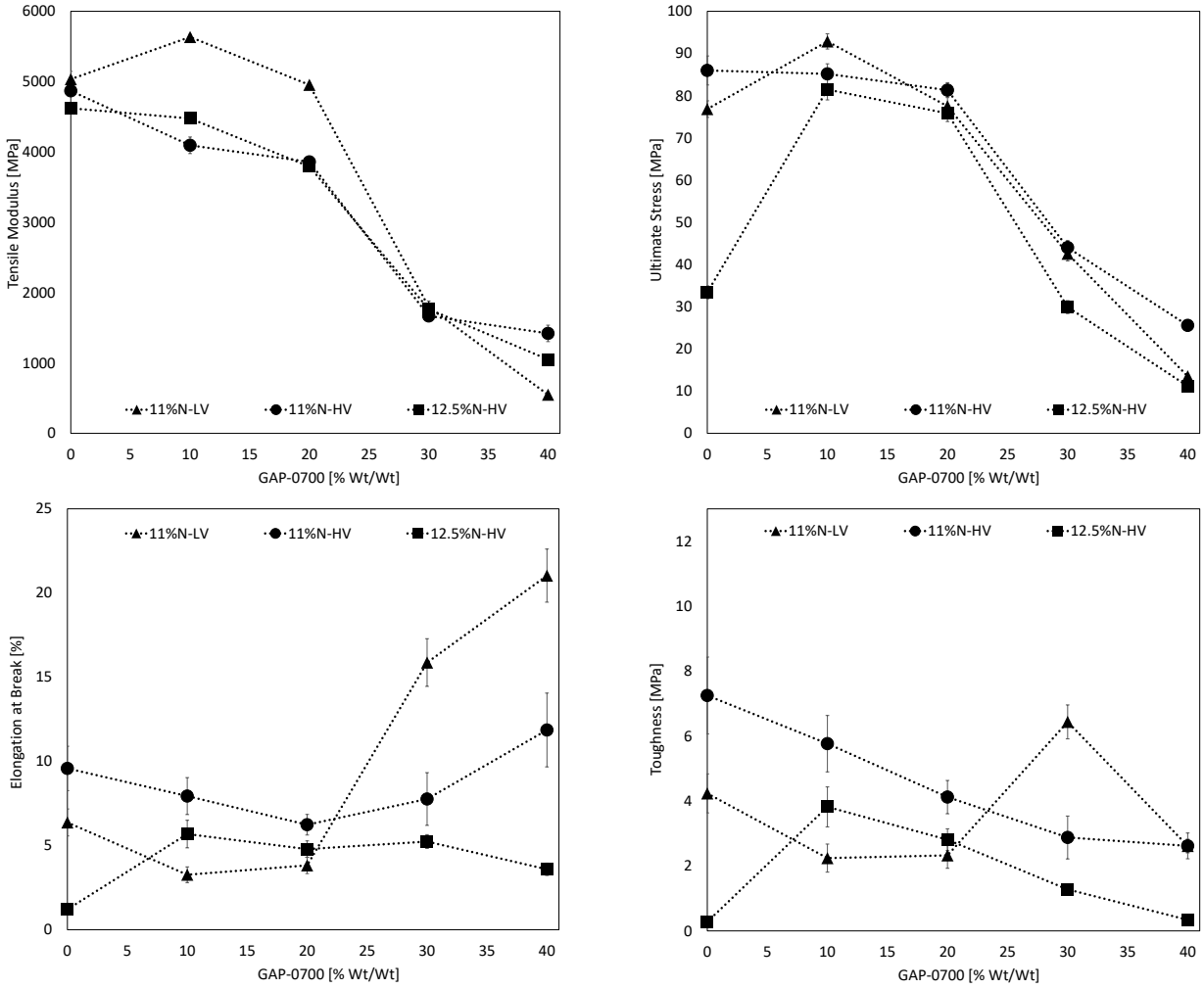

Figure 4-8 Tensile modulus, ultimate stress, elongation at break and toughness for NC11%N-LV, NC11%N-HV and NC12,5%N-HV plasticized at 0, 10, 20, 30 and 40 wt% GAP0700.

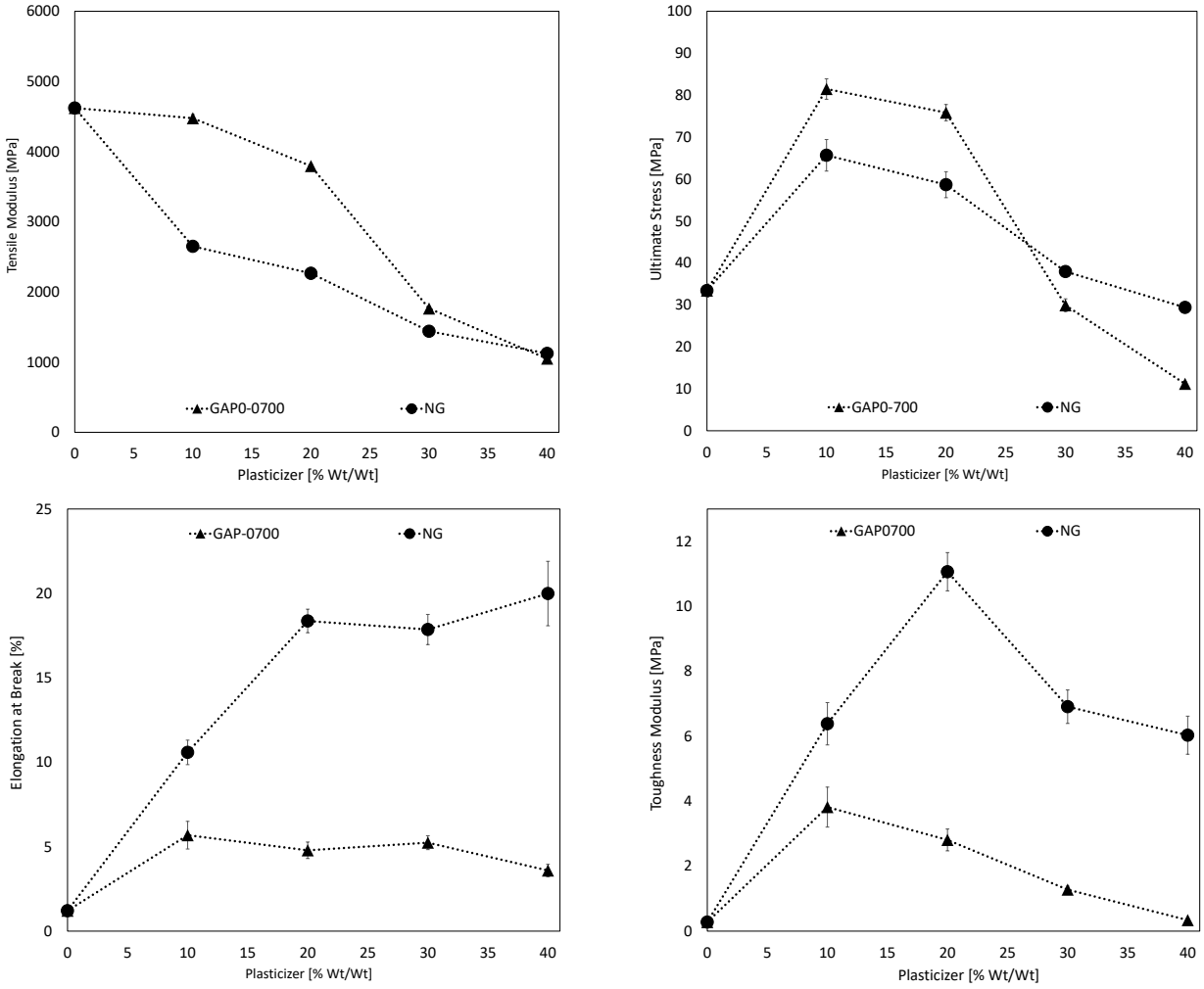

Figure 4-9 Tensile modulus, ultimate stress, elongation at break and toughness for NC12.5%N-HV plasticized at 0, 10, 20, 30 and 40 wt% GAP0700 and NG.

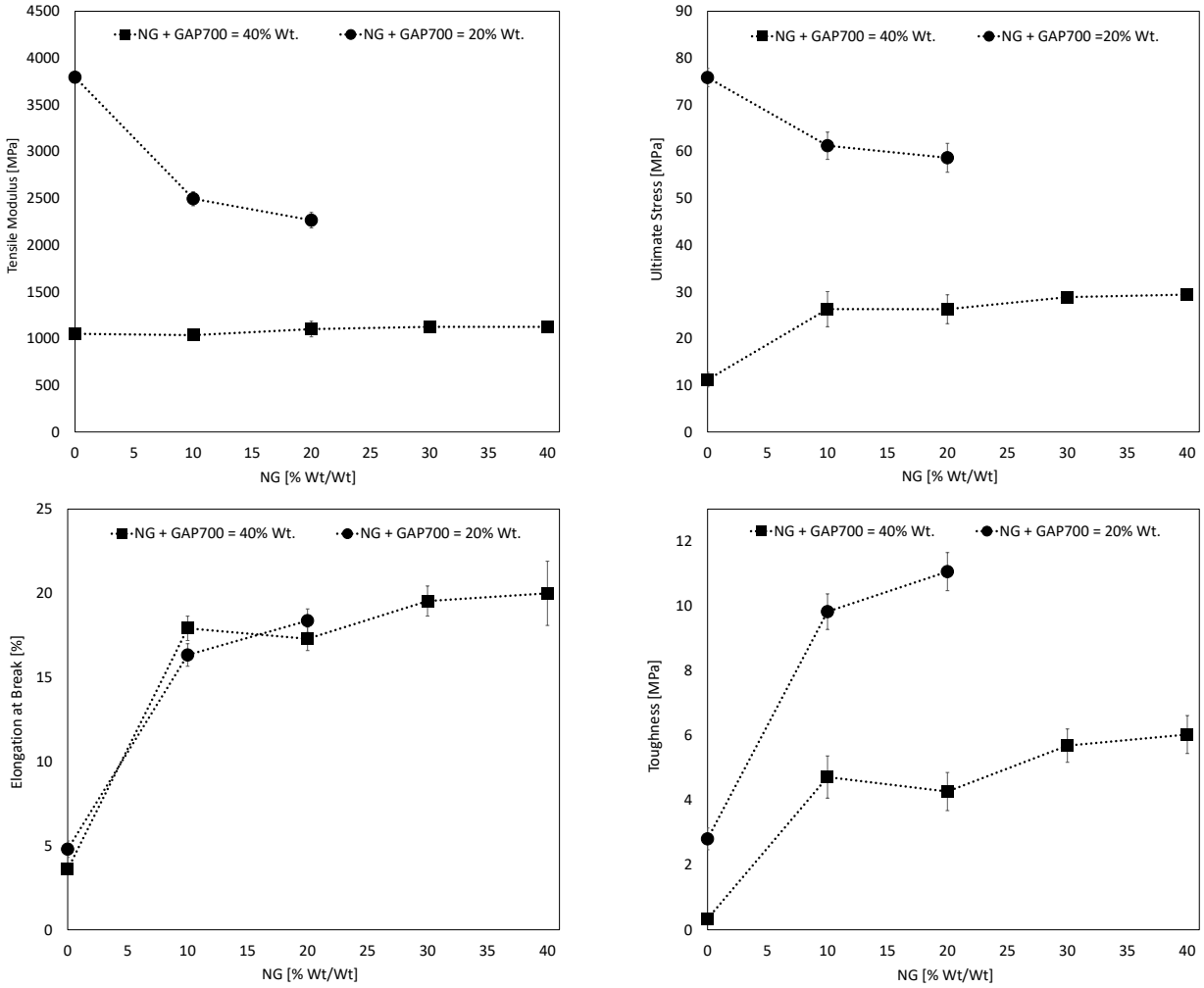

Figure 4-10 Tensile modulus, ultimate stress, elongation at break and toughness for NC12.5%N HV plasticized at a total concentration in plasticizer of 20 and 40 wt and the addition of GAP0700.

4.5 Conclusion

This paper reports on the plasticisation of NC with GAP, NG or a mixture of GAP and NG and on the improvement of the mechanical properties of NC plasticized with GAP by the addition of NG.

Although DMA is in accordance with the Gordon-Taylor equation, it is found that a large quantity of GAP must be added to observe the presence of a plasticizer rich phase and a reduction in the tensile modulus of the plasticized NC and that SEM micrographs show exudation of pure liquid GAP droplets in the material at concentration as low as 10 wt%

The addition of NG to NC plasticized with GAP eliminates the presence of exudation, allows for the presence of a plasticizer-rich phase and for a reduction in tensile modulus at lower GAP concentration. This confirms the understanding that GAP as a sole plasticizer, is not capable of perfectly inserting itself in between NC polymer chains and therefore does not act as a plasticizer until a high enough concentration is added. A small molecular weight plasticizer, such as NG, has sufficient mobility to situate between and separate the NC chains, allowing GAP to then be inserted and act as a plasticizer.

This capability of replacing a significant portion of NG with GAP in the combined GAP-NG plasticizer approach is an excellent outcome and appears to demonstrate that excellent plasticization of NC can be achieved at significantly lower levels of NG while maintaining good mechanical properties. Since NG has a number of serious environmental/toxicity consequences, this approach, which could reduce NG concentration by half and still achieve equivalent levels of plasticization, could have significant potential for NC plasticization.

Future work will look at the combustion property of NC plasticized with NG and GAP as well as the manufacturing of sheets of the material to evaluate thermoforming capabilities.

4.6 Acknowledgements

The authors would like to thank General Dynamics Canada Valleyfield for providing the time, materials, funding and equipment needed for the manufacturing and characterisation of the samples. The authors would also like to thank Mr. Alain Gagnon, Mrs. Fanny Charest, Mr. Ian Levac, Mr. Pierre-Yves Paradis, Mr. Marc Boileau and Mr. Daniel Lepage from GDOTS for their time and effort in making this project a reality.

CHAPTER 5 ARTICLE 2: LINEAR BURNING RATE AND EROSIVITY PROPERTIES OF NITROCELLULOSE PROPELLANT FORMULATIONS PLASTICIZED BY GLYCIDYL AZIDE POLYMER AND NITROGLYCERINE

Étienne Comtois, Charles Dubois and Basil D. Favis

Submitted to *Propellants, Explosives, Pyrotechnics*

The aim of this article was to evaluate how a mixture of plasticizers comprised of glycidyl azide (GAP) polymer and nitroglycerine (NG) will affect the combustion performance of nitrocellulose (maximum generated pressure, linear burning rate and erosivity) with a view to provide the necessary informations to perform ballistic simulation on the material.

The scientific contribution of this work is threefold. Firstly, it is demonstrated experimentally that formulation compounded with NG, GAP or a mixture of thereof is in agreement with the theoretical calculations obtained using thermodynamic software. Secondly, linear burning rate was obtained at -46, 21 and 63 ^{o}C for the proposed formulation allowing for improved modeling for such formulations. Lastly, relative erosivity data is in agreement with the Kimura-Arisawa model allowing ballisticians to predict the relative erosivity between two formulation.

The supporting information mentioned in this article is presented in Appendix A.

5.1 Abstract

The performance of the extruded cord geometry of nitrocellulose (NC) propellants plasticized by glycidyl azide polymer (GAP) and nitroglycerine (NG) has been evaluated using both closed and erosion vented vessel techniques in order to obtain the linear burning rate and the relative erosivity of these propellants. The closed vessel experiments performed at -46, 21 and 63 ^{o}C demonstrate that the measured maximum pressure is in accordance with the calculation obtained using the CHEETAH V2 thermochemical code. From the closed vessel analysis, the linear burning rates show that it is on average 89 ± 3 % that of the 21^{o}C propellant when fired at -46 ^{o}C. and 112 ± 4 % when fired at 63 ^{o}C. The addition of either GAP or NG increases the linear burning rate when compared to the neat NC formulation. Relative erosion data obtained in the erosion vented vessel

are in agreement with the Arisawa-Kimura models and it is found that the ratio of CO/CO_2 concentration in combustion gases is a better erosivity indicator than N_2/CO ratio.

5.2 Introduction

Nitrocellulose (NC) based binders are omnipresent in applications such as gun propellants, rocket propellants and as combustible containers. Low molecular weight nitrate esters are commonly used with NC in propulsion applications as plasticizers to improve mechanical properties and to increase the impetus of the propellant. Nitrate esters like nitroglycerine (NG) are effective but they possess drawbacks such as high migration rates, stability, toxicity, handling issues and high flame temperatures leading to premature wear of the gun barrel [30, 57]. It is therefore important to investigate novel energetic plasticizer systems for NC.

Recent developments have considered glycidyl azide polymer (GAP) as a potential replacement for nitrate esters in various propellant applications [59, 72, 82-90]. Also, work done in rocket propulsion have included NC into GAP based rocket formulations, but only at low concentration in order to improve mechanical properties [73].

Recent work from this laboratory, accepted for publication in Polymer Engineering & Science, has evaluated the plasticization properties of GAP and demonstrates that, by itself, it does not efficiently plasticize NC due to its high molecular weight. However, that same work also shows that an NG/GAP mixture is an efficient way to plasticize NC and leads to similar mechanical properties when compared to the NC-NG formulation.

Extensive work has been done to characterize the linear burning rate (LBR) of double base propellants such as JA2, GAP based Low Vulnerability Ammunition (LOVA) propellants and other highly plasticized propellants [18, 72, 82, 106-108]. All of these results have been performed at 21 ^oC and no data is available at high and low temperature for NC and GAP or for a mixture of GAP and NG limiting the simulation capability for such formulations.

Erosivity and wear of the gun barrel is a critical aspect as it can lead to a reduced operational effectiveness and an increased cost of maintenance over the lifecycle of the weapons' life and has yet to be investigated for NC/NG/GAP formulations [18].

Any combustible component can affect barrel wear in two ways; by thermal or chemical erosion. Thermal erosion occurs when the steel of the barrel becomes hot to the point of partially melting

as temperatures up to 1800 K are reached during the ballistic cycle and can be reduced by using low flame temperature propellant [109].

Chemical erosion is caused by the chemical interaction between the gun barrel and the combustion gases. Typical gas released from the combustion of gun propellants are mainly comprised of carbon dioxide (CO_2), carbon monoxide (CO), water (H_2O), nitrogen (N_2) and hydrogen (H_2). According to Lawton, Jaramaz and Kimura propellant erosivity can be expressed as a function of molecular gas composition. According to Lawton, the relative contribution of each gas to erosivity is H_2 > CO > N_2 > CO_2 > H_2O. On the other hand, Jaramaz ranks their effects according to Residual Gas > H_2O > CO > N_2 > H_2 > CO_2 and Kimura reports the following relationship CO_2 > CO > H_2O > H_2 > O > N_2 [6, 25, 110].

While theories conflict with each other, there is agreement that CO and H_2 will lead to an increase in erosivity and that N_2 will reduce it and improve barrel life. The erosion due to CO and CO_2 comes from the formation of iron carbide through the reaction between carbon monoxide, carbon dioxide and iron forming at the gas-bore interface, leading to the formation of solid carbon. At high temperature, the carbon is dissolved in the gun steel and with cool down, precipitates out of solution leading to the formation of iron carbide [28-30, 111]. The carburization effect lowers the melting point of the barrel wall by 50-400 ^oC thus resulting in a faster wear [29].

The increase in erosion from hydrogen comes from the decarburization of the steel. This decarburization occurs when hydrogen reacts with the gun steel leading to the formation of carbides. This softens the steel allowing an increase in erosivity.

Nitrogen reduces the erosivity by allowing the formation of nitride. At high content N_2 dissolves in the steel allowing the formation of nitride thus hardening the steel. It is also proposed that dissolved N_2 increases the melting point temperature of the steel protecting it from thermal erosivity [112]. Due to the protective effect of N_2 and the negative effect of CO_2 the ratio of N_2/CO and CO/CO_2 has been used as an approximation to evaluate the erosivity of a propellant. From the information mentioned above, the manufacturing of propellant binders containing high nitrogen and low flame temperature are a good avenue to reduce barrel wear.

The objective of this research is to evaluate how a mixture of plasticizers comprised of GAP and NG will influence the LBR of plasticized NC at -46, 21 and 63 ^oC as well as to evaluate the relative erosivity of NC/NG/GAP based propellant formulations.

5.3 Experimental Section

5.3.1 Materials

High viscosity low nitrogen content grade NC ("NC11%N") was purchased from Sichuan Nitroellulose Corporation (Luzhou, China). Grade A high viscosity NC ("NC12.5%N") was purchased from Eurenco (Bergerac, France). Grade B high viscosity NC ("NC13.4%N") was purchased from Eurenco (Bergerac, France). Low molecular weight GAP plasticizer GAP-0700 ("GAP", Mw = 1.1 kDa, PDI = 1.2, OH_{value} = 1.27) was purchased from 3M. 1-methyl-1,3-diphenylurea ("Akardite II") was purchased from Synthesia (Pardubice, Czech Republic). NG ("NG", Mw = 0.23 kDa, PDI = 1) was manufactured onsite by General Dynamics Ordnance and Tactical Systems Canada (Salaberry-de-Valleyfield, Canada) using the Biazzi process. Molecular weight of NG is taken from literature [1].

All NCs were received water wet and dehydrated prior to processing using a dehydration hydraulic press typical in the solvent extruded propellant industry in order to replace the water with ethanol. The ethanol-wet NC was then broken up in a sigma blade mixer to expose the fibers and then dried in conductive trays until total volatiles are less than 1 wt% when measured using gas chromatography and Karl Fisher titration.

GAP was used without further processing.

NG was desensitized in acetone at a concentration of 30 wt% for safe handling.

5.3.2 Preparation of NC/GAP/NG Formulation

Dry NC was weighed and added to a polyethylene bag. GAP and desensitized NG solution were weighed and added to a separate beaker. A solution of acetone and ethanol (50 wt%) and Akardite II (1 wt% by dry weight of the total formulation) was added to the plasticizer solution and agitated using a magnetic stirrer. The resulting solution was mixed with the dry NC fibers and the bag was hermetically sealed. The total concentration of polymer and plasticizer in the solution was set at 50 wt% The bag was stored at 35°C for no less than 4 days and mixed sporadically by hand to form a homogenous mass.

The propellant dough was placed on a two-roll mill to ensure proper mixing and to evaporate the solvent. The rolls were adjusted to a temperature of 50°C in order to keep the material warm to the touch throughout the evaporation process.

The propellant dough was mixed on the two-roll mill until it was stiff enough to be laminated and formed into a sheet of uniform thickness, free of air bubbles. The propellant sheet was then removed from the roll mill, placed in a 102 mm diameter extrusion press and extruded through a 3.2 mm non-perforated cylindrical die in a single strand. The strand was suspended in a 35 °C room and allowed to air dry until the recorded weight was constant for three days and was then left an extra seven days to fully dry. The grains were then cut to 25.4 mm in length into cord geometry. The samples were kept in a desiccator until needed. Prior to testing, 30 grains were randomly selected for geometrical measurements. The length was measured at one location and the diameter was measured at three locations. Dimensions are provided in Supporting Information Table S1.

A total of 14 formulations were manufactured and tested in the closed vessel (CV). The nomenclature for each of the formulations is as follow: the nitrogen content on the NC used followed in parentheses by its concentration, the concentration in parentheses of the NG and finally the concentration of GAP in parentheses. As an example the following "NC12.5%N(60)/NG(20)/GAP(20)" indicates a formulation manufactured using 60 wt% NC12.5%N , 20 wt% NG and 20 wt% GAP.

5.3.3 Gas pycnometer

Absolute density was measured using a Quantachrome Instrument Pentapyc 5220e automatic density analyser. The density was measured on 100 cm^3 of bulk propellant using nitrogen.

5.3.4 Closed vessel analysis

CV analysis was performed following MIL-DTL-286C method 801.1. Each sample was conditioned for no less than 4 hours at -46, 21 or 63 °C. CV tests were performed using a 97.6 cm^3 CV equipped with a Kistler 6215 probe with a calibration of 27.58 MPa V^{-1}. The loading density for all samples was done at 0.2 g cm^{-1}. The ignition was performed using a Pyrodex® .50 Caliber Pellet suspended with a tungsten wire. After each ignition, the interior of the CV was observed for residues. If residues were found, they were recovered and weighed. The CV was then cleaned and the temperature of the CV is taken using an infrared thermometer ensuring the temperature of the

combustion chamber was at 21 ± 1°C before loading the next sample. A minimum of three tests were performed for each formulation and for each temperature.

Thermochemical properties for each formulation were obtained from CHEETAH 2.0 using the gun calculation tool at 0.2 g $cm^3$and enabling BLAKE library compatibility [113]. From the thermochemical properties, the pressure time curve and the grains measurements, LBR rate regression was performed using BRLCB V3.0 [114].

5.3.5 Erosion evaluation

Erosion evaluation was performed using an erosivity vented vessel (EVV) in which the propellant was burned in a 200 cm^3 hermetic chamber sealed with a 70 MPa rupture disc. Following the rupture disc, a 1 mm perforated cylindrical AISI A36 steel erosion piece having a outside diameter of 19 mm and a length of 20 mm was installed so that upon rupture of the disc the combustion gases were forced through the perforation of the erosion piece. In order to take into account the heat loss and the subsequent pressure drop in the EVV, the loading density was adjusted from the CV data for each propellant formulation to obtain 77 MPa thus ensuring the opening of the rupture disc. For every formulation, one erosion piece was used and three subsequent firings were performed. The erosivity is evaluated by measuring the weight loss of the erosion piece before and after the test. The EVV diagram is available in Supporting Information Figure S7.

5.4 Results and discussion

5.4.1 Thermochemical calculations and maximum pressure

The chemical formulation, the thermodynamic properties and maximum pressure obtained in CV are presented in Supporting Information Table S1.

On average, the recorded maximum pressure in the CV (P_{Max}^{CV}) is 81 ± 4 % that of the pressure evaluated using CHEETAH ($P_{Max}^{CHEETAH}$). This variation in pressure is explained by the heat losses with the walls of the CV and was confirmed using double base propellant in CV of various volumes. The pressure generated at a loading density of 0.2 g cm^{-1} was 95, 93 and 84 % $P_{Max}^{CHEETAH}$ for respectively 700, 200 and 100 cm^3 and are presented in Supporting Information Figure S8.

Therefore, measuring 81 ± 4 % of the theoretical pressure is expected.

Figure 5-1 presents the P_{Max}^{CV} and the $P_{Max}^{CHEETAH}$ for NC12.5%N compounded with GAP and NG and Figure 5-2 NC12.5%N compounded at a constant weight fraction (40 wt%) using different ratios of GAP and NG.

In both cases, the maximum pressures measured in CV follows a trend in accordance with the theoretical calculations which confirms that the addition of a small amount of GAP (10 wt%) to an NG based formulation does experimentally generate a similar pressure to a formulation comprised solely of NG.

Figure 5-3 presents the calculated flame temperature and the average molecular weight of gas and the gas composition of the propellants at a fixed ratio to NG and GAP. It can be seen that the increase in total product concentration and reduced average gas molecular weight compensate for the lower flame temperature of the formulations. It follows that propellants: NC12.5%N(60)/NG(0)/GAP(40) and NC12.5%N(60)/NG(30)/GAP(10) generate similar pressure as demonstrated from the experimental data in CV (253 and 254 MPa). The gas composition is presented in Supporting Information Figure S9. The increase in overall gaseous products concentration is caused by a less favorable oxygen balance, leading to the formation of increased H_2 and CO reducing the formation of CO_2 and H_2O. This is beneficial as H_2 and CO are much lighter species and thus for the same mass of propellant, more gases are produced.

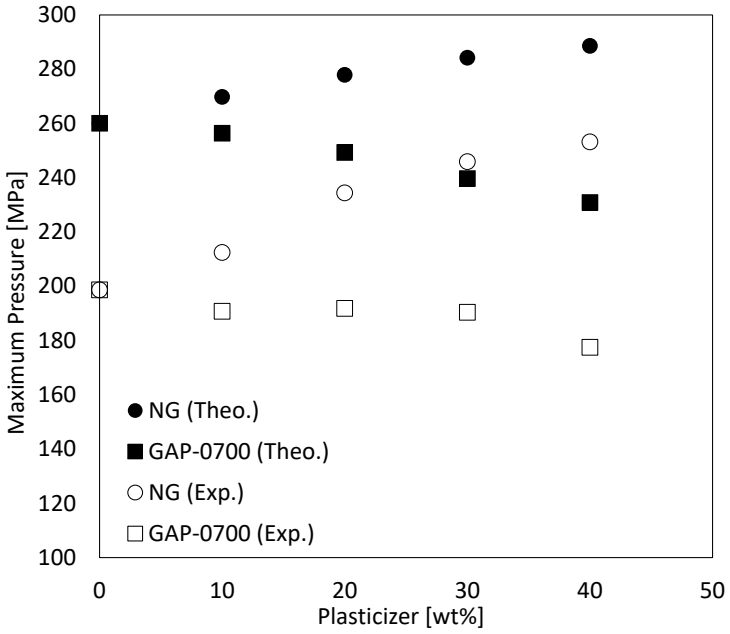

Figure 5-1 P_{Max}^{CV} and the $P_{Max}^{CHEETAH}$ obtained for NC12.5%N compounded with GAP and NG.

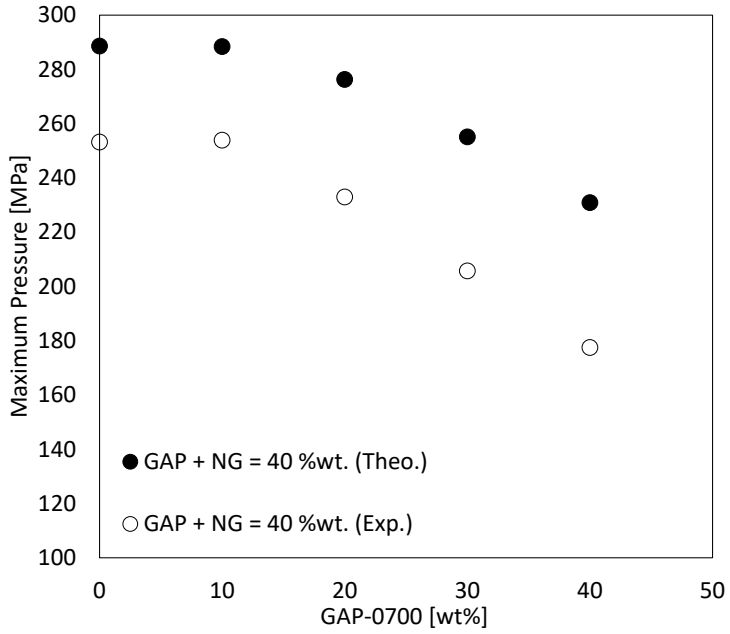

Figure 5-2 P_{Max}^{CV} and the $P_{Max}^{CHEETAH}$ obtained for NC12.5%N compounded with GAP and NG at constant concentration (GAP + NG = 40 wt%).

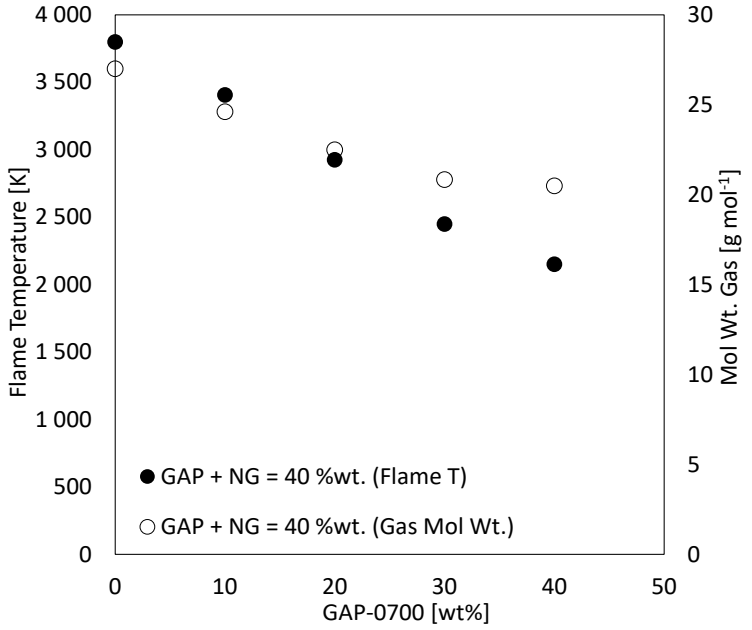

Figure 5-3 Flame temperature and average gas molecular weight obtained from CHEETAH for NC12.5%N compounded with GAP and NG at constant concentration (GAP + NG = 40 wt%).

5.4.2 Linear burning rate

LBR is estimated from the pressure-time curves obtained in CV, the thermochemical properties obtained by CHEETAH and the geometrical dimensions of the propellant grains. Density is measured using a gas pycnometer and is found to be ranging between 97.5 and 99.0 % of the theoretical maximum density (TMD) obtained using CHEETAH. This change in density can be attributed to either having the wrong chemical composition or to the presence of small occlusions in the material. The manufacturing process used dried raw material or precise desensitized solution. The risk of having the wrong formulation is therefore negligeable and the change density is more likely caused by small occlusion in the material. To perform LBR regression, the BRLCB software uses the density, the geometrical measurements and the loading density to evaluate the volume of propellant in the CV. For the scope of this work a 1.0 to 2.5 % decrease in TMD is acceptable as it will not dramatically affect the calculated surface on which the regression is performed.

Using BRLCB, the LBR curves are obtained and the burning parameters are calculated according to Vielle's Law (5.1) from 40 MPa to 90 $\%P_{Max}$.

$$r = \beta P^{\alpha} \quad (5.1)$$

Where r is the LBR in cm s^{-1}, β is the LBR coefficient, P is the pressure expressed in MPa and α is the pressure exponent. The α and β parameters are presented in Supporting Information Table S2.

5.4.2.1 Influence of temperature

For the sake of clarity, only the reference (NC12.5%N(100)/NG(0)/GAP(0)) formulation compounded with 40 wt% NG (NC12.5%N(100)/NG(0)/GAP(0)) and 40 wt% GAP (NC12.5%N(60)/NG(0)/GAP(40)) are presented in Figure 5-4 to observe the influence of temperature on the LBR. All evaluated formulations show an increase in LBR at 63 ºC and a decrease in LBR at -46 ºC when compared to the values at 21 ºC. This is explained by the combustion mechanism that takes place in solid gun propellant.

A burning propellant can be described in four discrete regimes, the condensed phase, the sub-surface liquid region, the gas phase and the flame front [112]. As heat is applied to the propellant, the surface temperature of the condensed phase increases until it starts decomposing either through sublimation, evaporation or decomposition giving rise to the sub-surface liquid region. The decomposition products are then converted into an intermediate gaseous species. At the flame front the intermediate species are decomposed into their final decomposition products as they reach a state of thermal equilibrium [13].

By having a propellant at 63 ºC instead of 21 ºC, less energy is needed to reach the decomposition point leading to the sub-surface liquid region and therefore the burning rate is increased. Inversely, if the propellant temperature is lowered to -46 ºC, more energy is needed to decompose the propellant as a greater quantity of thermal energy is needed to heat the propellant to its decomposition point and the burning rate is therefore decreased.

On average, all formulations fired at -46ºC exhibited a LBR 89 ± 3 % that of the propellant fired at 21 ºC. This value is increased to 112 ± 4 % when fired at 63 ºC.

All evaluated propellants complied with this behaviour and for the purpose of comparison, curves at 21 ºC are presented in Figure 5-6 and Figure 5-7.

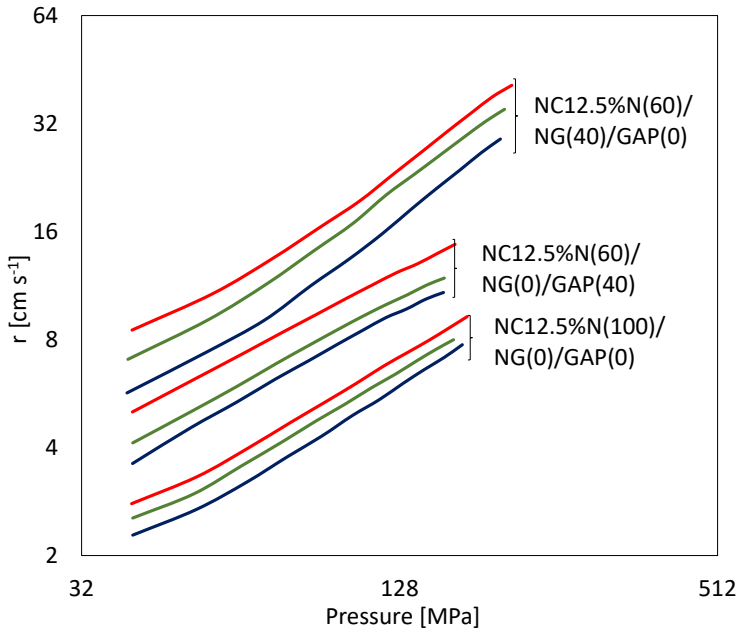

Figure 5-4 Influence of propellant temperature (-46 in blue, 21 in green and 63 °C in red) for various propellants on LBR.

It is also important to note that from our previous work on the thermomechanical properties of similar formulations there seems to be a correlation between the presence of the β relaxation and a sharp increase in the LBR at high temperature [115]. In order to better observe this phenomenon, the ratio of LBR at 63 °C and -46 °C for both NG and GAP concentration ranging from 0 to 40 wt% is traced in Figure 5-5.

When compounding NC with GAP, the presence of a β relaxation between -40 °C and 10 °C could only be measured in DMA for 30 wt% GAP and above. The same β relaxation could be measured with NG at a concentration of 20 wt% and it is suspected that it is also present at a much lower concentration although this has yet to be measured by DMA.

From Figure 5-5, a sharp increase in the ratio of LBR is observed between 30 and 40 wt% in GAP which coincides with the apparition of the β relaxation. More work is needed to obtain definitive results, but one explanation could be that the presence of the β relaxation associated with molecular movement in the plasticizer rich domains allows for greater thermal conductivity, an increased evaporation rate, in the case of NG and an overall increase in LBR at temperature above β

relaxation. More work is planned to evaluate the presence of the β relaxation with greater accuracy for both NG and GAP as well as doing CV at temperatures above 63 °C.

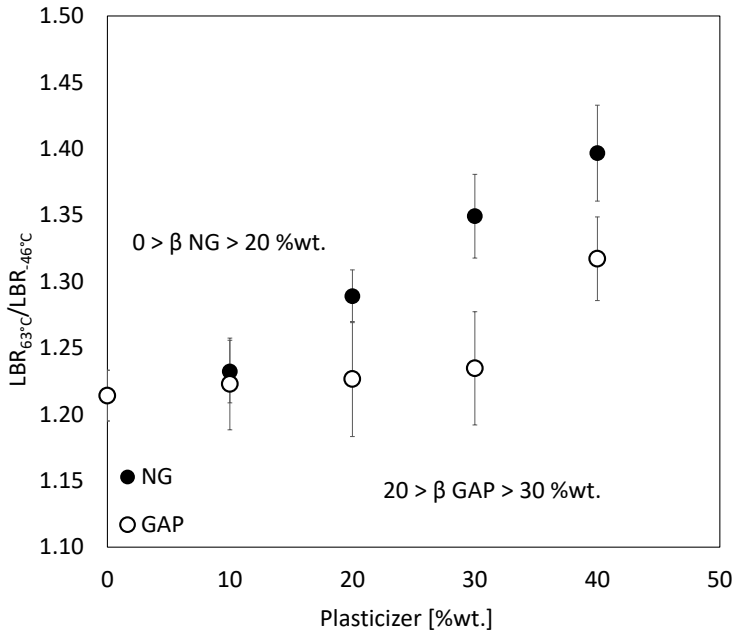

Figure 5-5 Ratios of LBR at 63 °C and -46 °C as a function of GAP and NG concentration.

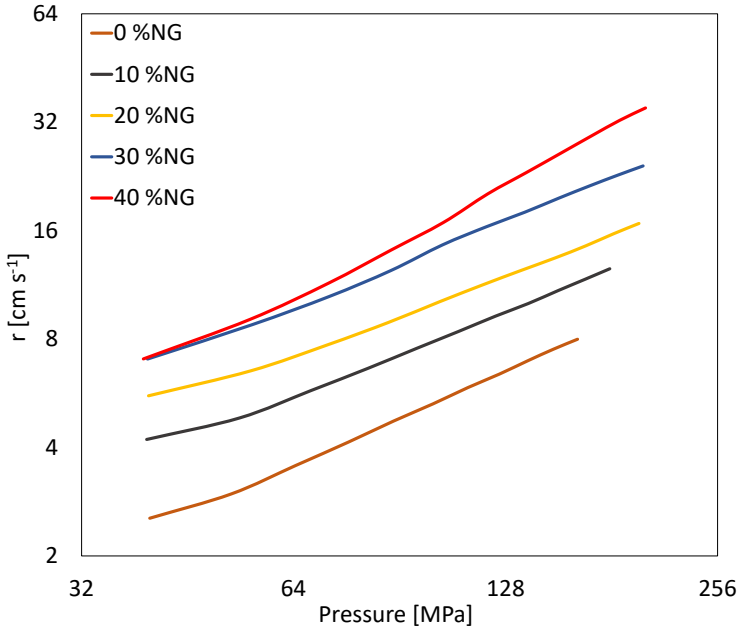

Figure 5-6 Influence of NG concentration on NC12.5%N formulation at concentration of 0, 10, 20, 30 and 40 wt% on LBR.

5.4.2.2 Influence of NG and GAP concentration

The influence of NG concentration at 0, 10, 20, 30 and 40 wt% on LBR is presented in Figure 5-6 and shows an increase in LBR as a function of NG concentration. This is caused by the tendency of NG to decompose and evaporate at a lower temperature than NC [116]. The hypothesis is that, as the flame front gets closer to the surface of the propellant, NG evaporates at a much faster rate than NC decomposes thus increasing the overall LBR of the propellant. Between 30 and 40 wt% there is a sharp increase in the pressure exponent from 0.8 to 1. A similar pressure exponent has been reported for this type of propellant [117, 118].

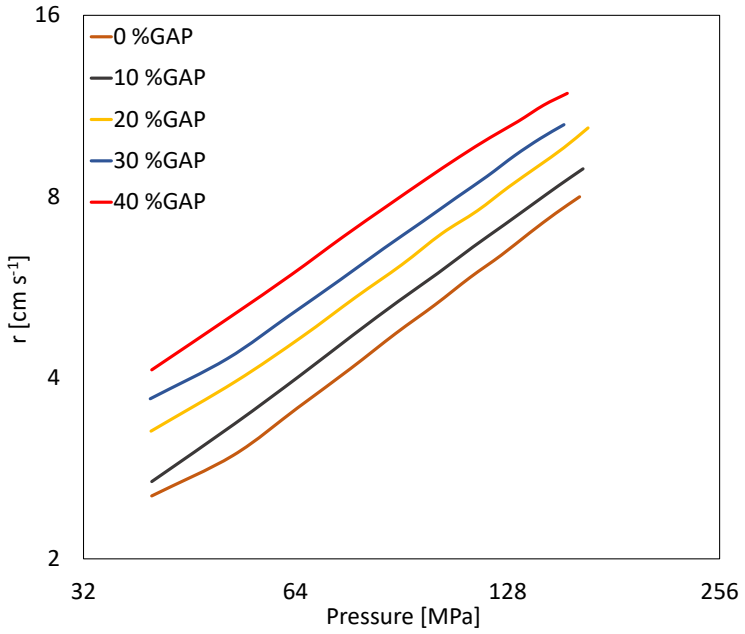

Figure 5-7 Influence of GAP concentration on NC12.5%N at concentration of 0, 10, 20, 30 and 40 wt% on LBR.

When using GAP (Figure 5-7), the linear burning still increases as a function of the GAP concentration, but the exponent value is not influenced as compared to the NG propellant formulations. This can be explained by the fact that unlike NG, GAP does not evaporate as readily since it has a higher molecular weight, 0.23 for NG and 1.1 kDa for GAP, as presented in the materials section. For this reason, the increase in burning rate associated with the evaporation of the liquid polymer is not present. Also, compared to NG, the flame temperature of GAP based

formulations are lower than that of unplasticized NC and an increase in LBR is therefore not associated with an increase in heat transfer to the surface of the propellant. For both these reasons the increase in LBR can be attributed to an increase in the decomposition kinetics of GAP based propellants.

The influence of replacing a portion of NG with GAP on the LBR is presented in Supporting Information Figure S10. As expected from previous results, the addition of GAP to a NG base formulation reduces the overall LBR. A similar explanation as previously stated is proposed for this behaviour. The addition of GAP to NG base formulations reduces the overall flame temperature and reduces the NG volatile content in the propellant thus reducing the overall LBR of the propellants.

The fact that GAP displays a lower LBR when compared to NG is, in itself, neither an advantage nor a disadvantage, but has to be known in order to tailor a propellant to a given application. Knowing that GAP based propellants have a lower LBR than NG propellants, one can adjust the geometry of the propellant or make use of surface coatings to obtain a similar pressure curve.

To evaluate the reference material, three propellant formulations comprised of 11%N, 12.6%N and 13.4%N NC were compounded using 40 wt% of GAP. LBR values are presented in Supporting Information Figure S11. As expected, the LBR increases as a function of %N due to the increase in flame temperature of the combustion gases which increases the heat transfer at the surface of the propellant.

5.4.3 Relative erosivity

Seven formulations were evaluated to measure erosivity. The recorded weight loss, the relative erosivity, the ratio of N_2/CO and CO/CO_2 are presented in Table 5-1 . The relative erosivity is defined here as the weight loss of the sample divided by the weight loss measured for the reference formulation NC12.5%N(100)/NG(0)/GAP(0).

Figure 5-8 shows a picture of the erosion pieces for the following formulations : NC12.5%N(100)/NG(0)/GAP(0), NC12.5%N(60)/NG(40)/GAP(0) and NC12.5%N(60)/NG(0)/GAP(40) as well as an uneroded piece. Each picture are taken after three consecutive firings in each erosion piece.

Figure 5-8 clearly shows the increased erosivity of the high nitroglycerine formulation.

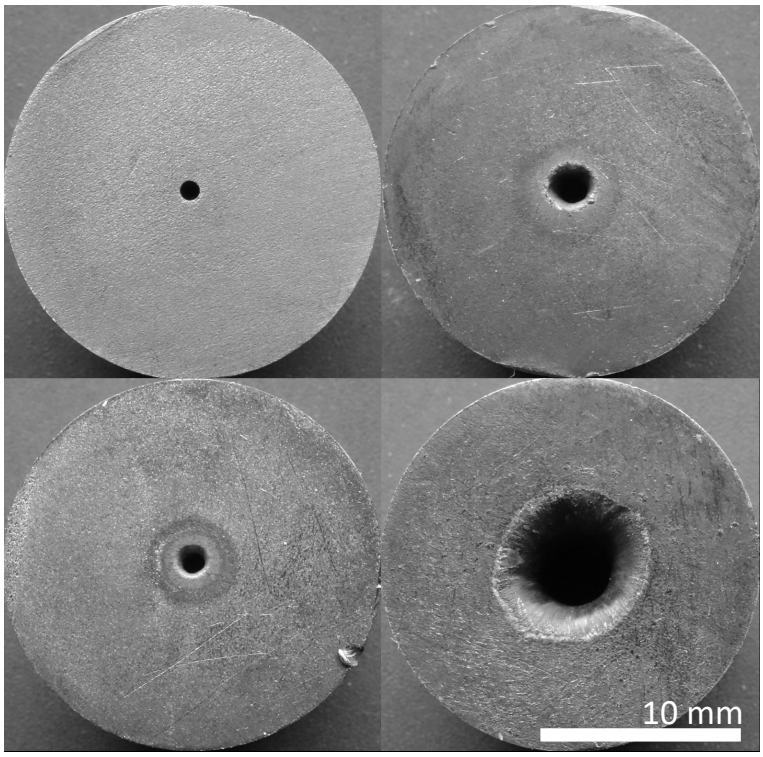

Figure 5-8 Erosion pieces prior to testing (top left), NC12.5%N(100)/NG(0)/GAP(0) (top right), NC12.5%N(60)/NG(0)/GAP(40) (bottom left) and NC12.5%N(60)/NG(40)/GAP(0) (bottom right).

Table 5-1 Chemical composition, erosion and relative erosion of the tested formulations.

ID	**Erosion [g]**	**Relative erosivity**	**N_2 / CO**	**CO / CO_2**
NC12.5%N(100)/NG(0)/GAP(0)	0.1004	1.0	0.26	3.58
NC12.5%N(80)/NG(20)/GAP(0)	0.4385	4.4	0.35	2.30
NC12.5%N(80)/NG(10)/GAP(10)	0.1175	1.2	0.31	5.51
NC12.5%N(80)/NG(0)/GAP(20)	0.0392	0.4	0,30	12.05
NC12.5%N(60)/NG(40)/GAP(0)	1.8725	18.7	0.48	1.45
NC12.5%N(60)/NG(20)/GAP(20)	0.2257	2.2	0.36	8.36
NC12.5%N(60)/NG(0)/GAP(40)	0.0138	0.1	0.36	N/A

Two models predict erosivity as a function of the flame temperature and of the average molecular weight of the combustion gases of a propellant : the Kimura (5.2) and the Arisawa-Kimura (5.3) [32, 33]. The Arisawa-Kimura evolved from the Kimura model to reconcile the thermal effects and chemical reactions taking place in gun erosion and will be used in this work.

Figure 5-9 show that the models fit the data each with a determination coefficient of 0.97 and that the values follow the same trend as the work of Lavoie et al [119].

It is important to note that three data points superimposed at 600 K $g^{0.5}$ $mol^{-0.5}$. They are in order of erosivity NC12.5%N(60)/NG(20)/GAP(20), NC12.5%N(80)/NG(10)/GAP(10) and NC12.5%N(100)/NG(0)/GAP(0).

This variation indicates that, although they have a similar value of $T_f/M_w^{0,5}$, one can look at the chemical composition of the gas and the flame temperature to better understand the cause of the increased erosion.

$$lnW \approx \left(\frac{Tf}{Mw}\right)^{0.5} \quad (5.2)$$

$$lnW \approx \frac{Tf}{Mw^{0.5}} \quad (5.3)$$

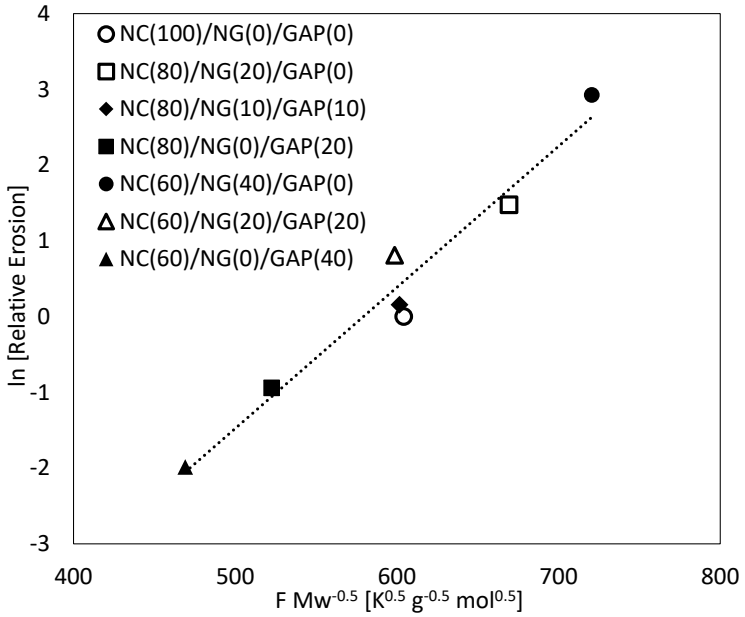

Figure 5-9 Influence of flame temperature and gas molecular weight on erosion.

The flame temperature for the formulations are respectively 2925, 3007 and 3094 ºC for NC12.5%N(60)/NG(20)/GAP(20), NC12.5%N(80)/NG(10)/GAP(10) and NC12.5%N(100)/NG(0)/GAP(0).

If only the flame temperature is considered, the single base propellant would present a higher erosivity value compared to the two double base formulation. Here, the opposite is observed. One can then assume that the gas composition is the cause of the higher erosivity. Gas compositions of the three formulations, as calculated from CHEETAH, are presented in Figure 5-10.

In Figure 5-10 the calculated CO and N_2 concentrations increase, while CO_2 and H_2O amounts decrease, a consequence of the lower oxygen balance of the propellent. From Table 5-1 the values of N2/CO are 0.26, 0.31, 0.36 and the values of CO/CO_2 are 3.58, 5.81, 8.36 respectively. The ratio of N_2/CO is therefore not a good indication of the erosivity at similar $T_f/M_w^{0,5}$ compared to the ratio of CO/CO_2. This can be explained since the ratio of N_2/CO was mainly used when comparing high nitrogen formulations [120].

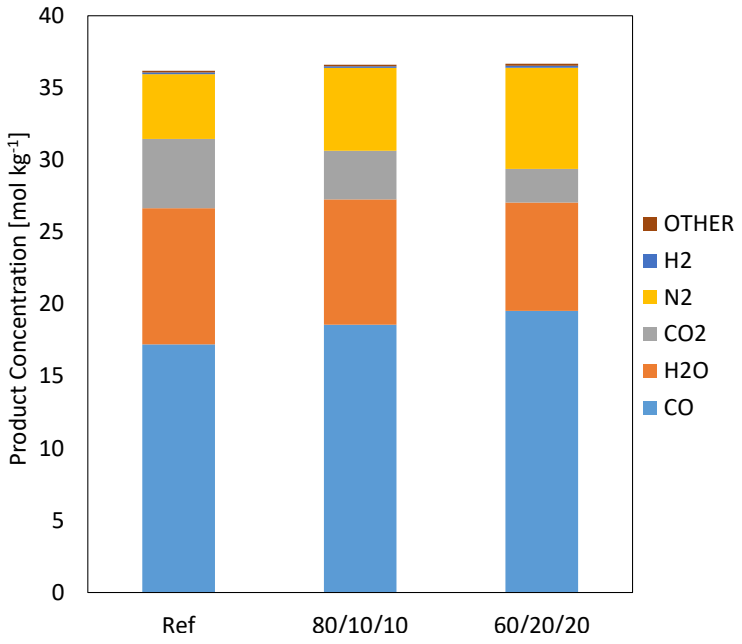

Figure 5-10 Gas composition for formulation NC12.5%N(100)/NG(0)/GAP(0), NC12.5%N(80)/NG(10)/GAP(10) and NC12.5%N(60)/NG(20)/GAP(20)

From the presented values obtained it is clear that a binder containing a higher concentration of GAP will perform better in terms of erosivity when compared to a binder comprised solely of NG and that at similar $T_f/M_w^{0.5}$ the ratio CO/CO_2 can be used to evaluate the relative erosivity between multiple formulations.

Finally, when including the values obtained from LBR, one can tailor the ballistic properties of a propellant to a desired erosivity value. As an example, a propellant having low erosivity such as NC12.5%N(100)/NG(0)/GAP(0) (Relative Erosivity = 1; α = 0.845 ; β = 0.108; $P_{Max}^{CHEETAH}$ = 260 MPa) could be replaced by a propellant having similar erosivity value such as NC12.5%N(80)/NG(10)/GAP(10) (Relative Erosivity = 1.2 ; α = 0.780 ; β = 0.249; $P_{Max}^{CHEETAH}$ = 268 MPa) but would burn on average at 130 % the LBR of the original propellant.

5.5 Conclusion

The objective of this research was to evaluate how the concentration of GAP, the concentration of NG and the nitrogen content of the nitrocellulose influences the combustion and erosivity characteristics of nitrocellulose based propellant formulations. Closed vessel measurements show that GAP performs as expected from thermochemical gun simulations. LBR calculations were performed from 40 MPa to 90 $\%P_{Max}$ at -46, 21 and 63 °C and show that LBRs are respectively 89 ± 3 % and 112 ± 4 % that of the LBR at 21 °C. From preliminary results, it appears that the presence of the β relaxation is associated with a sharp increase in LBR at high temperature compared to cold temperatures.

Both GAP and NG increase the LBR when compared to the neat NC formulation, although NG increases LBR much more than GAP. This is explained by its higher flame temperature and increased volatility reaching a pressure exponent greater than 1 at 40 wt%

Erosivity was measured using an erosivity vented vessel and was found to follow the Kimura-Arisawa model. GAP formulations show lower erosivity compared to NG formulations as expected from their low flame temperature and it was also observed that for formulations comprised of NC, NG and GAP, the ratio of CO/CO_2 can be used to evaluate relative erosivity between two propellants of similar $T_f/M_w^{0,5}$ when using the Kimura-Arisawa model.

In conclusion, this work demonstrates that a mixture of NG and GAP can be added to NC in order to influence both its erosivity and LBR properties. It was also found that one can tailor a propellant

formulation to obtain a desired effect either from the erosivity or from the linear burning rate standpoint.

Future work will look at the addition of solid high nitrogen fillers, the incorporation of cellulosic-based high nitrogen binder to the formulation, as well as the influence of other energetic plasticizers and the relationship between the β relaxation and it's influence on the LBR.

5.6 Acknowledgements

The authors would like to thank General Dynamics Canada Valleyfield for providing the time, materials, funding, and equipment needed for the manufacturing and characterization of the samples. The authors would also like to thank Mr Marc Boileau, and Mr Daniel Lepage from General Dynamics Canada for their time and effort in making this project a reality.

CHAPTER 6 ARTICLE 3: LINEAR BURNING RATE OF DOUBLE BASE PROPELLANT CONTAINING AZIDODEOXYCELLULOSE

Étienne Comtois, Charles Dubois and Basil D. Favis

Submitted to *Journal of Energetic Materials*

The aim of this article was to evaluate how the concentration of azidodeoxycellulose (AC) affects the combustion performance of nitrocellulose (NC) plasticized at a concentration of 30 wt% in nitroglycerine (NG), for the purpose of providing the necessary information to perform ballistic simulation on the material.

The scientific contribution of this work is twofold. First, it is demonstrated experimentally that formulations compounded with AC, NG and NC agree with the theoretical calculations obtained using thermodynamic software. Second, a linear burning rate was obtained at 21 ^{o}C for the proposed formulations, allowing simulations to be performed on the material.

The supporting information for this article is presented in Appendix A.

6.1 Abstract

Azidodeoxycellulose (AC) is evaluated in a closed vessel as part of a propellant formulation containing nitrocellulose (NC) and nitroglycerine (NG) as binders. It is found that the AC systematically generates greater pressure and a faster linear burning rate when compared to a formulation having a similar concentration of a mixture of cellulose and NC that is meant to replicate a comparable substitution degree. An additional finding is that a formulation containing 13 wt% of AC generates higher pressure in a closed vessel than the mixture of NC and NG alone. These results are evidence that AC is an adequate solid filler for propellant formulations.

6.2 Introduction

Binders used in many low-vulnerability ammunitions (LOVA) are comprised of cellulose acetate butyrate (CAB) and other cellulose derivatives such as cellulose acetate (CA) [121, 122]. In order to improve the energetic output of the formulation while keeping the concentration of nitrate ester to a minimum, a portion of nitrocellulose (NC) can be added to the binder formulation to improve processing and energetic output [16, 123].

Therefore, the bulk of the energy in LOVA formulations comes from solid fillers such as 1,3,5-trinitro-1,3,5-triazine (RDX) and 1,3,5,7-tetranitro-1,3,5,7-tetrazoctane (HMX), which can reach concentrations in the propellant of more than 85 wt% [16, 123].

The work of Kirshenbaum et al. [124] found that all propellants containing nitrate ester are less sensitive than their LOVA counterparts. Based on these conclusions, and in order to improve the mechanical properties and increase the energetic content, a cured energetic thermoplastic elastomer (ETPE) based on glycidyl azide polymer (GAP) has been evaluated as a binder for a RDX-based LOVA formulation that demonstrates the application of azide-based binders in both gun and rocket propulsion [90, 125, 126].

Work from this research group evaluated NC, nitroglycerine (NG) and GAP formulations and showed that, although not capable of plasticizing NC by itself, GAP can efficiently plasticize NC when a quantity of NG is added [115]. Furthermore, it was found that replacing a portion of NG with GAP allows for reduced erosivity while generating similar pressure in a closed vessel (CV), indicating the effectiveness of the azide explosophoric group as part of propellant formulations.

AC, much like NC, is a derivative of cellulose where the hydroxyl group is replaced with azide moieties. It is currently being investigated as a means to manufacture membranes in which click chemistry can occur with the azide moieties on the AC chain. [45, 127].

The azidation of cellulose is a two-step process. First, a leaving group such as tosylate or mesylate is added to the cellulose backbone, followed by the replacement of the leaving group with the azide moieties.

Two reaction pathways are proposed for the tosylation of cellulose tosylate. In the first pathway, cellulose is dissolved in a DMA/LiCl solution [49, 52], while in the second, the tosylation is performed in an ionic liquid solution [8].

Substitution degrees (DS_{Ts}) for tosylate on cellulose found in the literature are reported in Table 6-1. In this current research, in order to reach the maximum degree of substitution, the synthesis proposed by Rahn et al. [49] was followed and is presented in Figure 6-1.

Table 6-1 DSTs present in the literature.

DS_{Ts}	Ref.
0.40 – 0.68	[52]
0.43 – 0.95	[8]
038 – 2.30	[49]
0.74 – 1.29	[53]

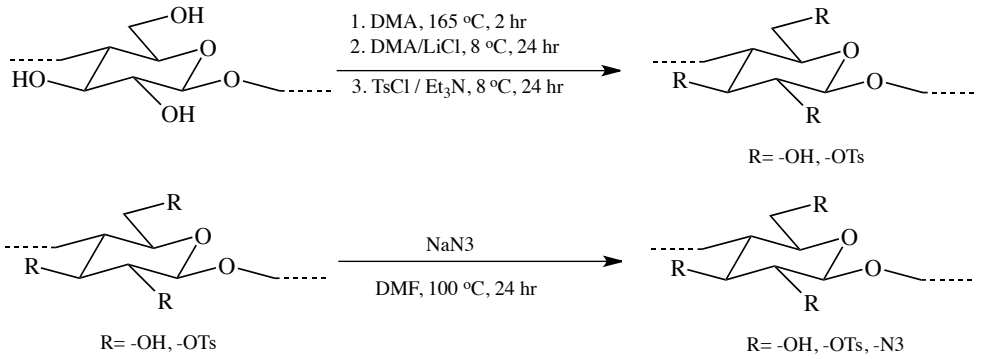

Figure 6-1 Synthesis pathways: tosylation of cellulose (top) and azidation of Cel-Ts (bottom) [8, 49].

The azidation of Ts-Cell is successfully demonstrated in the work of Schmidt et al., where Ts-Cell is dissolved in dimethylformamide (DMF) in the presence of sodium azide (NaN_3), forming AC and sodium p-toluenesulfonate by nucleophilic displacement. The final substitution degree in azide moieties (DS_{N3}) is measured to be of 0.82 and a residual DS_{Ts} of 0.05 Schmidt et al [8]. Chemical reactions and conditions are presented in Figure 6-1.

The stability of AC as a energetic material has been evaluated by DSC and proved to be similar to that of NC [50, 51]. This is of interest as it is expected that AC with a DS_{N3} of 1, 2 and 3 would, respectively, have a nitrogen content (%N) of 22.3, 39.8 and 53.2, making this material very interesting from a high-nitrogen energetic binder standpoint.

The objective of this research will be to evaluate the AC combustion property and linear burning rate (LBR) as part of a propellant formulation. To carry out this analysis, AC will be synthesized and compounded in a typical formulation and tested in comparison with a reference.

6.3 Materials and method

6.3.1 Materials

The Cellulose ("PB400") was provided by Rayonier Advanced Materials (Gradignan, France). N,N-Dimethylacetamide (reagent), Lithium Chloride (Certified) ("LiCl"), Triethylamine (Reagent) ("Et_3N"), p-Toluenesulfonyl chloride (99+%) ("TsCl"), N,N-Dimethylformamide (Certified ACS) and sodium azide (99% extra pure) ("NaN_3") were purchased from Fisher Scientific. Grade A high-viscosity NC ("NC12.5%N") was purchased from Eurenco (Bergerac, France). N-Methyl-N',N'-diphenylurea was purchased from Synthesia (Pardubice, Czech Republic). The NG was manufactured onsite by General Dynamics Ordnance and Tactical Systems Canada (Salaberry-de-Valleyfield, Canada) using the Biazzi process.

The NC was received water wet and had to be dehydrated prior to processing. The excess water was removed by rinsing the slurry with a continuous flow of ethanol in a dehydration press. The excess ethanol was removed by applying pressure that formed a consolidated block of NC. The ethanol-wet NC was then broken up in a sigma blade mixer to expose the fibres. The loose NC fibres were placed in a conductive tray and air dried until total volatility was less than 1 wt% when measured using gas chromatography and Karl Fisher titration.

The NG was desensitized in acetone at a concentration of 30 wt% for safe handling.

Fourier Transform Infrared Spectroscopy (FTIR) spectrum was obtained using an ABB FTLA2000-104-T in transmission and used to confirm the presence of the azide group on the tosylated cellulose.

The decomposition temperature peak ($T_{d,peak}$), onset ($T_{d,onset}$) and heat of decomposition (ΔH_d) were measured using a TA Instrument Q20 DSC. Samples were sealed in a hermetic aluminium pan and the analysis was performed at a heating rate of 5 $^oC\ min^{-1}$ under nitrogen flow at 50 mL/min.

Elemental analysis was performed using a Perkin Elmer 2400 CHNS/O Series II system in CHNS mode. The degree of substitution was evaluated using the ratio of sulfur compared to the theoretical concentration found in pure, substituted samples. The oxygen concentration was found by difference.

H^1 – NMR spectra were recorded using a Bruker AVANCE III 400 spectrometer in DMSO-d_6.

The number average molecular weight (M_n) and the polydispersity indes (PDI) was obtained using a Viscotek VE 2001 GPCmax. The columns were from Tosoh Bioscience (TSKgel α-2500, TSKgel α-3000 and TSKgel α-5000). The detection train was composed of a right-angle light-scattering detector, a low-angle light-scattering detector and a refractive index detector (Malvern 270 Dual Detector and Viscotek VE3580). The operating temperature was 40ºC, the sample concentration was 5 mg mL^{-1}, the flow rate was 0.8 mL min^{-1} and the injection volume was 100 uL. The mobile phase was DMF (0.01 M LiBr) and the system was calibrated using broad and narrow polymethyl methacrylate standards in multi-detector mode.

The density of both PB400-N3 and the propellant formulations were measured with a Quantachrome Intrument Pentapyc 5220e automatic density analyser using nitrogen.

The heat of formation (ΔH_f^o) was calculated from the heat of combustion (ΔH_c^o), obtained using a Parr 6200 bomb calorimeter. From the elemental analysis, the quantities of CO_2, H_2O, SO_2 and N_2 were obtained assuming complete combustion of PB400-N3. From the difference in the heat of combustion and the heat of formation of the associated gaseous products, the heat of formation of PB400-N3 was obtained [128].

6.3.2 Synthesis of tosylated cellulose (PB400-Ts)

Synthesis of PB400-Ts was based on the procedure described by Rahn et al. [49]. 40.0 g of air dry PB400 (245 mmol AGU) was suspended in 1500 mL of DMA and boiled for one hour under mechanical stirring and nitrogen flow, during which 60 mL of DMA were removed by distillation to replace water-bound water in PB400. The slurry was allowed to cool to 100 ºC under agitation and 128 g of LiCl were added to the suspension. After 18 hours, the cellulose was dissolved and transferred in a 3 L glass-jacketed reactor vessel equipped with a mechanical stirrer and the temperature was adjusted to 8 ºC. 240 mL of Et_3N (1726 mmol) dissolved in 160 mL of DMA was added dropwise to the cellulose solution under constant stirring using a peristaltic pump at a rate of 10 mL min^{-1} followed by 161 g of TsCl (850 mmol) dissolved in 240 mL of DMA added at a rate of 3 mL min^{-1}. The reaction was stirred for 36 hours at 8 ºC. The solution was slowly added to 16 L of water and 8 L of crushed iced in a vessel equipped with an overhead stirrer and baffles under strong agitation. The polymer was filtered and dried in a vacuum oven overnight. Once dry, the polymer was pulverized using a blender, suspended in 1000 mL of ethanol, filtered, suspended

in 3 L of acetone, precipitated in 10 L of water, washed with ethanol and dried at 50 ºC under vacuum to obtain a final dry weight of 95.43 g.

The obtained yield was 88%. The elemental analysis obtained in was C, 50.81 wt%; H, 4.65 wt%; N, 0.19 wt%; S, 13.05 wt%; O, 31.30 wt%. This was associated to a DS_{TS} of 1.80 and the calculated elemental analysis was C, 51.20 wt%; H, 4.20 wt%; N, 0.23 wt%; S, 12.99 wt%; O, 31.39 wt% with less than 1 wt% of residual solvent. The M_n of the polymer was obtained by GPC and was116 kDa with a PDI of 2.86. DSC evaluation proved that $T_{d,peak}$ was 178 ºC, $T_{d,onset}$ was 158 ºC and ΔH_d was 0.250 kJ g^{-1}. FTIR analysis showed the following distinct band 3400 (ν OH), 2920 (ν CH), 1629 (ν C=C cyclic alkene), 1360 (ν S=O) and 1177 (ν S=O).

6.3.3 Synthesis of azidodeoxycellulose (PB400-N3)

Synthesis of PB400-N3 was based on the procedure described by Schmidt et al. [8]. 92.0 g of PB400-Ts (209 mmol AGU) were added to 2500 mL of DMF in a 3 L glass-jacketed reactor equipped with a mechanical stirrer. 50 g of NaN_3 (769 mmol) were added to the reactor vessel and allowed to react at 100 ºC for 24 hours under stirring. The solution was slowly added to 16 L of water and 8 L of crushed iced in a vessel equipped with an overhead stirrer and baffles under strong agitation. The polymer was filtered and dried in a vacuum oven overnight. Once dry, the polymer was pulverized using a blender in fractions of less than 10 g until all the material could pass through an ASTM E-11 No. 70 standard-test sieve with an opening mesh size of 212 μm. It was then suspended successively in 1000 mL of ethanol, 1000 mL of water, filtered, washed with ethanol and dried at 50 ºC under vacuum to obtain a final dry weight of 40.23 g.

The obtained yield was 85%. The elemental analysis obtained in was C, 39.45 wt%; H, 4.21 wt%; N, 27.51 wt%; S, 2.60 wt%; O, 26.23 wt%. This was associated to a DS_{N3} of 1.52 and a residual DS_{Ts} of 0.19. The calculated elemental analysis was C, 38.33 wt%; H, 4.22 wt%; N, 27.89 wt%; S, 2.61 wt%; O, 26.93 wt%. The M_n of the polymer was obtained by GPC and was 67 kDa with a PDI of 1.76. DSC evaluation proved that $T_{d,peak}$ was 226 ºC, $T_{d,onset}$ was 180 ºC and ΔH_d was 2.030 kJ g^{-1}. FTIR analysis showed the following distinct band 3400 (ν OH), 2920 (ν CH), 2108 (ν N_3), 1629 (ν C=C cyclic alkene), 1360 (ν S=O) and 1177 (ν S=O). Calorimetry evaluation showed that ΔH_c^o was 186.1 kJ g^{-1}, ΔH_f^o was 170.0 kJ mol^{-1}. Density was 1.49 g cm^{-3} when evaluated using gas pycnometer.

6.3.4 Preparation of propellant formulation

The dry NC, cellulose and ground PB400-N3 were weighed and added to a polyethylene plastic bag. A desensitized NG solution was weighed and added to a separate beaker. A solution of acetone and ethanol (50/50 wt%) and N-Methyl-N', N'-diphenylurea (1 wt% by dry weight of the total formulation) was added to the plasticizer solution and agitated using a magnetic stirrer. The solution was added to the dry NC fibres and the bag was hermetically sealed. The total concentration of polymer and plasticizer in the solution was set at 50 wt%. The bag was stored at 35 °C for no less than four days and mixed sporadically by hand to form a homogenous mass.

The material was hand mixed and spread to remove excess solvent. Once the material did not feel tacky to the touch, it was folded onto itself, placed in the plastic bag and laminated between the rolls of the two-roll mill. This step was repeated until the material formed a uniform sheet. The sheet was cut into 30 mm wide ribbons and allowed to dry for four days at 35 ºC. The ribbons were then placed in a 73 ºC convection oven until the recorded weight was constant for three days.

Prior to firing, the ribbons were cut into 25.4 mm squares to better accommodate the CV. 10 grains were randomly selected for geometrical measurement.

6.3.5 Closed vessel analysis

CV analysis was performed following the MIL-DTL-286C method 801.1. Each formulation was conditioned for a minimum of four hours at 21 ºC. CV analysis was performed using a 97.6 cm^{-3} CV equipped with Kistler 6215 with a calibration of 27.58 MPa V^{-1}. The loading density for all samples was done at 0.2 g cm^{-3}. The ignition was performed using a Pyrodex® .50 Caliber Pellets suspended with a tungsten wire. After each ignition, the CV was allowed to cool for five minutes and pressure was released prior to opening the CV. The interior of the CV was observed for residues. If residues were present, they were recovered and weighed. The CV was then cleaned and the temperature of the CV was taken using an infrared thermometer ensuring the temperature of the combustion chamber was at 21 ± 1 ºC. Two tests were performed for each formulation.

Thermochemical properties for each formulation were obtained from CHEETAH 2.0 using the gun calculation tool at 0.2 g cm^{-3} and enabling BLAKE library compatibility.

Based on the thermochemical property, the pressure-time curve and the grains measurements, LBR regression was performed using BRLCB V3.0.

6.4 Results and discussion

6.4.1 Synthesis of PB400-Ts

The synthesis of PB400-Ts shows a degree of substitution of DS_{Ts} = 1.80 when evaluated using elemental analysis and it proves to be soluble in acetone, dimethyl sulfoxide, dimethylacetamide and dimethylformamide, which is consistent with the results presented by Rahn and Heinze [49, 129]. DSC analysis (Figure 6-2) shows a first decomposition peak at 178 ºC with a decomposition energy of 330 J $g^{-1,}$ which is in accordance with Heinze [129] where tosylated cellulose showed a first peak of decomposition ranging from 161 to 195 ºC and with decomposition energy values between 200 and 380 J g^{-1}. Ft-IR analysis (Figure 6-3) showed that for PB400-Ts, distinct bands are associated with the presence of SO_2 at 1360 and 1177 cm^{-1}. 1H NMR analysis (Figure 6-4) was not conclusive in evaluating the degree of substitution, since the peaks could not be sufficiently separated to be integrated due to the high viscosity of the polymer in DMSO. Using MestReNova software, integral values are obtained. Protons associated with the tosylate ring are visible at 2.4 for the protons on the methyl group, and at 7.5 and 7.8 ppm for the protons on the aromatic ring. Protons associated with the anhydroglucose unit were reported to be between 3.2 and 5.3 ppm [130]. The sums of the protons associated with the tosylate ring were compared to the anhydroglucose protons contained on the cellulose ring to obtain DS_{Ts} = 1.56. This value is inferior to that measured using elemental analysis.

6.4.2 Synthesis of PB400-N3

The synthesis of PB400-Ts shows a degree of substitution of DS_{N3} = 1.52 and a residual DS_{Ts} = 0.19 when evaluated using elemental analysis. It is soluble in acetone, DMSO, DMA and DMF, but proves to be insoluble in a mixture of 75 wt% acetone and 25 wt% ethanol. DSC analysis (Figure 6-2) shows a single decomposition peak at 226 ºC with decomposition energy of 2030 J g^{-1}. FTIR analysis (Figure 6-3) shows that for PB400-Ts, distinct bands are associated with the presence of residual SO_2 at 1360 and 1177 cm^{-1} and a strong peak is associated with the azide functionality at 2108 cm^{-1}. Similar conclusions with the PB400-Ts are obtained in 1H NMR. Due to the high viscosity of the polymer in DMSO, 1H NMR analysis (Figure 6-4) was not conclusive in evaluating the degree of substitution since the peaks could not be sufficiently separated to be

integrated individually due to chemical shift anisotropy. Using a similar approach as that used for PB400-Ts, the substitution degree was evaluated to be DS_{TS} = 0.28 and DS_{N3} = 1.28 by difference.

Although the NMR spectroscopy substitution degree is different than that of the substitution degree calculated using elemental analysis, all characterisation methods (NMR, FTIR and elemental analysis) point in the same direction — a majority of the tosylate groups have been removed from the anhydroglucose ring and have been replaced with azide moieties. GPC analysis indicates that a high-molecular weight polymer is obtained (M_n = 67 kDa).

The heat of combustion is obtained using bomb calorimetry, ΔH_c^o = 186.1 kJ g^{-1}. The heat of formation of PB400-N3 is obtained from elemental analysis assuming complete combustion to CO_2, H_2O, N_2 and SO_2 ($\Delta H_{f\,PB400-N3}^o$ = 170.0 kJ mol^{-1}). The elemental analysis results are used in this case since they are more reproducible than 1H NMR results. Density was measured using gas pycnometry and is evaluated as ρ = 1.49 g cm^{-3}. From the heat of explosion, density and elemental analysis, the thermodynamic property of PB400-N3 using CHEETAH V2 thermochemical code can be evaluated.

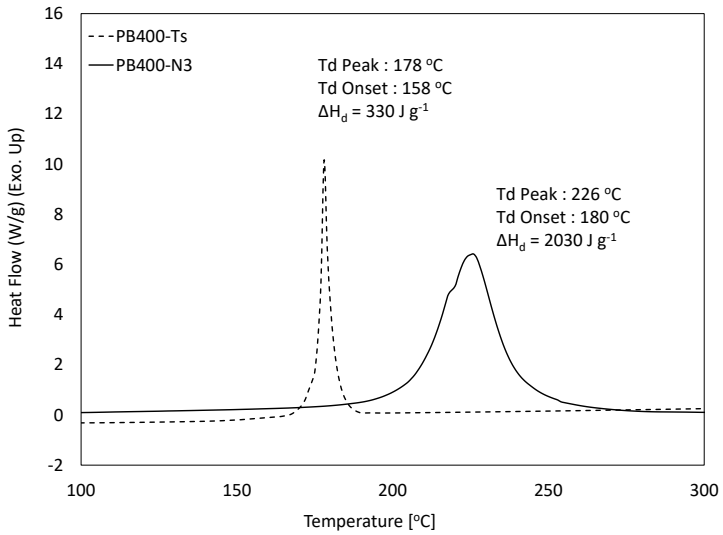

Figure 6-2 DSC thermogram of PB400-Ts and PB400-N3.

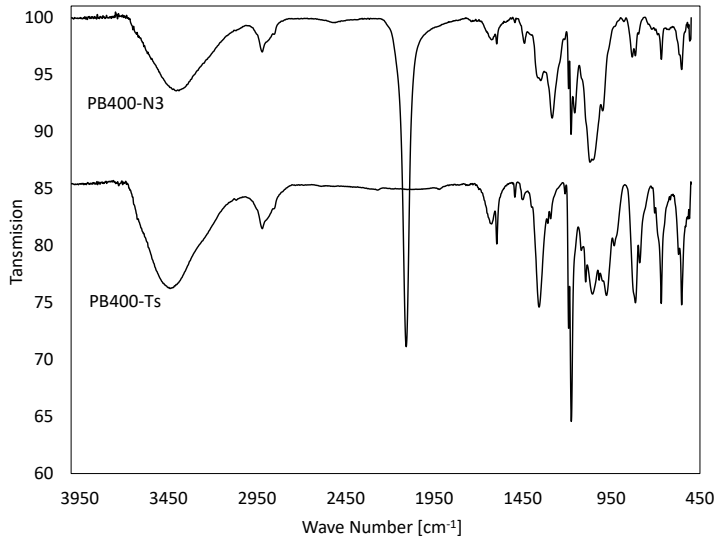

Figure 6-3 Ft-IR spectrum of PB400-N3 (top) and PB400-Ts (bottom).

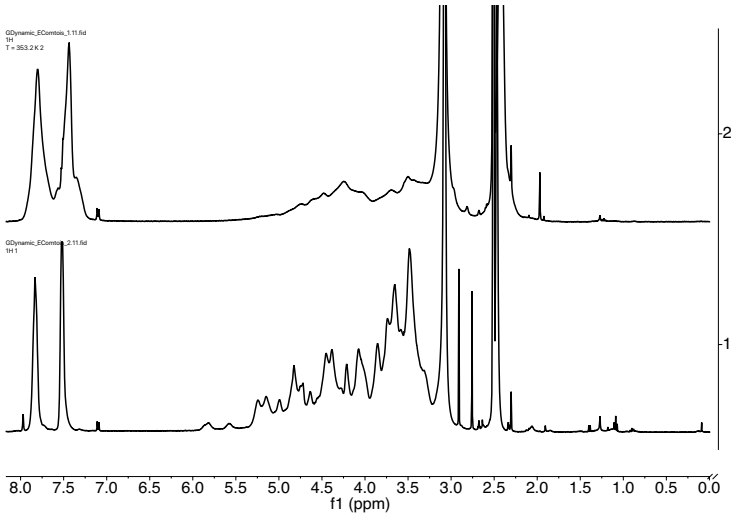

Figure 6-4 1H NMR analysis of PB400-Ts (top) and PB400-N3 (bottom).

6.4.3 Thermochemical properties and maximum pressure

A total of seven formulations were manufactured using the roll-milling method and were tested in CV. The binder was chosen to be 70 wt% NC12.5%N and 30 wt% in NG. To this binder 13, 26 and 40 wt% of PB400-N3 were added to the formulation. In order to have a comparison between

the combustion property of PB400-N3 and NC, the two materials were compared at a similar substitution degree (DS_{NO2} = DS_{N3+Ts} =1.71). A DS_{NO2} of 1.71 in NC would represent a value of 910 %N. Such NCs are not commercially available. For this reason, it was decided that a mixture of NC12.5%N and PB400 would be added in a ratio of 80 wt% NC and 20 wt% cellulose to obtain an equivalency between AC and NC. The chemical compositions are presented in Table 6-2.

The thermochemical properties calculated using CHEETAH properties are reported in Table 6-3. The nomenclature is as follows: DB stands for double base and refers to the binder comprised of 70 wt% of NC and 30 wt% of NG, MDB-N3 stands for a modified double base with PB400-N3 added and MDB–Cell stands for a modified double base in which a mixture of NC and cellulose is added so that that DS_{NO2} = 1.71. For example, MDB-N3(26) refers to a propellant formulation in which 26 wt% of PB400-N3 is added and MDB-Cell(26) refers to a propellant formulation in which 26 wt% of a mixture of cellulose and NC is added.

Table 6-2 Chemical compositions and oxygen balance of the evaluated formulations.

	NC12.5%N [wt%]	**NG [wt%]**	**PB400 [wt%]**	**PB400-N3 [wt%]**	**%OB**
DB	70.00	30.00	-	-	-23
MDB-N3(13)	60.9	26.1	-	13.0	-34
MDB-N3(26)	51.8	22.2	-	26.0	-45
MDB-N3(40)	42.0	18.0	-	40.0	-57
MDB-Cell(13)	71.0	26.1	2.9	-	-27
MDB-Cell(26)	72.1	22.2	5.7	-	-31
MDB-Cell(40)	73.2	18.0	8.8	-	-35

Table 6-3 Thermochemical properties and maximum pressure recorded in CV.

	T [K]	**Impetus [J g^{-1}]**	**Gas Mw [g mol^{-1}]**	**$P_{Max}^{CHEETAH}$ [MPa]**	**P_{Max}^{CV} [MPa]**
DB	3656	1149	26.461	284.2	228.8
MDB-N3(13)	3350	1133	24.587	284.3	246.0
MDB-N3(26)	3009	1091	22.933	278.3	223.3
MDB-N3(40)	2636	1022	21.448	265.7	212.8
MDB-Cell(13)	3474	1119	25.810	277.8	231.2
MDB-Cell(26)	3275	1082	25.157	269.6	215.6
MDB-Cell(40)	3048	1036	24.468	259.1	196.4

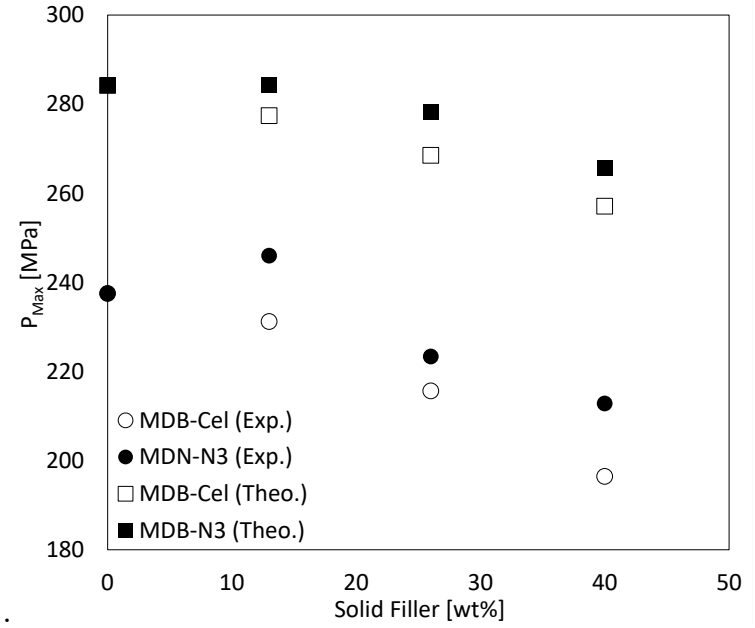

Figure 6-5 The P_{Max}^{CV} and $P_{Max}^{CHEETAH}$ obtained for MDB-Cell and MDB-N3 at various filler concentrations.

On average, the recorded maximum pressure in the CV (P_{Max}^{CV}) is 82 ± 3 % of the pressure evaluated using CHEETAH ($P_{Max}^{CHEETAH}$). This variation in pressure is explained by the heat losses with the walls of the CV and was confirmed using double base propellant in CVs of various volume. Previous work, showed that the pressure generated in 700, 200 and 100 cm^{-3} CV at a loading density of 0.2 g cm^{-3} was respectively 95, 93 and 84 % $P_{Max}^{CHEETAH}$. Values are presented in Supporting Information Figure S8.

Measuring 82 ± 3 % of the theoretical pressure is therefore expected. Also, the theoretical pressure is in accordance with the pressure generated in the CV given that they both follow the same trend as depicted in Figure 6-5.

From the thermochemical results and the observed pressure in the CV, one can see the advantage of using AC compared to NC at an equivalent substitution degree. At all concentrations, the theoretical and experimental pressures are higher for the MDB-N3 formulation, while flame temperatures are lower (Figure 6-6).

This increase in pressure is explained since the average molecular weight of the combustion gases of MDB-N3 formulations are lower than that of MDB-Cel as shown in Figure 6-5. Consequently, an increase in total product concentration is expected.

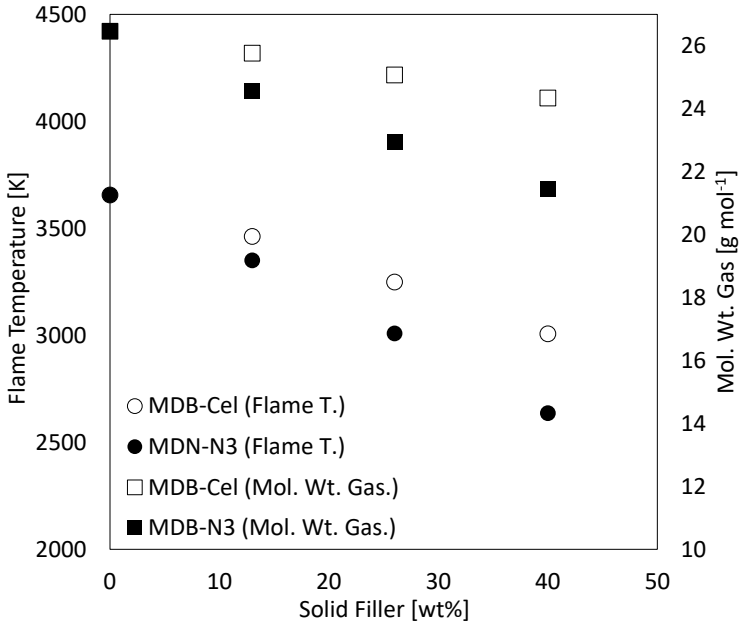

Figure 6-6 Flame temperature and average gas molecular weight obtained from CHEETAH for MDB-Cell and MDB-N3 at various solid filler concentrations.

From Figure 6-7, both modified propellant formulations show that the total product concentration from combustion gases increases as a function of the concentration of both solid filler in the propellant formulation. The maximum product concentration for MDB-Cel(40) and MDN-N3(40) are, respectively, 41 and 46 mol kg^{-1}. In comparison, the total product concentration for the DB formulation is 37 mol kg^{-1}. The increase for MDB-Cel is associated with the reduced production of CO_2 and H_2O and with the increased production of CO and H_2 due to the reduced oxygen balance in the formulation. The addition of a mixture of tosylate and azide on the cellulose moieties not only leads to a reduced oxygen balance and an increase in CO and H_2 generation, but also to an increase in N_2 production. For this reason, the total product concentration is increased for MDB-N3 as well.

From the theoretical pressure predicted by thermochemical code, there is an advantage to using cellulose, which is substituted with azide moieties, as compared to NC when both are substituted at DS = 1.71. The results have been confirmed using CV measurements.

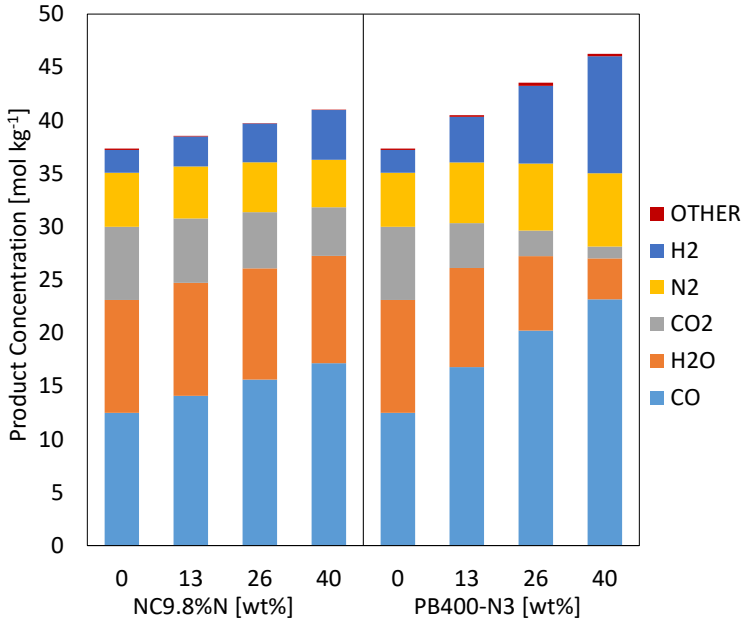

Figure 6-7 Product concentration obtained from CHEETAH for MDB-Cell and MDB-N3.

6.4.4 Linear burning rate

The LBR is estimated from the pressure-time curves obtained in the CV, the thermochemical properties obtained using CHEETAH and the geometrical dimensions of the propellant formulation. The density was measured using a gas pycnometer and is found to be within 3% of the theoretical value obtained using CHEETAH, indicating that no porosity is present in the propellant. Using the burning rate regression software BRLCB, the LBR curves were obtained and the burning parameters were calculated according to Vieille's Law from 40 MPa to 90 $\%P_{Max}$ measured in CV.

$$r = \beta P^{\alpha} \qquad (6.1)$$

Where r is the LBR in cm s^{-1}, β is the LBR coefficient, P is the pressure expressed in MPa and α is the pressure exponent. The α and β parameters are presented in Table 6-4 and LBR curves for MDB-Cel and MDB-N3 are presented in Figure 6-8.

Table 6-4 LBR parameters obtained in CV at 21 ºC calculated from 40 MPa to 90 %PMax.

	α	β	R^2
DB	0.71 ± 0.01	0.56 ± 0.03	1.00
MDB-N3(13)	0.73 ± 0.01	0.47 ± 0.02	1.00
MDB-N3(26)	0.75 ± 0.01	0.39 ± 0.02	1.00
MDB-N3(40)	0.77 ± 0.02	0.32 ± 0.01	1.00
MDB-Cell(13)	0.71 ± 0.02	0.52 ± 0.03	1.00
MDB-Cell(26)	0.69 ± 0.01	0.49 ± 0.03	0.99
MDB-Cell(40)	0.68 ± 0.03	0.41 ± 0.03	0.99

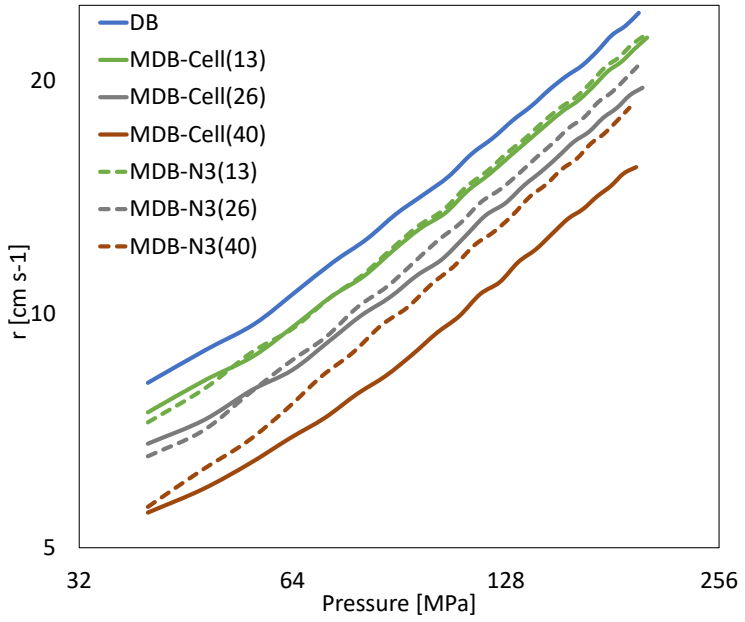

Figure 6-8 LBR for DB, MDB-Cell and MDB-N3 propellant formulations.

From Table 6-4 and Figure 6-8, one notes that the Vieille law parameters for the double-base propellant is $\alpha = 0.71 \pm 0.01$ and $\beta = 0.56 \pm 0.03$. The LBR results are similar to those obtained in

recent unpublished research using the same apparatus and the identical composition on formulation extruded with a cylindrical geometry. The Vielle coefficients were found to be $\alpha = 0.79 \pm 0.01$ and $\beta = 0.38 \pm 0.02$ which are very close to those measured with the rectangular strip propellant in this study. This result is to be expected.

Prior work on the evaluation of NC12.5%N plasticized with NG without the presence of solid fillers demonstrates that an increase in NG concentration increases the α of the propellant. From the ratio of NG and NC12.5%N for both formulations in Table 6-2, it can be observed that the ratio is kept constant for MDB-N3 formulations, while it diminishes for MDB-Cell formulations since a mixture of NC and Cellulose is added. From the binder composition alone, it is expected that α will diminish for MDB-Cell, but remain unchanged for MDB-N3. It can be observed in the results obtained that α for the MDB-N3 formulations increases while it should remain unchanged, and that the value for MDB-Cell is kept constant while it should diminish. Both findings indicate that, in this case, the addition of a solid filler influences the burning rate in a way that increases the pressure exponent.

One possible explanation is that the addition of the fibrous cellulose in MDB-Cell or the pulverised PB400-N3 acts as a discontinuity in the material, allowing an increase in flame propagation and an overall increased burning rate. The fact that the concentration in solid filler is 2.9, 5.7 and 8.8 for MDB-Cell formulations, compared to 13.0, 26.0 and 40.0 wt%, accounts for the high increase in the overall burning rate between both formulations.

6.5 Conclusion

The objective of this research was to evaluate propellant formulations using NC plasticized with NG and containing AC as a solid filler. AC was obtained in a two-step synthesis and displays a partial substitution of the hydroxyl group and an incomplete substitution of the tosylate moieties ($DS_{N3} = 1.52$ and $DS_{TS} = 0.19$). The material generates more pressure in a CV when compared to a mixture of NC and cellulose having a similar substitution degree in a hydroxyl group. The CV analysis of a formulation containing 13 wt% of AC also proves to generate greater pressure than the binder itself, which is in accordance with the theoretical calculation obtained with CHEETAH V2. Finally, the LBR was calculated. The presence of both solid fillers increased the LBR pressure

exponent when compared to similar propellant binder formulations evaluated in the same experimental setup, but without the presence of solid fillers.

Overall, the addition of partially-tosylated AC proves to be an effective way of increasing the maximum pressure of a propellant and does not generate LBR behaviour outside of what can be used for a propellant application.

Further research is necessary to increase the substitution degree of tosylated cellulose and to improve the conversion of tosylate to azide. In addition, other synthesis pathways such as the one proposed by Schmidt et al. [8] should be investigated, as the method in this study used large quantities of harmful organic solvents, making it impractical for large-scale production.

6.6 Acknowledgements

The authors would like to thank Mrs. Sophie Balaguer and Mr. Denis Sens from Rayonier Advanced Material and to Mr. Claude Guillaume from Manuco for providing the material needed for this work. The authors are extremely grateful to all the laboratory and pilot plant technicians involved in this project from General Dynamics Ordnance and Tactical Systems Canada Valleyfield. We would like to especially thank Mrs. Annie Fergusson, Mr. Denis Paquin, Mr. Guillaume Côté, Mr. Richard Beaulieu, Mr. Jean-Maxime Chatigny and Mr. Mathieu Lafleur for their work on the closed vessel, without whom it would not have been possible to complete this study.

CHAPTER 7 COMPLEMENTARY RESULTS

The findings presented in Chapter 6 show that AC cannot be compounded with traditional solvent used in the manufacturing of extruded propellant. In order to better understand the interaction between the selected polymers (NC, NG and GAP), this section will use the Flory-Huggins Solution and the approximation proposed by Scott to predict polymer compatibility.

7.1 Flory-Huggins Solution Theory

According to the Flory-Huggins Solution Theory, the free energy of mixing (ΔG_{mix}) can be described using (7.1):

$$\Delta G_{mix} = RTV\left\{\frac{\phi_A \ln \phi_A}{\widetilde{V_A}} + \frac{(1-\phi_A)\ln(1-\phi_A)}{\widetilde{V_B}}\right\} + \widetilde{V_{AB}}\phi_A(1-\phi_A) \qquad (7.1)$$

Where $\Delta G_{mix}$is the free energy of mixing; R, the universal constant; T, the temperature; V, the volume; ϕ_i, the volume fraction of species i; $\widetilde{V_i}$, the molar volume of I; and $\widetilde{V_{AB}}$, the interaction parameters between both species [131].

From equation (7.1), Scott developed the following formula for the interaction between two polymers (A and B) (7.2):

$$\Delta G_{mix} = \frac{RTV}{V_R}\left\{\frac{\phi_A}{x_A}\ln \phi_A + \frac{\phi_B}{x_B}\ln \phi_B + \chi_{AB}\phi_A\phi_B\right\} \qquad (7.2)$$

Where V_R is the reference volume taken as close to the molar volume of the smallest repeating unit; x_i, the degree of polymerization of i; and χ_{AB}, the enthalpy of interaction of the polymer repeating unit. χ_{AB} can be expressed using the solubility parameters (7.3) [131].

$$\chi_{AB} = \frac{V_R}{RT}(\delta_A - \delta_B)^2 \qquad (7.3)$$

Where $\delta_i$is the solubility parameter of i.

By having T = 25°C and by assuming a reference volume of V_R= 100 cm^3 mole^{-1}, which is a good first approximation, one can simplify (7.3) into (7.4).

$$\chi_{AB} \approx \frac{(\delta_A - \delta_B)^2}{6} \quad (7.4)$$

From (7.2), Scott showed that the critical condition for the solubility of a system (7.5) is met under three conditions (7.6)(7.7)(7.8).

$$\frac{\delta^2 \Delta G_{mix}}{\delta {\phi_A}^2} = \frac{\delta^3 \Delta G_{mix}}{\delta {\phi_A}^3} = 0 \quad (7.5)$$

$$(\chi_{AB})_{cr} = \frac{1}{2}\left[\frac{1}{{x_A}^{0.5}} + \frac{1}{{x_B}^{0.5}}\right]^2 \quad (7.6)$$

$$(\phi_A)_{cr} = \left[\frac{{x_B}^{0.5}}{{x_A}^{0.5} + {x_B}^{0.5}}\right]^2 \quad (7.7)$$

$$(\phi_B)_{cr} = \left[\frac{{x_A}^{0.5}}{{x_A}^{0.5} + {x_B}^{0.5}}\right]^2 \quad (7.8)$$

Furthermore, x_i can be described using the molar volume of the repeating unit ($\tilde{V}$), the reference volume (V_r) and the degree of polymerization (x) (7.9).

As a first approximation, (7.10) can be used, where (M_A) is the molecular weight of polymer A. (7.6) can then be rewritten as (7.11).

$$x_A = \frac{\tilde{V}}{V_R} \quad (7.9)$$

$$x_A \approx \frac{M_A}{100} \quad (7.10)$$

$$(\chi_{AB})_{cr} \approx \frac{1}{2}\left[\frac{1}{\left(\frac{M_A}{100}\right)^{0.5}} + \frac{1}{\left(\frac{M_B}{100}\right)^{0.5}}\right]^2 \quad (7.11)$$

From the critical condition, Scott established that when $\chi_{AB} > (\chi_{AB})_{cr}$, it is expected that the two polymers will be incompatible at some concentration.

Therefore, polymer compatibility can be predicted as long as the solubility parameters and molecular weights of the polymers are known.

7.2 Molecular weight determination using gel permeation chromatography

From Chapter 4, NC11%N-LV, NC11%N-HV, NC12.5%N-HV, GAP-0700 and GAP5527 are obtained (see Table 7-1).

Using the GPC procedure described in Chapter 4, molecular weight for NC13.4%N-HV from Eurenco (Bergerac, France) is obtained (see Table 7-1).

From Chapter 6, the molecular weight for AC is obtained (see Table 7-1).

Table 7-1 Mn and polydispersity index (PDI) of NCs, GAPs and AC (PB400-N3) measured by GPC.

ID	Mn [kDa]	PDI
NC11%N-LV	27	2.78
NC11%N-HV	59	3.44
NC12.5%N-HV	42	3.57
NC13.4%N-HV	35	3.06
GAP-5527	4.8	1.24
GAP-0700	0.9	1.20
PB400-N3	67	1.76

7.3 Solubility parameter determination

The solubility parameter is a numerical estimate of the degree of solubility between two liquids or polymers. Liquids with similar solubility parameters will be miscible in one another and polymers will be solvated by solvents having similar solubility parameters — or, “like dissolves like” [132].

The Hansen solubility parameters (δ_T) are described as three parameters representing the energy from the dispersion forces (δ_d), from the dipole forces (δ_p) and from the hydrogen bonds (δ_h) between molecules. Each parameter is expressed as $MPa^{0.5}$.

$$\delta_T{}^2 = \delta_d{}^2 + \delta_p{}^2 + \delta_h{}^2 \qquad (7.12)$$

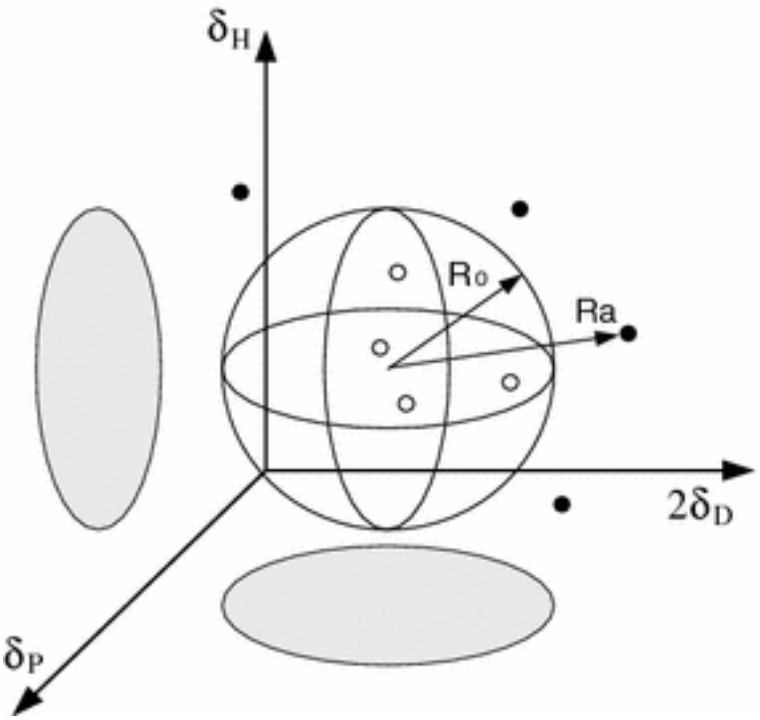

Figure 7-1 Solubility sphere of a polymer [133].

Hansen solubility parameters for common solvents are known and available in the literature [132]. The solubility parameter of a polymer can be established by taking the polymer and attempting to dissolve it in a series of solvents. In time, the solutions are observed, and a score assigned depending on the solubility of the polymer in the solvent.

By tracing the solvent interaction in a three-dimensional graph, a solute sphere of radius *R* is obtained where the good solvents are located inside the sphere and the bad solvents on the outside. The solubility parameters of the polymer are in the centre of the sphere. (Figure 7-1) [133].

Following this procedure, a sample of approximately 0.2 g of NCs, GAPs and AC was placed in contact with a series of solvents. After 48 hours at ambient temperature, a score of 1 was assigned to a clear solution and a score of 0 to a solution where the polymer did not dissolve. An example is provided in Figure 7-2 for NC11%N-LV. The experimental solubility results are presented in Annex A Table S 3.

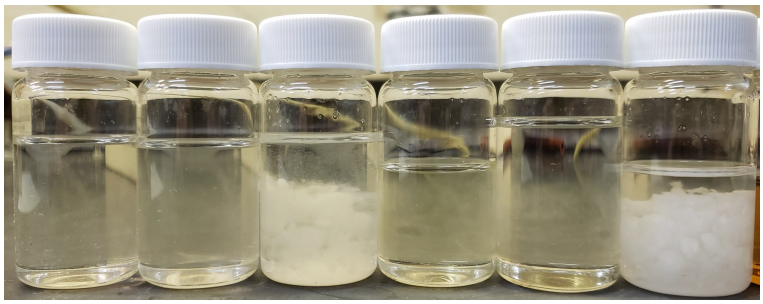

Figure 7-2 NC11%N-LV in (from left to right): acetic glacial, methyl isobutyl ketone, cyclohexanol, ethylene glycol monoethyl ether acetate, di propylene glycol, and 4-methyl-2-pentanol scores are, respectively, 1, 1, 0, 1, 1 and 0.

$$D^2_{(1,2)} = (\delta_{d1} - \delta_{d2})^2 + \left(\delta_{p1} - \delta_{p2}\right)^2 + (\delta_{h1} - \delta_{h2})^2 \qquad (7.13)$$

Using the HSPiP software, the Hansen solubility parameters are obtained and are presented in Table 7-2.

From Table 7-2, the NCs all present identical values, except for NC13.4%N, which did not solubilize in methanol. This is expected as the lower hydroxyl value of the NC will reduce its solubility in polar solvent. In addition, the GAPs show similar values. For both these reasons, Table 7-2 can be simplified into Table 7-3.

Using the three-dimensional graph as a representation (Figure 7-1), the distance between two points can be used to evaluate the affinity between two polymers and is obtained using (7.13). If the two centres are very close to one another, affinity between both polymers will be high; if they are far apart, affinity will be diminished.

From the values in Table 7-3 and (7.13), the distance between the centre sphere for NCs, GAPs and AC is calculated and presented in Table 7-4.

Chapter 4 demonstrated that GAP is not an efficient plasticizer for NCs. Table 7-4 shows that the affinity between GAPs and NCs is superior than the affinity between GAP and AC. One can thus conclude it is even more difficult to combine AC and GAPs together and that, as in the case of NCs, a low-molecular weight plasticizer will have to be used.

Table 7-2 Hansen solubility parameters for NCs, GAPs and AC (PB400-N3).

	δ_d	δ_h	δ_P	δ_T	R
11%N-LV	16.7	12.4	6.9	21.9	9.3
11%N-HV	16.7	12.4	6.9	21.9	9.3
12.6%N-HV	16.7	12.4	6.9	21.9	9.3
13.4%N-HV	17.0	12.1	7.0	21.9	9.2
GAP-0700	17.2	11.0	5.3	21.1	10.3
GAP-5527	17.3	10.5	5.0	20.8	9.7
PB400-N3	19.8	14.4	13.4	27.9	9.7

Table 7-3 Simplified Hansen solubility parameters of NCs, GAPs and AC.

	δ_d	δ_h	δ_P	δ_T	R
NCs	16.7	12.4	6.9	21.9	9.3
GAP	17.3	10.5	5.2	21.0	10.0
PB400-N3	19.8	14.4	13.4	27.9	9.7

Table 7-4 Distance between the centre of the solubility sphere between NCs, GAPs and AC (PB400-N3) given in $MPa^{0.5}$.

	NCs	**PB400-N3**
PB400-N3	7.5	-
GAPs	2.2	9.2

7.4 Predicting compatibility

Having the molecular weight and solubility parameters of the polymers, it is possible to perform a first evaluation of the compatibility between the polymers.

From the critical condition, it can be stated that when $\chi_{AB} > (\chi_{AB})_{cr}$, it is expected that the two polymers are insoluble at some concentration. This can also be written as $\chi_{AB}/(\chi_{AB})_{cr} > 1$.

Using the data from Table 7-1, Table 7-2, (7.4) and (7.11), $\chi_{AB}/(\chi_{AB})_{cr}$ is calculated and the values presented in Table 7-5.

Table 7-5 $\chi_{AB}/(\chi_{AB})_{cr}$ for NCs, GAPs and AC (PB400-N3).

	11%N LV	**11%N HV**	**12.5%N HV**	**13.4%N HV**	**GAP 0700**	**GAP 5527**
11%N-HV	0.0					
12.5%N-HV	0.0	0.0				
13.4%N-HV	0.0	0.0	0.0			
GAP-0700	1.3	1.5	1.4	1.4		
GAP-5527	9.8	12.0	11.0	11.0	0.1	
PB400-N3	1212	1884	1570	1415	106	513

Based on the results presented in Table 7-5, six conclusions can be drawn:

- NCs are compatible with one another. This is expected as all solubility parameters were identical or very similar.
- Even though $\chi_{AB}/(\chi_{AB})_{cr}$ is greater than 1 for GAP-0700 and GAP-5527 with regard to NCs, due to the approximation made, it is likely that NCs are incompatible with GAPs on a narrow range of concentration.
- GAP-0700 and GAP-5527 are compatible with one another. This is expected as all solubility parameters were very similar and from the low-molecular weight.
- NCs are incompatible with PB400-N3 on a wide range of concentration.
- GAPs are incompatible with PB400-N3 on a wide range of concentration.
- NCs are expected to be incompatible with GAP on a much narrower range of concentration when compared to PB400-N3.

The results observed in this chapter are consistent with the observations in Chapter 4 and Chapter 6, where the higher-molecular weight GAP-5527 showed less affinity with NCs and where AC would not solubilize with a mixture of solvent typically used in propellant processing.

According to these findings, it is unlikely that NCs and AC alone will form an efficient binder system and that compatibilization of both polymers will be required.

More studies are necessary as the substitution degree of the AC here was incomplete and the tosylate residual groups were still present (DS_{N3} = 1.47; DS_{TS} = 0.18). Having a completely

substituted cellulose backbone will more likely affect the solubility parameters of the resulting polymer.

CHAPTER 8 GENERAL DISCUSSION AND FUTURE CONSIDERATIONS

One of the principal conclusions that can be drawn from the three previous chapters is that the use of azido polymers, either as a plasticizer, ballistic modifier or solid fillers, allows for better control of the modification combustion properties (LBR and erosivity) of an energetic formulation based solely on nitro-bearing energetic material, without contributing adversely to its mechanical properties.

One aims of this research was to demonstrate the usefulness of low-molecular weight azido polymers as part of an energetic plasticizer system for energetic polymers and to obtain their mechanical and combustion properties. The choice of energetic polymers and energetic plasticizers was based on commercial availability, ease of transportation and safety concerns. The choice of NC was based on the fact that is readily available in many ranges of viscosity and nitrogen content, is inexpensive, and is proven to have affinities with various plasticizers such as low-molecular weight nitro plasticizer. NG and GAP were chosen as both are commercially available and have been used as part of the NC binder system in propellant applications.

Although GAP alone did not prove to be an efficient plasticizer, due to its inability to situate between NC polymer chains, when used as part of a plasticizer system with NG, good plasticization of NC is obtained. This is covered in detail in Chapter 4, where it is shown that small-molecular weight energetic plasticizer has sufficient mobility to situate between and separate the NC chains, allowing larger polymeric plasticizers to then be inserted, thus acting as an effective plasticizer.

The usage of a plasticizer system comprised of plasticizers and low-molecular weight polymers is not common in industry. From a migration standpoint, it is expected that having a mixture of plasticizers will reduce mobility of the low-molecular weight polymer when one is of larger molecular weight. In Chapter 4, it was demonstrated that it was possible to replace a portion of the quantity of NG with GAP without reducing mechanical properties. Because NG is a volatile compound, it is expected that a mixture of NG and GAP will reduce migration of NG in the material. This has yet to be proven and will be addressed in future work.

From the combustion standpoint, it is found that the addition of GAP to a NC/NG formulation allows for reduced erosivity and a reduced linear burning rate. It is also found that pressure

reduction can be avoided with the help of a thermochemical calculator such as CHEETAH, as it is demonstrated experimentally that both theoretical and experimental pressure are in accordance with one another for formulations comprised of GAP, NC and NG.

When looking at more specific applications, such as the manufacturing of thermoplastic-sheeted material used in the thermoforming of combustible items, the T_g of the material has to be low enough to allow for the safe processing of the material, yet high enough to provide suitable mechanical properties throughout the operating temperature of the item, while ensuring the complete combustion of the item throughout the ballistic cycle.

An example of such an application is the design of a thermoformable combustible container used in a mortar application as depicted in Figure 2-26. Its T_g must be no greater than 130 ^{o}C and no less than 90 ^{o}C and its combustion must be completed no later than 10 ms after ignition of the main propellant charge. The pressure generated by the main propellant charge is shown in Figure 8-1.

Using the information in Chapter 4, T_gs ranging from 90^{o}C to 130^{o}C can be obtained as a function of various plasticizer conditions. For this example, a formulation comprised of 80 wt% of NC12.5%N, 10 wt% of NG and 10 wt% of GAP is chosen.

From the LBR parameters obtained in Chapter 5 and using the pressure-time curve (Figure 8-1), one can use the Vieille's law to calculate the thickness burned for the selected formulation. From the calculation a thickness of up to 1.02 mm of material would have been consumed as shown in Figure 8-1 at 10 ms. One can then also assume that a container having a wall thickness of 1.02 mm thick would have completely burned in such an application. Also, from the CHEETAH calculations, no solid carbon in generated by such formulation. It can therefore be assumed that the material is going to achieve complete combustion with no residual soot.

Such calculations can be used by engineers and scientists working with EMs to better select the choice of materials when developing combustible applications.

Another application of this work is in the design of novel gun propellants. In **Error! Reference source not found.**, it was explained that a propellant must have a specific shape in order to be suited for a particular application and that a propellant formulation could be used for both a hunting rifle and an artillery round as long as the geometry is adjusted.

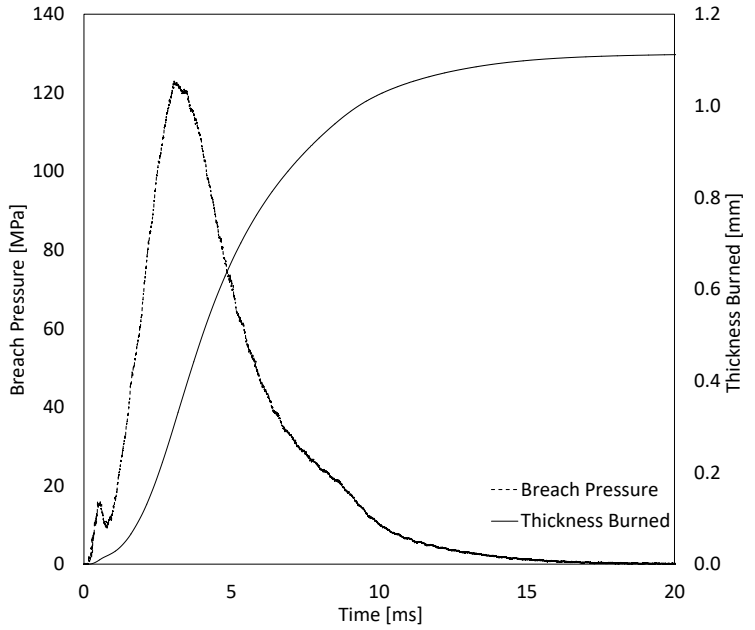

Figure 8-1 Typical breach pressure-time curve in a 120 mm mortar and total thickness burned for a propellant container manufactured with NC12.5%N/NG(10)/GAP(10).

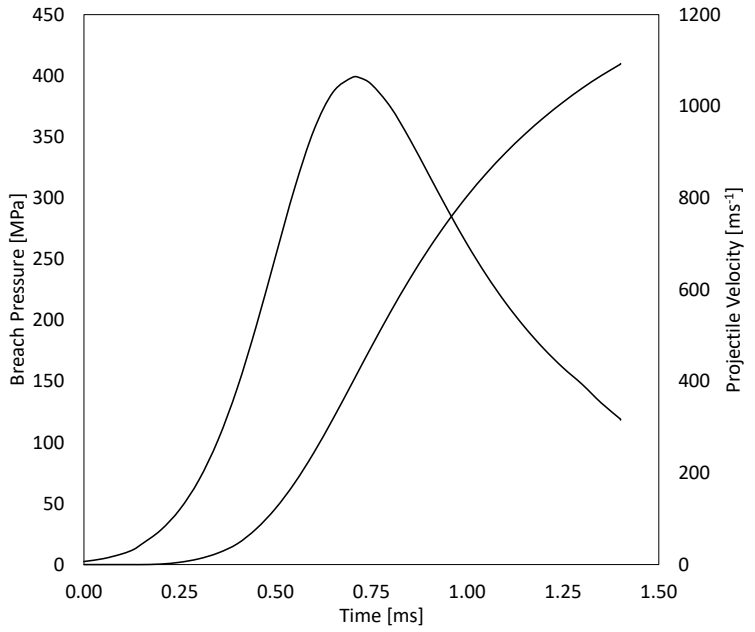

Figure 8-2 Calculated pressure-time curve and projectile velocity when using a charge of 14.5 g of a single perforated propellant (NC12,.5%N/NG(10)/GAP(10)) in a 12.7 mm caliber carbine and a light 24 g projectile using PLAYBALL ballistic software.

Using ballistic simulation software such as PLAYBALL by Denis Lester, the ballistic performance for a propellant in a gun system can be predicted if the following information is known:

- Thermochemistry of the propellant formulation
- LBR of the propellant
- Geometry of the propellant
- Gun parameters (bore diameter, rifling, caliber, maximum breach pressure, etc.)
- Projectile parameters (mass, length, caliber, driving band etc.)
- Allowable case volume

Not all of these parameters have been reviewed in this work. Fortunately, thermochemical software such as CHEETAH are able to provide thermochemical properties of the propellant and PLAYBALL already has in its database a series of guns and projectiles for which calculations can be performed. Using the LBR obtained in Chapter 5 or Chapter 6, in combination with the thermochemical properties of a chosen propellant and ballistic software, the propellant geometry for a given system can be determined.

As an example, a charge of 14.5 g of a single perforated propellant comprised of 80 wt% of NC12.5%N, 10 wt% of NG and 10 wt% of GAP, having an outside diameter of 1.08 mm, a perforation diameter of 0.108 mm and a height of 1.08 mm, would generate 398 MPa measured at the breach face and a projectile velocity of 1093 ms^{-1} when using a 12.7 mm caliber carbine and a light 24 g projectile (Figure 8-2).

This calculation was performed using ambient temperature data (21 ^{o}C), but data is now available for it to be carried out at -46 ^{o}C and 63 ^{o}C as well.

Depending on the weapon systems, there is frequently a trade-off between erosivity and performance. For example, it is reported that the average life expectancy of a tank crew during the Second World War ranged from two to six weeks [134], while a tank like the Sherman had a duration of approximately 1,500 to 2,000 miles [135]. To ensure the crew's safety, the ability to engage targets at long distance takes precedence over the erosivity of the propellant.

In comparison, artillery support has always been based on a sustained and extensive volley of fire. The German artillery guns near Aachen fired an average of 22.5 rounds per gun per day between

October 2 and October 21,1944 [136]. From this point of view, the erosivity of a propellant becomes a logistical issue as it will increase the maintenance associated with the bore replacement.

From this previous example, it was demonstrated that ballistic cycle could be evaluated. Using the results presented in Chapter 5, erosivity can also be included in the modeling to help decide which formulation would provide enough impetus while keeping erosivity to a minimum.

The combination of the results from Chapter 4 and Chapter 5 can be used as a first approximation of the properties of a NC/NG/GAP binder with precaution as the manufacturing method used was not the same for samples. The mechanical properties were obtained using the film-casting method, while the combustion properties were obtained using the two-roll mill solvent extruded process. It is known in the polymer industry that the properties of a material is not only affected by it's chemical composition, but by its macro and micro structure and both are altered by the manufacturing process. As an example, the manufacturing of sheeted material using large quantity of solvent would allow for better dissolution of the NC fibers and increased mobility of the plasticizers when compared to the solvent extruded method.

An indication of this is that, a film comprised of 80 wt% 12.5%N-HV, 10 wt% GAP-0700 and 10 wt% NG manufactured using the solvent-casting method was flexible and firm to the touch. When preparing the same formulation using the two-roll mill the material felt brittle and tough and would even snap when cutting it. SEM analysis of the solvent extruded formulation comprised of 60 wt% 12.5%N-HV and 40 wt% were taken following the procedure described in 4.3.4. Compared to the film-casting sample, no distinct GAP phase was present.

This is a good indication that the manufacturing process of NC/NG/GAP does affect the property of the material. A way of explaining these observations is that the mobility of GAP is reduced due to the low concentration of solvent and NG in the two-roll mill process. This reduces it's ability to situate between NC chains reducing the overall plasticization of NC chains. The lack of distinct GAP phase can be explained by the high shear from the two-roll mill mixing not allowing for the formation of liquid GAP droplet in the material.

This is only a hypothesis and it will be interesting to see in the future how the manufacturing process influences the properties of NC/NG/GAP material.

From Chapter 3, the evaluation of the LBR on film material is not recommended. For this reason, the understanding of the combustion behavior of films could be improved from their characterisation in sub-systems such as the gun interrupted burning method.

The synthesis of AC proved to be a challenge on many fronts. The difficulty to solubilize cellulose, the viscosity of the resulting solution, the large quantity of water trapped in the polymer after tosyalation, the vast amount of solvent needed to isolate and purify the samples meant that only a small quantity of AC could be obtained. For these reasons, it was decided that it would be best to characterise its combustion properties as part of a traditional propellant formulation and getting a first idea of the material properties.

AC proved unsuitable in a typical solvent ratio used in the compounding of a typical propellant. It did, however, prove to be a good substitute as a high-nitrogen additive at concentration below 26 wt%, as it does have some oxygen on the cellulosic backbone. This proves to be advantageous, since the low molecular weight of CO and H_2 reduces the overall gas molecular weight of the combustion species. If too much AC is added, however, the OB becomes too low, which can in turn lead to the generation of heavier gas species and ultimately to solid carbon. This could however be addressed using oxidizers in the formulation such as perchlorates and nitrates to increase the overall oxygen balance of the formulation.

As mentioned, the lack of material didn’t allow the erosivity of AC as part of a propellant formulation to be evaluated. Due to the similarity with the cellulosic backbone of NC and the azide moieties similar to that of GAP, it is possible to hypothesize that the erosivity will be in agreement with the Kimura-Arisawa theory [33] and that lower erosivity is expected.

CHAPTER 9 CONCLUSION

As was shown in Chapter 3, the manufacturing of an improved propellant formulation and of thermoformable combustible containers was limited by two factors: the lack of clean-burning thermoplastic binders and the lack of nitrogen-rich polymeric binders that allow for reduced erosion.

In order to address both these restrictions, polymers and plasticizers were selected according to their commercial availability, cost and ease of synthesis.

The main conclusions and contributions are as follows:

On the evaluation of the plasticization of NC with GAP. It was found that GAP alone does not have the ability to eficently plasticized NC. Although when mixed with a small molecular weight, such as NG, good plasticization is measured. The evaluation of plasticization using mixtures of plasticizers is not a subject well covered in the literature and allows for improved control over various properties of the material such as it's thermomechanical properties and combustion behavior.

On the evaluation of the LBR of NC/NG/GAP formulation. It was found that both GAP and NG have the ability to increase LBR of the resulting propellant, are following the thermodynamic predictions of the CHEETAH software. The evaluation of the LBR of such formulations were never evaluated as a function of temperature and from the thermomechanical results there seems to be a correlation between the increase in the LBR at 63 ^{o}C and the presence of a β relaxation. The erosivity of the formulation are in agreement with the Arisawa-Kimura relation. Using the results it is therefore possible to tailor a propellant formulation to a desired LBR or a desired relative erosivity.

On the evaluation of AC as part of a propellant formulation. It was found that it is a suitable candidate as a solid filler when compared to a NC with similar substitution degree. The resulting propellant showed a reduced LBR formulation when compared to the double based binder and proved to generate similar pressure in closed vessel.

From these conclusions, did we achieve our goals? Were we able to successfully manufacture a clean-burning thermoplastic binder and were we able to manufacture nitrogen-rich polymeric binders that allow for reduced erosion?

After all, thermoforming properties were expected since, T_gs ranging from 90 to 130 ºC were obtained, which is similar to that of other NC-based thermoplastic material. In addition, clean burning was expected since modeling can predict the material thickness at which complete combustion of the material occurs.

Although these are optimistic signs, we cannot claim with certainty that we achieved the manufacture of a clean-burning thermoplastic binder.

One reason for this is that the term "thermoplastic binder" is application-dependent and the thermal forming process must first be considered in order to develop a specific formulation that meets the requirements of the desired application. Also, the precise definition of "clean burning" is highly dependent on the firing conditions as demonstrated in the previous chapter.

For example, the conclusive demonstration of manufacturing of a clean-burning thermoformed material used in an application would require large quantities of sheeted material to be manufactured, would require access to a thermoforming machine capable of handling EMs and would require that the finished part be evaluated in a relevant environment, such as a instrumented test bed or a range using the actual system.

This is no small feat, since the manufacturing of sheets, the thermoforming of EMs. and the actual evaluation of prototypes all pose challenges related to the associated safety issues.

This study established the groundwork for subsequent research. We showed that, although GAP alone did not prove to be an efficient plasticizer, when used as part of a GAP/NG plasticizer system, good plasticization of NC can be measured. This may serve as the beginning of a larger research project on the influence of various energetic and non-energetic plasticizers on the mechanical and combustion properties of NCs.

The manufacturing of energetic binders for reduced erosion proved to be challenging. The insolubility of AC in most solvents prevents its transformation in the traditional propellant process. Other solvents such as DMF and pyridine may be used for processing but fell outside the scope of this study.

Although AC proved to be an efficient solid filler as part of NC/NG propellant formulations, it will be interesting to see if novel synthetic approaches will permit increased azide-moiety substitution

leading to improved ballistic performances and possibly increased compatibility in more common solvents.

Finally, methodological choices were made at the start of the research project with regard to the polymers and plasticizers studied. Since then, advances in energetic plasticizers [137] and polymers have been published in the literature [138], and the increasing availability of EMs suggests that low-molecular weight energetic polymers such as polyGLYN could be used as part of plasticizer systems in the coming years.

Finally, the successful synthesis of azido polymers using a tosylated route permits development of further novel compounds. Future research may consider the synthesis of other azido plasticizers for use in similar systems.

REFERENCES

[1] J. P. Agrawal and R. Hodgson, *Organic Chemistry of Explosives*. Wiley, 2007.

[2] R. Meyer, J. Köhler, and A. Homburg, "Explosives, Fifth, Completely Revised Edition," in *Explosives*: Wiley-VCH Verlag GmbH & Co. KGaA, 2003, pp. 1-23.

[3] H. G. Ang and S. Pisharath, *Energetic Polymers: Binders and Plasticizers for Enhancing Performance*. Wiley, 2012.

[4] M. Young *et al.*, "Propellant increment container, useful in mortar and artillery propulsion systems, comprises foamed celluloid containing nitrocellulose and camphor," Patent US8617328-B1 Patent Appl. US8617328-B1 US483420 12 Jun 2009, [Online]. Available: <Go to ISI>://DIIDW:2014A45508

[5] J. Akhavan, *The Chemistry of Explosives*. Royal Society of Chemistry, 2011.

[6] S. Jaramaz, D. Micković, and P. Elek, "Determination of gun propellants erosivity: Experimental and theoretical studies," *Experimental Thermal and Fluid Science,* vol. 34, no. 6, pp. 760-765, 2010/09/01/ 2010, doi: https://doi.org/10.1016/j.expthermflusci.2010.01.005.

[7] D. A. Reese, L. J. Groven, and S. F. Son, "Formulation and Characterization of a New Nitroglycerin-Free Double Base Propellant," *Propellants, Explosives, Pyrotechnics,* vol. 39, no. 2, pp. 205-210, 2014, doi: 10.1002/prep.201300105.

[8] S. Schmidt, T. Liebert, and T. Heinze, "Synthesis of soluble cellulose tosylates in an eco-friendly medium," *Green Chemistry,* 10.1039/C3GC41994K vol. 16, no. 4, pp. 1941-1946, 2014, doi: 10.1039/C3GC41994K.

[9] J. Kelly, *Gunpowder: Alchemy, Bombards, and Pyrotechnics: The History of the Explosive That Changed the World*. Basic Books, 2009.

[10] B. N. Agrawal and M. F. Platzer, *Standard Handbook for Aerospace Engineers, Second Edition*. McGraw-Hill Education, 2018.

[11] *Centra Control, Centra Intense, Centra Intense LD, Safety Data Sheet*, Safety Data Sheet O. USA, 2013.

[12] *Red Emergency Flare - No Perchlorate (NPC) Formulation*, Material Safety Datasheet O. S. Product, 2015.

[13] N. Kubota, *Propellants and Explosives: Thermochemical Aspects of Combustion*. Wiley, 2007.

[14] T. M. Klapötke, *Chemistry of high-energy materials*. Walter de Gruyter GmbH & Co KG, 2019.

[15] U. Teipel, *Energetic materials: particle processing and characterization*. John Wiley & Sons, 2006.

[16] J. P. Agrawal, *High Energy Materials: Propellants, Explosives and Pyrotechnics*. Wiley, 2010.

[17] A. K. Sikder and N. Sikder, "A review of advanced high performance, insensitive and thermally stable energetic materials emerging for military and space applications," *Journal of Hazardous Materials,* vol. 112, no. 1, pp. 1-15, 2004/08/09/ 2004, doi: https://doi.org/10.1016/j.jhazmat.2004.04.003.

[18] J. Lavoie, C.-F. Petre, P.-Y. Paradis, and C. Dubois, "Burning Rates and Thermal Behavior of Bistetrazole Containing Gun Propellants," *Propellants, Explosives, Pyrotechnics,* vol. 42, no. 2, pp. 149-157, 2017, doi: 10.1002/prep.201600091.

[19] T. Urbanski, *Chemistry and technology of explosives Vol.1*. Pergamon, 1964.

[20] A. Provatas, Aeronautical, M. R. L. W. S. Division, D. Science, and T. Organisation, *Energetic Polymers and Plasticisers for Explosive Formulations: A Review of Recent Advances*. DSTO Aeronautical and Maritime Research Laboratory, 2000.

[21] A. Mukhtar and H. Nasir, "Comparative Closed Vessel Firing-Ballistic Parameters Evaluation for Development of Base Bleed Composite Solid Propellant," *Engineering, Technology & Applied Science Research,* vol. 8, no. 6, pp. 3545-3549, 2018.

[22] M. Grivell, "The closed vessel test and determination of ballistic properties of gun propellants," Weapons Systems Research Lab Adelaide (Australia), 1982.

[23] D. E. Carlucci and S. S. Jacobson, *Ballistics: Theory and Design of Guns and Ammunition, Second Edition*. CRC Press, 2013.

[24] C. A. Heller and A. S. Gordon, "Structure of the Gas Phase Combustion Region of a Solid Double Base Propellant," *The Journal of Physical Chemistry,* vol. 59, no. 8, pp. 773-777, 1955/08/01 1955, doi: 10.1021/j150530a019.

[25] B. Lawton, "Thermo-chemical erosion in gun barrels," *Wear,* vol. 251, no. 1, pp. 827-838, 2001/10/01/ 2001, doi: https://doi.org/10.1016/S0043-1648(01)00738-4.

[26] D. Izod and R. Baker, "Gun wear: an account of recent UK research and new wear mechanisms," in *Proc. Tri-service Gun Tube Wear and Erosion Symp.*, 1982, p. 221.

[27] P. Conroy, C. Leveritt, J. Hirvonen, and J. Demaree, "The Role of Nitrogen in Gun Tube Wear and Erosion," p. 28, 05/01 2006.

[28] P. J. Cote and C. Rickard, "Gas–metal reaction products in the erosion of chromium-plated gun bores," *Wear,* vol. 241, no. 1, pp. 17-25, 2000/06/01/ 2000, doi: https://doi.org/10.1016/S0043-1648(00)00311-2.

[29] S. Sopok, P. O'Hara, G. Pflegl, S. Dunn, D. Coats, and G. Nickerson, "Unified Computer Model for Predicting Thermochemical Erosion in Gun Barrels," *Journal of Propulsion and Power,* vol. 15, no. 4, pp. 601-612, 1999, doi: 10.2514/2.5469.

[30] I. A. Johnston, "Understanding and predicting gun barrel erosion," in "Technical Report," Defense Science and Technology, Australia, DSTO–TR–1757, 2005.

[31] J. K. Hirvonen *et al.*, "Gun barrel erosion studies utilizing ion beams," *Surface and Coatings Technology,* vol. 196, no. 1, pp. 167-171, 2005/06/22/ 2005, doi: https://doi.org/10.1016/j.surfcoat.2004.08.218.

[32] J. Kimura, "Hydrogen gas erosion of high-energy LOVA propellants," in *16th Internal Ballistics Symposium*, 1996, vol. 1, p. 307.

[33] H. Arisawa and J. Kimura, "Applicability of the hydrogen gas erosion theory to conventional gun propellants," in *19th International Symposium of Ballistics*, Interlaken, Switzerland, 2001.

[34] D. Åberg, P. Hermansson, A. Sättler, and D. Rakus, "Plasma Ignition Response for LOVA Gun Propellant at Low Loading Densities," *IEEE Transactions on Plasma Science,* vol. 43, no. 5, pp. 1316-1320, 2015, doi: 10.1109/TPS.2015.2415591.

[35] J. Hunley, "The history of solid-propellant rocketry-What we do and do not know," in *35th joint propulsion conference and exhibit*, 1999, p. 2925.

[36] A. Elbeih, J. Pachman, W. A. Trzciński, S. Zeman, Z. Akštein, and J. Šelešovský, "Study of Plastic Explosives based on Attractive Cyclic Nitramines Part I. Detonation Characteristics of Explosives with PIB Binder," *Propellants, Explosives, Pyrotechnics,* vol. 36, no. 5, pp. 433-438, 2011, doi: 10.1002/prep.201000070.

[37] T. L. Davis, *The Chemistry of Powder and Explosives* (no. v. 1-2). Angriff Press, 1943.

[38] R. M. Kozlowski and M. Mackiewicz-Talarczyk, *Handbook of natural fibres: volume 1: types, properties and factors affecting breeding and cultivation*. Woodhead Publishing, 2020.

[39] H. P. Company, *Hercules Nitrocellulose, Properties and Uses*. 1944.

[40] C. W. Saunders and L. T. Taylor, "A review of the synthesis, chemistry and analysis of nitrocellulose," *Journal of Energetic Materials,* vol. 8, no. 3, pp. 149-203, 1990/09/01 1990, doi: 10.1080/07370659008012572.

[41] B. Medronho, A. Romano, M. G. Miguel, L. Stigsson, and B. Lindman, "Rationalizing cellulose (in)solubility: reviewing basic physicochemical aspects and role of hydrophobic interactions," *Cellulose,* vol. 19, no. 3, pp. 581-587, 2012/06/01 2012, doi: 10.1007/s10570-011-9644-6.

[42] C. M. Selwitz, *Cellulose nitrate in conservation*. Getty Publications, 1988.

[43] T. Heinze, T. Liebert, and A. Koschella, *Esterification of polysaccharides*. Springer Science & Business Media, 2006.

[44] J. Zhanning, "The glass transition temprature measurement of nitrocellulose by torsional braid analysis," *Propellants, Explosives, Pyrotechnics,* vol. 17, no. 1, pp. 34-37, 1992, doi: 10.1002/prep.19920170109.

[45] N. Binke, L. Rong, C. Xianqi, W. Yuan, R. Z. Hu, and Y. Qingsen, "Study on the melting process of nitrocellulose by thermal analysis method," (in English), *Journal of Thermal Analysis and Calorimetry,* Article vol. 58, no. 2, pp. 249-256, Nov 1999, doi: 10.1023/a:1010138827699.

[46] F. Aftalion, *A history of the international chemical industry*. University of Pennsylvania Press, 1991.

[47] D. W. Rossell, "Exploding Teeth, Unbreakable Sheets and Continuous Casting: Nitrocellulose from Gun-Cotton to Early Cinema," ed: Fédération Internationale des Archives du Film, 2002.

[48] A. A. Nada, F. H. H. Abdellatif, A. A. F. Soliman, J. Shen, S. M. Hudson, and N. Y. Abou-Zeid, "Fabrication and bioevaluation of a medicated electrospun mat based on azido-cellulose acetate via click chemistry," *Cellulose,* vol. 26, no. 18, pp. 9721-9736, 2019/12/01 2019, doi: 10.1007/s10570-019-02739-9.

[49] K. Rahn, M. Diamantoglou, D. Klemm, H. Berghmans, and T. Heinze, "Homogeneous synthesis of cellulose p-toluenesulfonates in N,N-dimethylacetamide/LiCl solvent system," *Die Angewandte Makromolekulare Chemie,* vol. 238, no. 1, pp. 143-163, 1996, doi: 10.1002/apmc.1996.052380113.

[50] S. M. Pourmortazavi, S. G. Hosseini, M. Rahimi-Nasrabadi, S. S. Hajimirsadeghi, and H. Momenian, "Effect of nitrate content on thermal decomposition of nitrocellulose," *Journal of Hazardous Materials,* vol. 162, no. 2, pp. 1141-1144, 2009/03/15/ 2009, doi: https://doi.org/10.1016/j.jhazmat.2008.05.161.

[51] M. Shamsipur, S. M. Pourmortazavi, S. S. Hajimirsadeghi, and S. M. Atifeh, "Effect of functional group on thermal stability of cellulose derivative energetic polymers," *Fuel,* vol. 95, pp. 394-399, 2012/05/01/ 2012, doi: https://doi.org/10.1016/j.fuel.2011.09.036.

[52] L. S. Sletkina, A. I. Polyakov, and Z. A. Rogovin, "Some regularities in the nucleophilic substitution of various cellulose esters with halides," *Polymer Science U.S.S.R.,* vol. 7, no. 2, pp. 214-219, 1965/01/01/ 1965, doi: https://doi.org/10.1016/0032-3950(65)90037-7.

[53] T. Heinze, A. Koschella, L. Magdaleno-Maiza, and A. Ulrich, "Nucleophilic displacement reactions on tosyl cellulose by chiral amines," *Polymer Bulletin,* vol. 46, no. 1, pp. 7-13, 2001, doi: 10.1007/s002890170082.

[54] *Remarks on the Evolution of Explosives* (Propellants, Explosives, Pyrotechnics, no. 8). 2017, pp. 851-853.

[55] I. IPCS. "Nitroglycerine." IPCS. http://www.inchem.org/documents/icsc/icsc/eics0186.htm (accessed March 5, 2020).

[56] H. G. Ang and S. Pisharath, *Energetic Polymers*. Wiley, 2012.

[57] A. Provatas, "Energetic polymers and plasticisers for explosive formulations-A review of recent advances," in "Technical Report," Defence Science and Technology, Australia, DSTO-TR-0966, 2000.

[58] N. Kubota and T. Sonobe, "Combustion Mechanism of Azide Polymer," *Propellants, Explosives, Pyrotechnics,* vol. 13, no. 6, pp. 172-177, 1988, doi: 10.1002/prep.19880130604.

[59] M. B. Frankel, L. R. Grant, and J. E. Flanagan, "Historical Development of Glycidyl Azide Polymer," (in English), *Journal of Propulsion and Power,* vol. 8, no. 3, pp. 560-563, May-Jun 1992, doi: Doi 10.2514/3.23514.

[60] G. Wypych, *Handbook of Plasticizers*. Elsevier Science, 2013.

[61] M. Gordon and J. S. Taylor, "Ideal copolymers and the second-order transitions of synthetic rubbers. i. non-crystalline copolymers," *Journal of Applied Chemistry,* vol. 2, no. 9, pp. 493-500, 1952, doi: 10.1002/jctb.5010020901.

[62] L. Janssen and L. Moscicki, *Thermoplastic Starch*. Wiley, 2009.

[63] R. C. Warren, "Transitions and relaxations in plasticised nitrocellulose," *Polymer,* vol. 29, no. 5, pp. 919-923, 1988/05/01/ 1988, doi: https://doi.org/10.1016/0032-3861(88)90155-3.

[64] D. J. Townend and R. C. Warren, "Relaxations in double base propellants," *Polymer,* vol. 26, no. 1, pp. 79-83, 1985/01/01/ 1985, doi: https://doi.org/10.1016/0032-3861(85)90059-X.

[65] F. S. Baker and G. J. Privett, "Dielectric studies of nitrocellulose/nitroglycerine interaction," *Polymer,* vol. 29, no. 9, pp. 1594-1597, 1988/09/01/ 1988, doi: https://doi.org/10.1016/0032-3861(88)90268-6.

[66] R. Quintana, O. Persenaire, Y. Lemmouchi, L. Bonnaud, and P. Dubois, "Compatibilization of co-plasticized cellulose acetate/water soluble polymers blends by reactive extrusion," *Polymer Degradation and Stability,* vol. 126, pp. 31-38, 2016/04/01/ 2016, doi: https://doi.org/10.1016/j.polymdegradstab.2015.12.023.

[67] P. Bergo, P. J. A. Sorbal, and J. M. Prison, "Effect of glyceron on physical properties of cassava starch films," *Journal of Food Processing and Preservation,* vol. 34, no. s2, pp. 401-410, 2010, doi: 10.1111/j.1745-4549.2008.00282.x.

[68] L. Famá, S. Goyanes, and L. Gerschenson, "Influence of storage time at room temperature on the physicochemical properties of cassava starch films," *Carbohydrate Polymers,* vol. 70, no. 3, pp. 265-273, 2007/10/01/ 2007, doi: https://doi.org/10.1016/j.carbpol.2007.04.003.

[69] A. L. D. Róz, A. J. F. Carvalho, A. Gandini, and A. A. S. Curvelo, "The effect of plasticizers on thermoplastic starch compositions obtained by melt processing," *Carbohydrate Polymers,* vol. 63, no. 3, pp. 417-424, 2006/03/03/ 2006, doi: https://doi.org/10.1016/j.carbpol.2005.09.017.

[70] A. Taguet, M. A. Huneault, and B. D. Favis, "Interface/morphology relationships in polymer blends with thermoplastic starch," *Polymer,* vol. 50, no. 24, pp. 5733-5743, 2009/11/16/ 2009, doi: https://doi.org/10.1016/j.polymer.2009.09.055.

[71] Y. Wu, Y. Luo, and Z. Ge, "Properties and Application of a Novel Type of Glycidyl Azide Polymer (GAP)-Modified Nitrocellulose Powders," *Propellants, Explosives, Pyrotechnics,* pp. n/a-n/a, 2014, doi: 10.1002/prep.201400005.

[72] M. Niehaus, "Compounding of Glycidyl Azide Polymer with Nitrocellulose and its Influence on the Properties of Propellants," *Propellants, Explosives, Pyrotechnics,* vol. 25, no. 5, pp. 236-240, 2000, doi: 10.1002/1521-4087(200011)25:5<236::Aid-prep236>3.0.Co;2-c.

[73] Z. Wang, T. Zhang, B. Zhao, and Y. Luo, "Effect of nitrocellulose (NC) on morphology, rheological and mechanical properties of glycidyl azide polymer based energetic thermoplastic elastomer/NC blends," *Polymer International,* vol. 66, no. 5, pp. 705-711, 2017, doi: 10.1002/pi.5312.

[74] B. Vidéki, S. Klébert, and B. Pukánszky, "External and internal plasticization of cellulose acetate with caprolactone: Structure and properties," *Journal of Polymer Science Part B: Polymer Physics,* vol. 45, no. 8, pp. 873-883, 2007, doi: 10.1002/polb.21121.

[75] R. Willer, A. G. Stern, and R. S. Day, "Nitrated difunctional poly(glycidyl nitrate) oligomer - used as a plasticiser for binders in propellants, pyrotechnics and explosives," Patent US5380777-A, [Online]. Available: <Go to ISI>://DIIDW:1995060368

[76] H. H. Seck. "Marine probe blames human error in training accident." USA Today. https://www.usatoday.com/story/news/nation/2014/01/21/marines-mortar-accident-training/4739357/ (accessed 19 February, 2020).

[77] B. K. Brown, "The Use of Plasticizers in Lacquers," *Industrial & Engineering Chemistry,* vol. 17, no. 6, pp. 568-569, 1925/06/01 1925, doi: 10.1021/ie50186a005.

[78] L. A. Utracki, "History of commercial polymer alloys and blends (from a perspective of the patent literature)," *Polymer Engineering & Science,* vol. 35, no. 1, pp. 2-17, 1995, doi: 10.1002/pen.760350103.

[79] M. Young *et al.*, "Combustible thermoplastic material used in a container e.g. artillery propellant bag comprises foamed celluloid having specific density, where material is fast burning and low residue," Patent US8597444-B1, [Online]. Available: <Go to ISI>://DIIDW:2013W04079

[80] M. Young *et al.*, "Combustible thermoplastic material used in a container e.g. artillery propellant bag comprises foamed celluloid having specific density, where material is fast burning and low residue," Patent US8597444-B1 Patent Appl. US8597444-B1 US977374 23 Dec 2010, [Online]. Available: <Go to ISI>://DIIDW:2013W04079

[81] H. Austruy, "Chapter 9 - Double-base Propellants," in *Solid Rocket Propulsion Technology*, A. Davenas Ed. Amsterdam: Pergamon, 1993, pp. 369-413.

[82] R. Sanghavi, P. Kamale, M. A. R. Shaikh, T. Chakraborthy, S. Asthana, and A. Singh, "Glycidyl Azide Polymer-based Enhanced Energy LOVA Gun Propellant," *Defence Science Journal,* vol. 56, no. 3, pp. 407-416, 05/26 2006, doi: 10.14429/dsj.56.1907.

[83] R. R. Sanghavi, P. J. Kamale, M. A. R. Shaikh, T. K. Chakraborthy, S. N. Asthana, and A. Singh, "Glycidyl azide polymer-based enhanced energy LOVA gun propellant," 2006, vol. 56: Defense Scientific Information and Documentation Centre, in Defence Science Journal, 3 ed., pp. 407-416.

[84] R. S. Damse and A. S. Redkar, "High impetus cool burning gun propellants," *Defence Science Journal,* vol. 50, no. 3, pp. 281-288, 2000.

[85] R. S. Damse, A. Singh, and H. Singh, "High energy propellants for advanced gun ammunition based on RDX, GAP and TAGN compositions," *Propellants, Explosives, Pyrotechnics,* vol. 32, no. 1, pp. 52-60, 2007, doi: 10.1002/prep.200700007.

[86] Y. Hu, X. Jian, L. Xiao, and W. Zhou, "Microphase separation and mechanical performance of thermoplastic elastomers based on poly(glycidyl azide)/poly(oxytetramethylene glycol)," *Polymer Engineering & Science,* vol. 58, no. S1, pp. E167-E173, 2018, doi: 10.1002/pen.24831.

[87] Y. Zhang, J. Zhao, P. Yang, S. He, and H. Huang, "Synthesis and characterization of energetic GAP-b-PAEMA block copolymer," *Polymer Engineering & Science,* vol. 52, no. 4, pp. 768-773, 2012, doi: 10.1002/pen.22140.

[88] B. Gaur, B. Lochab, V. Choudhary, and I. K. Varma, "Azido Polymers—Energetic Binders for Solid Rocket Propellants," *Journal of Macromolecular Science, Part C,* vol. 43, no. 4, pp. 505-545, 2003/12/31 2003, doi: 10.1081/MC-120025976.

[89] K. Hori and M. Kimura, "Combustion mechanism of glycidyl azide polymer," (in English), *Propell Explos Pyrot,* vol. 21, no. 3, pp. 160-165, Jun 1996, doi: Doi 10.1002/Prep.19960210310.

[90] A. N. Nazare, S. N. Asthana, and H. Singh, "Glycidyl azide polymer (GAP) - an energetic component of advanced solid rocket propellants - a review," *Journal of Energetic Materials,* vol. 10, no. 1, pp. 43-63, 1992/03/01 1992, doi: 10.1080/07370659208018634.

[91] F. Baker, C. Turner, and G. Privett, "The interaction of dibutyl phthalate with 12.6 % N nitrocellulose," *Polymer International,* vol. 54, no. 1, pp. 54-57, 2005, doi: 10.1002/pi.1376.

[92] F. S. Baker and G. J. Privett, "Dynamic mechanical studies of nitrocellulose/nitroglycerine mixtures," *Polymer,* vol. 28, no. 7, pp. 1121-1126, 1987/06/01 1987, doi: http://dx.doi.org/10.1016/0032-3861(87)90253-9.

[93] F. S. Baker, M. J. Healey, and G. Privett, "The Rheological Properties of Plasticized Nitrocellulose as a function of nitrocellulose precursor," *Propellants, Explosives, Pyrotechnics,* vol. 13, no. 4, pp. 99-102, 1988, doi: 10.1002/prep.19880130402.

[94] G. Herder and W. d. Klerk, "Measurement of the relaxation transitions of nitrocellulose based gunpowder," *Journal of Thermal Analysis and Calorimetry,* vol. 85, no. 1, pp. 169-172, 2006, doi: 10.1007/s10973-005-7332-1.

[95] G. Számel, S. Klébert, I. Sajó, and B. Pukánszky, "Thermal analysis of cellulose acetate modified with caprolactone," *Journal of Thermal Analysis and Calorimetry,* vol. 91, no. 3, p. 715, 2008/06/14 2008, doi: 10.1007/s10973-007-8684-5.

[96] R. A. Pethrick and A. M. Wilton, "Plasticization of Fibrous Cellulose Acetate: Part II – Physical Property Measurement," *International Journal of Polymeric Materials and Polymeric Biomaterials,* vol. 62, no. 4, pp. 190-198, 2013/01/31 2013, doi: 10.1080/00914037.2011.617325.

[97] S. S. Ochigbo, A. S. Luyt, J. P. Mofokeng, Ž. Antić, M. D. Dramićanin, and V. Djoković, "Dynamic mechanical and thermal properties of the composites of thermoplastic starch and lanthanum hydroxide nanoparticles," *Journal of Applied Polymer Science,* vol. 127, no. 1, pp. 699-709, 2013, doi: 10.1002/app.37859.

[98] P. A. Sreekumar, M. A. Al-Harthi, and S. K. De, "Studies on compatibility of biodegradable starch/polyvinyl alcohol blends," *Polymer Engineering & Science,* vol. 52, no. 10, pp. 2167-2172, 2012, doi: 10.1002/pen.23178.

[99] M. M. Pang, M. Y. Pun, and Z. A. M. Ishak, "Thermal, mechanical, and morphological characterization of biobased thermoplastic starch from agricultural waste/polypropylene blends," *Polymer Engineering & Science,* vol. 54, no. 6, pp. 1357-1365, 2014, doi: 10.1002/pen.23684.

[100] B. W. Brodman, M. P. Devine, and M. T. Gurbarg, "Hydrogen bonding of deterrents to unesterified hydroxyl groups in nitrocellulose," *Journal of Applied Polymer Science,* vol. 18, no. 3, pp. 943-946, 1974, doi: 10.1002/app.1974.070180328.

[101] B. W. Brodman, J. A. Sipia Jr., and S. Schwartz, "Diffusion of deterrents into a nitrocellulose matrix. An example of diffusion with interaction," *Journal of Applied Polymer Science,* vol. 19, no. 7, pp. 1905-1909, 1975, doi: 10.1002/app.1975.070190711.

[102] B. W. Brodman, M. P. Devine, and M. T. Gurbarg, "An example of the effect of chemical interactions on transport phenomena," *AIChE Journal,* vol. 20, no. 4, pp. 819-820, 1974, doi: 10.1002/aic.690200426.

[103] M. Scandola and G. Ceccorulli, "Viscoelastic properties of cellulose derivatives: 1. Cellulose acetate," *Polymer,* vol. 26, no. 13, pp. 1953-1957, 1985/12/01/ 1985, doi: https://doi.org/10.1016/0032-3861(85)90173-9.

[104] L. Averous, L. Moro, P. Dole, and C. Fringant, "Properties of thermoplastic blends: starch–polycaprolactone," *Polymer,* vol. 41, no. 11, pp. 4157-4167, 2000/05/01/ 2000, doi: https://doi.org/10.1016/S0032-3861(99)00636-9.

[105] A. R. Shultz and A. L. Young, "DSC on Freeze-Dried Poly(methyl methacrylate)-Polystyrene Blends," *Macromolecules,* vol. 13, no. 3, pp. 663-668, 1980/05/01 1980, doi: 10.1021/ma60075a034.

[106] K. M. Boulkadid, D. Trache, S. Krai, M. H. Lefebvre, L. Jeunieau, and A. Dejeaifve, "Estimation of the Ballistic Parameters of Double Base Gun Propellants," *Propellants, Explosives, Pyrotechnics,* vol. 45, no. 5, pp. 751-758, 2020, doi: 10.1002/prep.201900341.

[107] E. Tırak, M. Moniruzzaman, E. Degirmenci, and A. Hameed, "Closed vessel burning behavior and ballistic properties of artificially-degraded spherical double-base propellants stabilized with diphenylamine," *Thermochimica Acta,* vol. 680, p. 178347, 2019/10/01/ 2019, doi: https://doi.org/10.1016/j.tca.2019.178347.

[108] R. S. Damse and A. Singh, "Evaluation of Energetic Plasticisers for Solid Gun Propellant," *Defence Science Journal,* vol. 58, no. 1, 2008, doi: 10.14429/dsj.58.1627. 2008/01/01.

[109] S. Sopok, C. Rickard, and S. Dunn, "Thermal–chemical–mechanical gun bore erosion of an advanced artillery system part one: theories and mechanisms," *Wear,* vol. 258, no. 1, pp. 659-670, 2005/01/01/ 2005, doi: https://doi.org/10.1016/j.wear.2004.09.031.

[110] J. Kimura, "Hydrogen Gas Erosion of High-Energy LOVA Propellants," in *16th International Symposium on Ballistics*, San Francisco, United States, 1996.

[111] N. R. C. C. o. G. T. Erosion and N. R. C. N. M. A. Board, *Erosion in Large Gun Barrels: Report of Committee on Gun Tube Erosion*. National Academy of Sciences, 1975.

[112] I. A. J. A. Harrland, "Review of Solid Propellant Ignition Models Relative to the Interior Ballistic Modelling of Gun Systems," in "Technical Report," Department of Defense Science and Technology, Australia, DSTO-TR-2735, 2012.

[113] E. F. Laurence , W. Michael Howard, and P. Clark Souers, "Cheetah 2.0 : User's Manual," Energetic Materials Center - Lawrence Livermore National Laboratory United States of America, Computer software manual 1998.

[114] W. F. Oberle and D. E. Kooker, "BRLCB: A Closed-Chamber Data Analysis Program. Part 1. Theory and User's Manual," in "Technical Report," Army Research Laboratory, United States of America, AD-A260 493, 1993. [Online]. Available: https://apps.dtic.mil/docs/citations/ADA260493

[115] E. Comtois, B. D. Favis, and C. Dubois, "Phase transitions and mechanical properties of nitrocellulose plasticized by glycidyl azide polymer and nitroglycerine," *Polymer Engineering & Science,* vol. 1, no. 13, 2020, doi: 10.1002/pen.25473.

[116] M. Sućeska, S. M. Mušanić, and I. F. Houra, "Kinetics and enthalpy of nitroglycerin evaporation from double base propellants by isothermal thermogravimetry," *Thermochimica Acta,* vol. 510, no. 1, pp. 9-16, 2010/10/20/ 2010, doi: https://doi.org/10.1016/j.tca.2010.06.014.

[117] N. Eisenreich *et al.*, "Burning Phenomena of the Gun Propellant JA2," *Propellants, Explosives, Pyrotechnics,* vol. 25, no. 3, pp. 143-148, 2000, doi: 10.1002/1521-4087(200006)25:3<143::Aid-prep143>3.0.Co;2-c.

[118] G. Gazonas, "The Mechanical Response of M30, XM39, and JA2 Propellants at Strain Rates from One One-hundredth to 250 per second," p. 63, 01/01 1991.

[119] J. Lavoie, C.-F. Petre, and C. Dubois, "Erosivity and Performance of Nitrogen-Rich Propellants," *Propellants, Explosives, Pyrotechnics,* vol. 43, no. 9, pp. 879-892, 2018, doi: 10.1002/prep.201700272.

[120] N. Fischer, D. Izsák, T. M. Klapötke, S. Rappenglück, and J. Stierstorfer, "Nitrogen-Rich 5,5′-Bistetrazolates and their Potential Use in Propellant Systems: A Comprehensive Study," *Chemistry – A European Journal,* vol. 18, no. 13, pp. 4051-4062, 2012, doi: 10.1002/chem.201103737.

[121] P. Gongwer, H. Arisawa, and T. Brill, "Kinetics and Species of Flash Pyrolysis of Cellulose Acetate Butyrate: The Binder of Lova," *MRS Online Proceedings Library Archive,* vol. 418, 1995.

[122] A. Pillai, M. Joshi, A. Barve, S. Velapure, and J. Karir, "Cellulose Acetate Binder-Based LOVA Gun Propellant for Tank Guns," *Defence Science Journal,* vol. 49, no. 2, p. 141, 1999.

[123] A. G. S. Pillai, R. R. Sanghavi, C. R. Dayanandan, M. M. Joshi, S. P. Velapure, and A. Singh, "Studies on RDX Particle Size in LOVA Gun Propellant Formulations," *Propellants, Explosives, Pyrotechnics,* vol. 26, no. 5, pp. 226-228, 2001, doi: 10.1002/1521-4087(200112)26:5<226::Aid-prep226>3.0.Co;2-9.

[124] M. Kirshenbaum, L. Avrami, and B. Strauss, "Sensitivity Characterization of Low Vulnerability (LOVA) Propellants," Army Armement Research and Development Center Dover, NJ, Larger Caliber Weapon System, 1983.

[125] J. S. You, S. C. Kang, S. K. Kweon, H. L. Kim, Y. H. Ahn, and S. T. Noh, "Thermal decomposition kinetics of GAP ETPE/RDX-based solid propellant," *Thermochimica Acta,* vol. 537, pp. 51-56, 2012/06/10/ 2012, doi: https://doi.org/10.1016/j.tca.2012.02.032.

[126] R. A. Pesce-rodriguez, F. J. Shaw, and R. A. Fifer, "Pyrolysis GC-FTIR studies of a LOVA propellant formulation series," *Journal of Energetic Materials,* vol. 10, no. 4-5, pp. 221-250, 1992/11/01 1992, doi: 10.1080/07370659208018924.

[127] F.-F. Yang, Z. Shao, N.-K. Li, F.-J. Wang, and Y. Zhang, "A Novel Cellulose-Based Azide Energetic Material: 1-Azido-2-hydroxypropyl Cellulose Ether," *Journal of Energetic Materials,* vol. 29, no. 3, pp. 241-260, 2011/07/01 2011, doi: 10.1080/07370652.2010.523755.

[128] E. W. Washburn, "Standard states for bomb calorimetry," *J. Res. Natl. Bur. Stand.(US),* vol. 10, pp. 525-558, 1933.

[129] T. Heinze, K. Rahn, M. Jaspers, and H. Berghmans, "Thermal studies on homogeneously synthesized cellulose p-toluenesulfonates," *Journal of Applied Polymer Science,* vol. 60, no. 11, pp. 1891-1900, 1996, doi: 10.1002/(sici)1097-4628(19960613)60:11<1891::Aid-app13>3.0.Co;2-4.

[130] H. Kono, H. Hashimoto, and Y. Shimizu, "NMR characterization of cellulose acetate: Chemical shift assignments, substituent effects, and chemical shift additivity," *Carbohydrate Polymers,* vol. 118, pp. 91-100, 2015/03/15/ 2015, doi: https://doi.org/10.1016/j.carbpol.2014.11.004.

[131] D. R. Paul, *Polymer Blends*. Elsevier Science, 2012.

[132] C. M. Hansen, *Hansen Solubility Parameters: A User's Handbook, Second Edition*. CRC Press, 2007.

[133] J. Ma and L. Zhou, "A new procedure for calculating Hansen solubility parameters of carbon nanotube/polymer composites," *Polymer Bulletin,* vol. 68, no. 4, pp. 1053-1063, 2012/03/01 2012, doi: 10.1007/s00289-011-0607-8.

[134] D. Render and S. Tootal, *Tank Action: An Armoured Troop Commander's War 1944–45*. Orion, 2016.

[135] S. Zaloga, *Armored Champion: The Top Tanks of World War II*. Stackpole Books, 2015.

[136] M. D. S. Wilson, *Evolution Of Artillery Tactics In General J. Lawton Collins' US VII Corps In World War II*. Lucknow Books, 2015.

[137] L. A. Wingard, P. E. Guzmán, E. C. Johnson, J. J. Sabatini, G. W. Drake, and E. F. C. Byrd, "Synthesis of bis-Isoxazole-bis-Methylene Dinitrate: A Potential Nitrate Plasticizer and Melt-Castable Energetic Material," *ChemPlusChem,* vol. 82, no. 2, pp. 195-198, 2017, doi: 10.1002/cplu.201600470.

[138] J.-C. St-Charles and C. Dubois, "Preparation of Azido Polycarbonates via Bulk Polymerization of Halogenated Diols," *Propellants, Explosives, Pyrotechnics,* vol. 45, no. 6, pp. 889-897, 2020, doi: 10.1002/prep.202000005.

APPENDIX A SUPPORTING INFORMATION

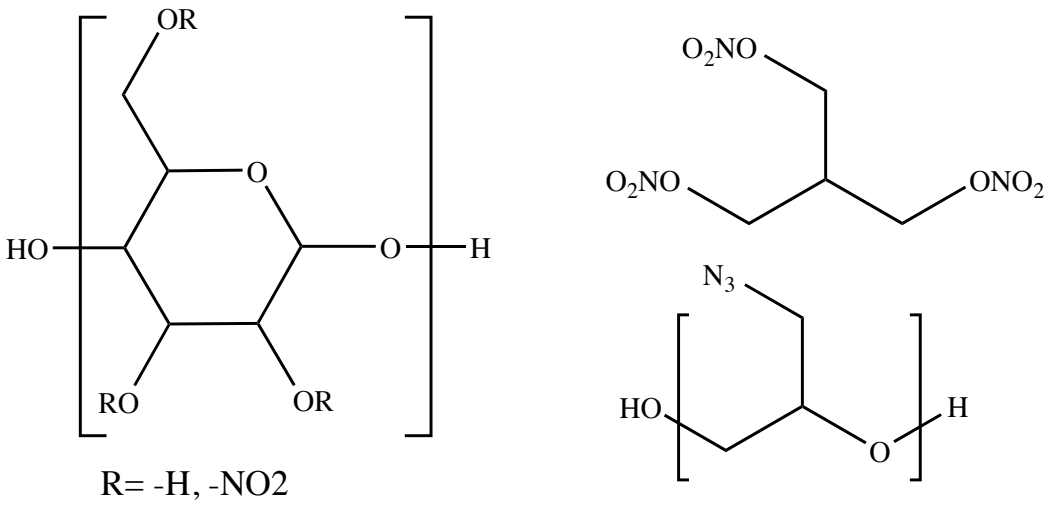

Figure S1 Nitrocellulose (left), nitroglycerine (top right) and glycidyl azide polymer (bottom right).

Figure S2 NC12,5%N-HV / NG(10%) / GAP0700(10%) after being removed from the glass plate.

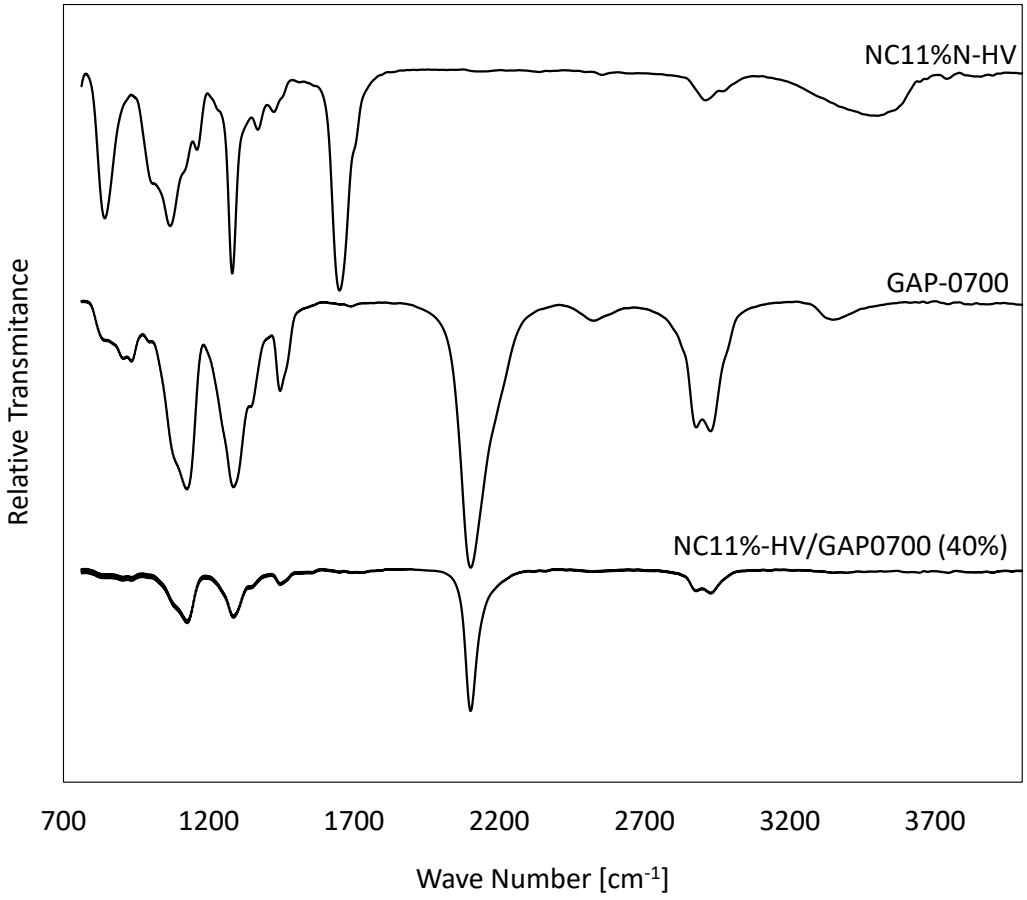

Figure S3 FTIR analysis of pure NC11%N-LV (top), GAP0700 (middle) and the leached solution of the sample NC11%N-HV/GAP0700 (40%) (bottom).

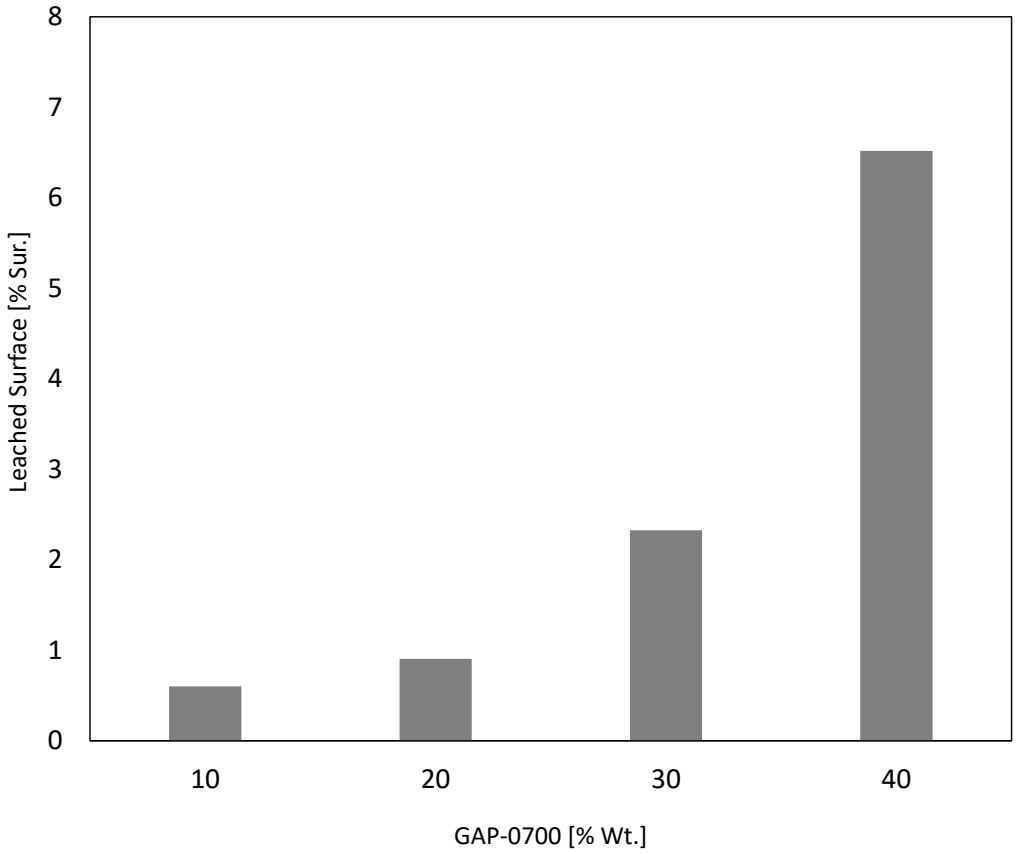

Figure S4 Leached surface of liquid GAP0700 phase in plasticized NC11%N at different concentrations.

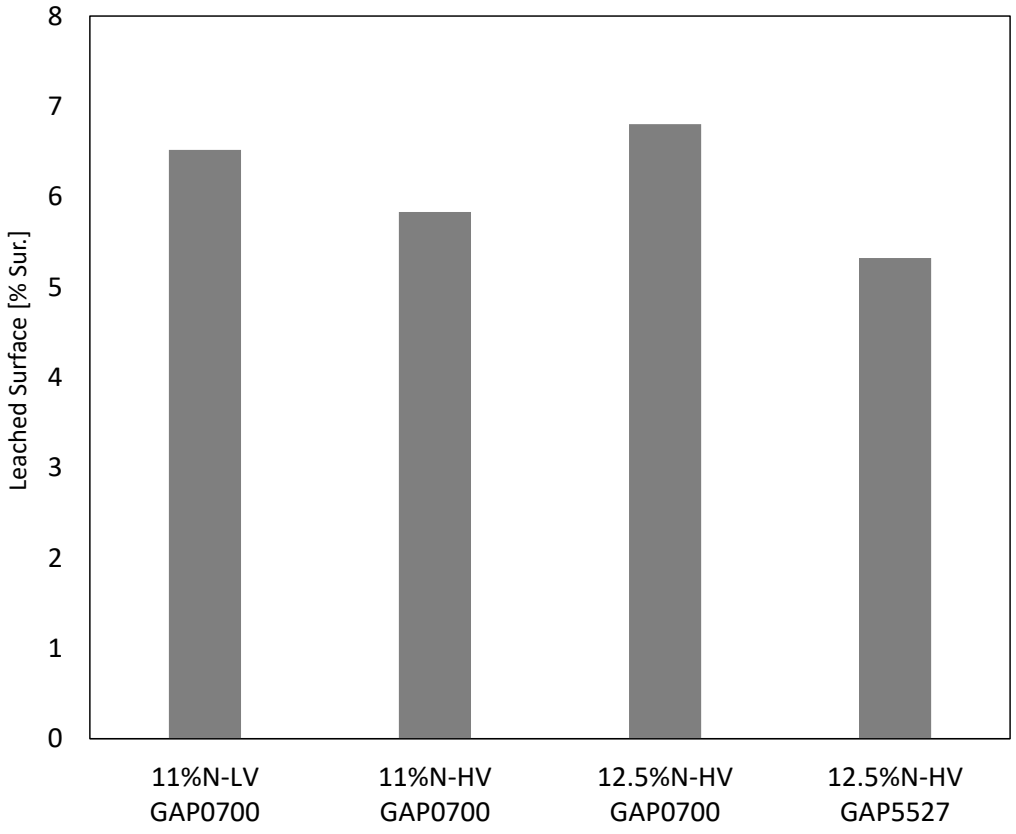

Figure S5 Leached surface of liquid GAP in plasticized NC at 40 wt%

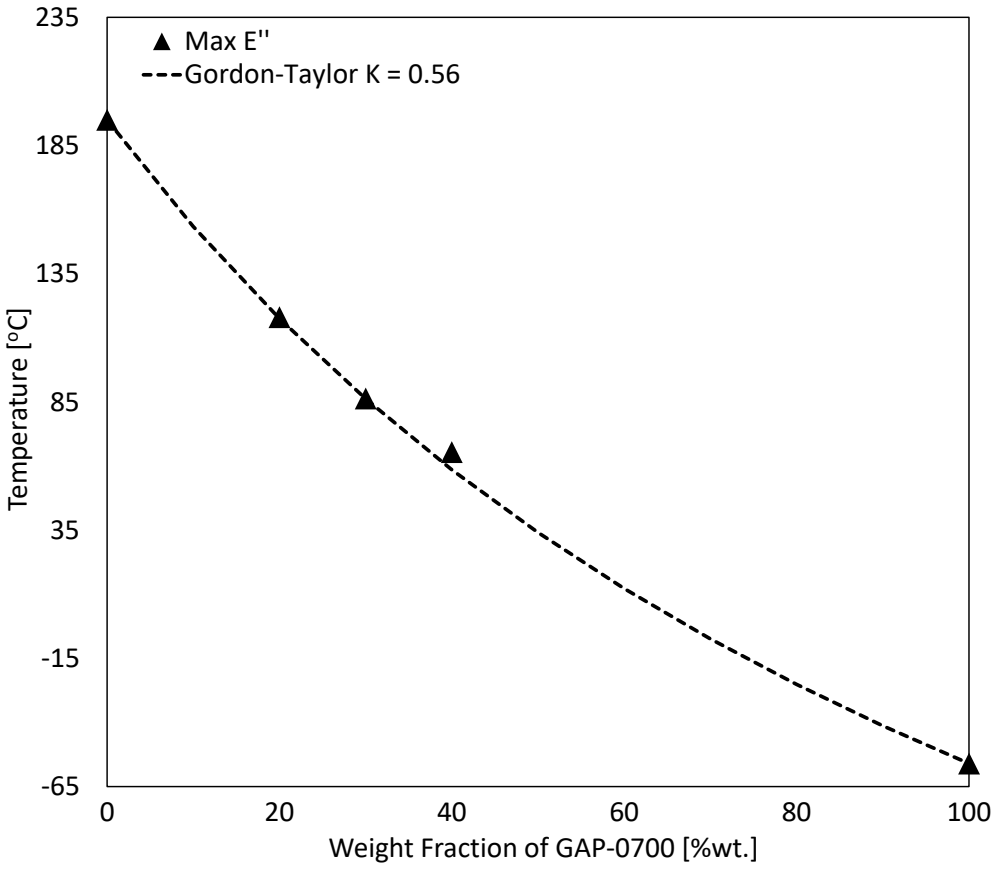

Figure S6 Influence of GAP-0700 concentration on α transition when using the max peak E'' obtained experimentaly and literature value of T_gs for pure GAP and NC.

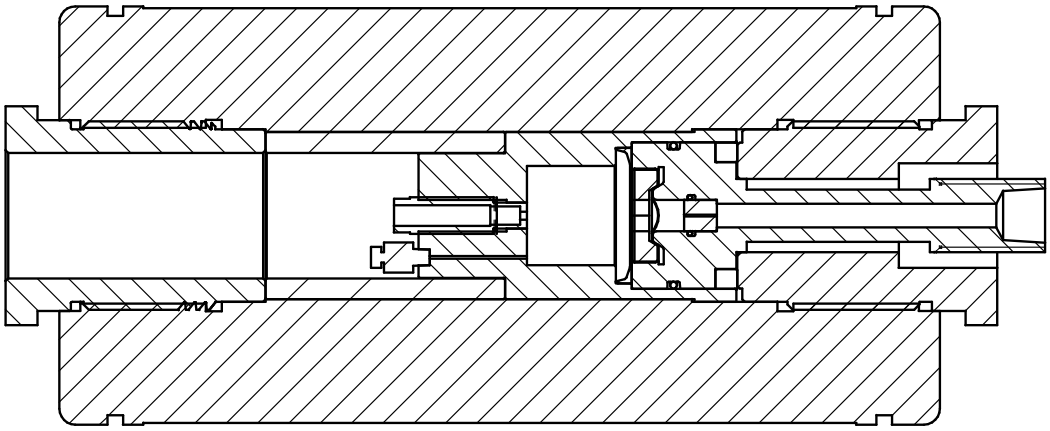

Figure S7 Erosivity vented vessel.

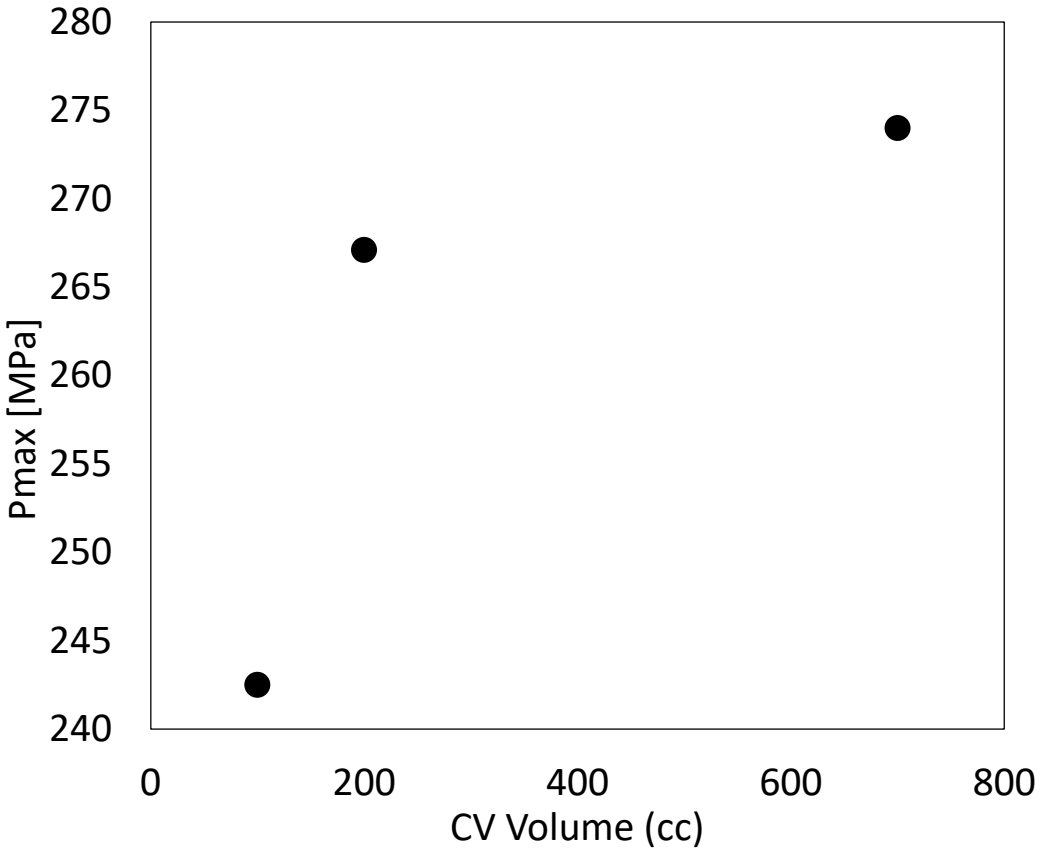

Figure S8 Maximum pressure recorded in 100, 200 and 700 cc CV using double base propellant.

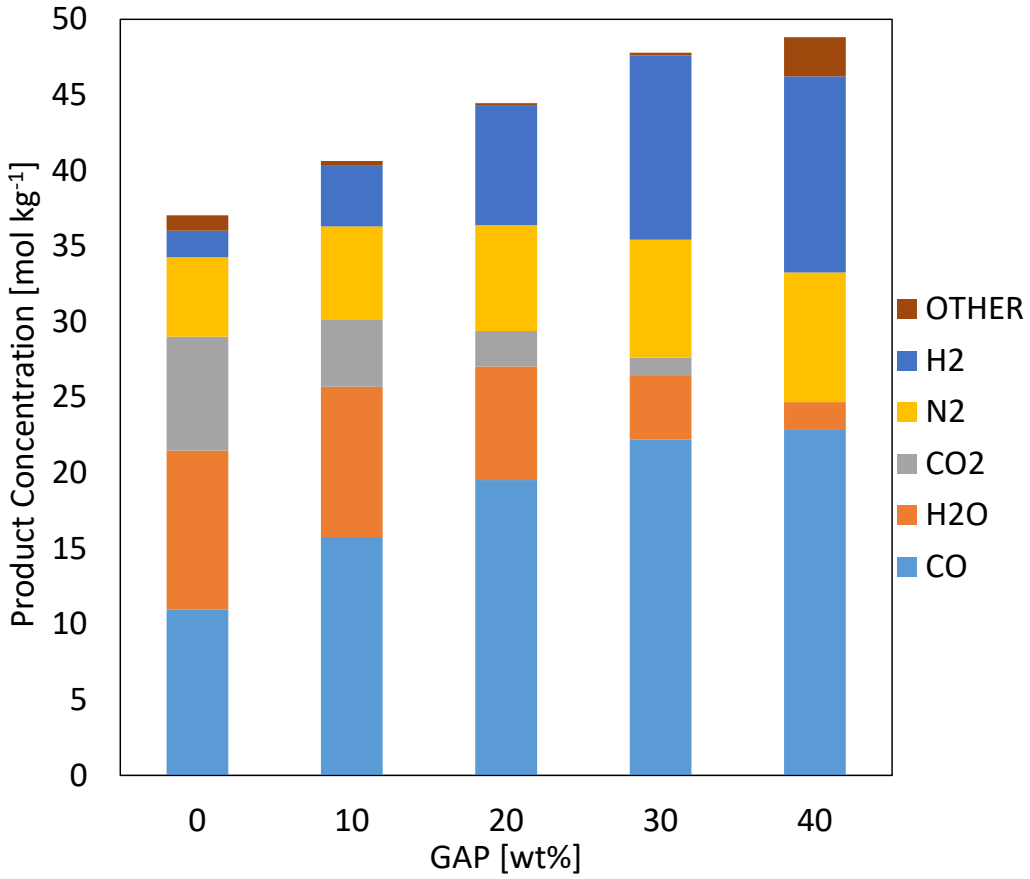

Figure S9 Product concentration obtained from CHEETAH for NC12.5%N compounded with GAP and NG at constant concentration (GAP + NG = 40 wt%).

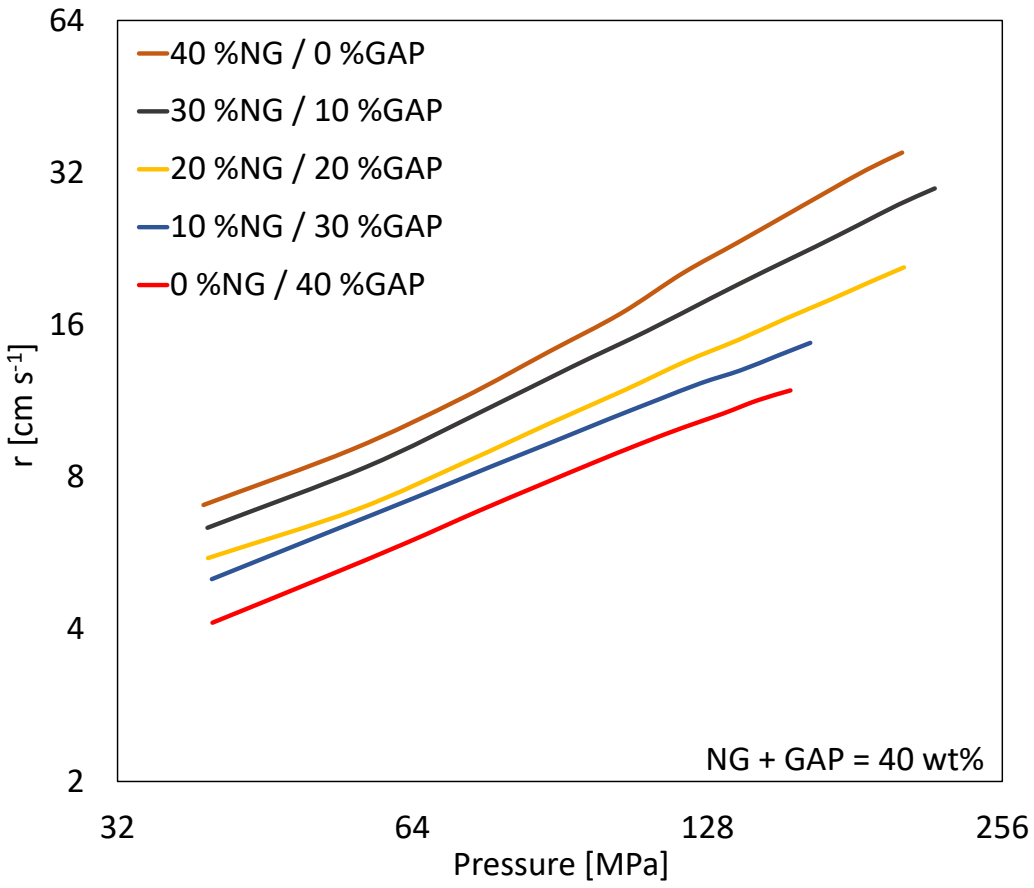

Figure S10 Influence of GAP concentration on NC12.5%N at concentration of 0, 10, 20, 30 and 40 wt% at constant concentration (NG + GAP = 40 wt%)

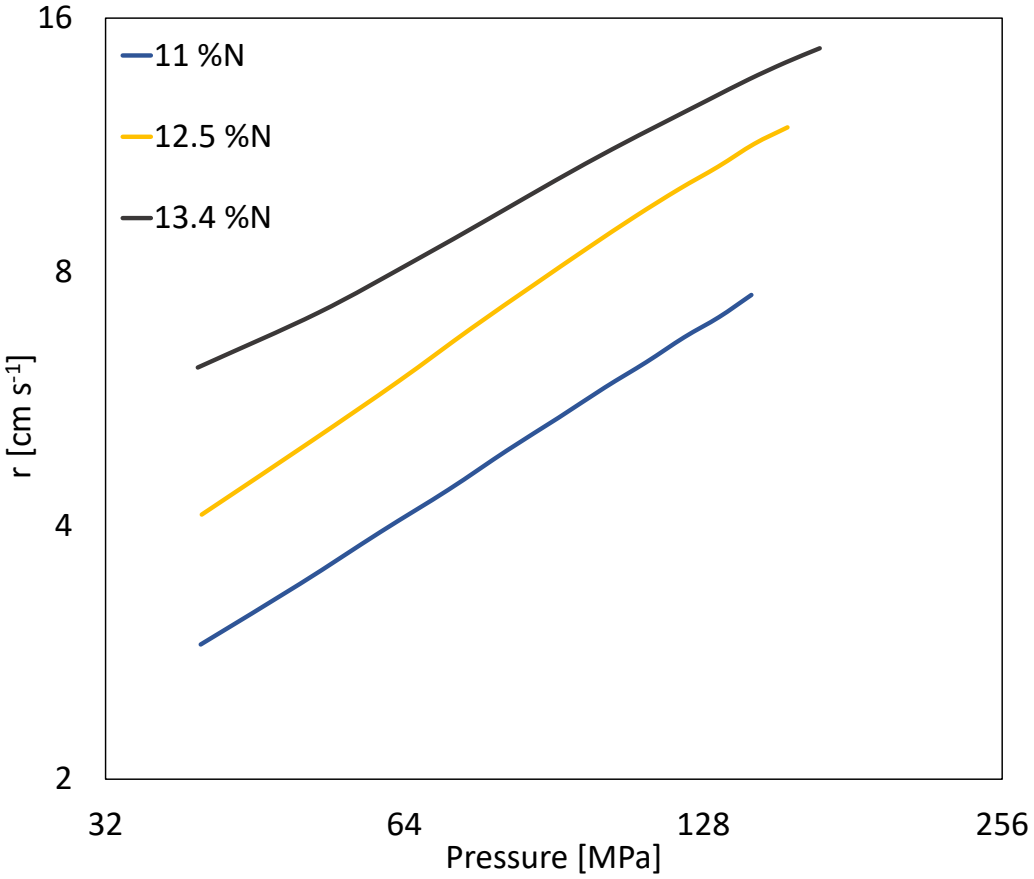

Figure S11 Influence of %N compounded with 40 wt% in GAP.

Table S1 Thermochemical properties and maximum pressure recorded in CV.

ID	**T [K]**	**Impetus [J g^{-1}]**	**Gas Mw [g mol^{-1}]**	**TMD [g cm^{-3}]**	**$P_{Max}^{CHEETAH}$ [MPa]**	**P_{Max}^{CV} [MPa]**	**OD [mm]**	**L [mm]**	**Rho [g cm^{-3}]**
NC12.5%N(100)/NG(0)/GAP(0)	3094	1039	24.8	1.656	260	199	2.9 ± 0.1	23.7 ± 0.7	1.638
NC12.5%N(90)/NG(10)/GAP(0)	3296	1082	25.3	1.647	270	212	3.4 ± 0.2	30.7 ± 2.0	1.610
NC12.5%N(80)/NG(20)/GAP(0)	3485	1119	25.9	1.642	278	234	3.4 ± 0.1	24.3 ± 0.3	1.602
NC12.5%N(70)/NG(30)/GAP(0)	3656	1149	26.5	1.637	284	246	3.4 ± 0.2	24.3 ± 0.9	1.615
NC12.5%N(60)/NG(40)/GAP(0)	3799	1170	27.0	1.631	289	253	3.6 ± 0.1	26.0 ± 1.4	1.611
NC12.5%N(90)/NG(0)/GAP(10)	2799	1009	23.1	1.610	256	191	3.3 ± 0.2	24.8 ± 1.3	1.569
NC12.5%N(80)/NG(0)/GAP(20)	2513	966	21.6	1.567	249	192	3.2 ± 0.2	24.9 ± 0.8	1.547
NC12.5%N(70)/NG(0)/GAP(30)	2276	915	20.7	1.527	240	190	3.5 ± 0.2	25.3 ± 0.9	1.505
NC12.5%N(60)/NG(0)/GAP(40)	2150	873	20.5	1.488	231	177	5.2 ± 0.1	24.9 ± 0.7	1.473
NC12.5%N(80)/NG(10)/GAP(10)	3007	1061	23.6	1.605	268	210	3.5 ± 0.2	26.8 ± 1.7	1.578
NC12.5%N(60)/NG(10)/GAP(30)	2449	977	20.8	1.522	255	206	4.9 ± 0.1	25.0 ± 1.1	1.489
NC12.5%N(60)/NG(20)/GAP(20)	2925	1081	22.5	1.555	276	233	3.3 ± 0.1	25.4 ± 0.9	1.520
NC12.5%N(60)/NG(30)/GAP(10)	3406	1151	24.6	1.592	288	254	3.4 ± 0.1	25.8 ± 0.7	1.555
NC13.4%N(60)/NG(0)/GAP(40)	2265	923	20.4	1.493	244	198	2.5 ± 0.1	21.4 ± 0.9	1.459
NC11%N(60)/NG(0)/GAP(40)	1995	796	20.8	1.486	210	164	3.5 ± 0.1	24.2 ± 0.7	1.465

Table S2 LBR parameters obtained in CV at -46, 21 and 63 ºC calculated from 40 MPa to 90%PMax.

	T [ºC]	α	β	R^2
NC12.5%N(100)/NG(0)/GAP(0)	-46	0.88 ± 0.02	0.09 ± 0.01	1.00
	21	0.85 ± 0.01	0.11 ± 0.01	1.00
	63	0.84 ± 0.01	0.12 ± 0.01	1.00
NC12.5%N(90)/NG(10)/GAP(0)	-46	0.77 ± 0.02	0.21 ± 0.02	0.99
	21	0.75 ± 0.02	0.25 ± 0.02	0.99
	63	0.73 ± 0.02	0.30 ± 0.03	0.99
NC12.5%N(80)/NG(20)/GAP(0)	-46	0.72 ± 0.02	0.33 ± 0.03	0.99
	21	0.71 ± 0.02	0.39 ± 0.03	0.99
	63	0.70 ± 0.02	0.47 ± 0.03	1.00
NC12.5%N(70)/NG(30)/GAP(0)	-46	0.81 ± 0.01	0.29 ± 0.02	1.00
	21	0.79 ± 0.01	0.38 ± 0.02	1.00
	63	0.85 ± 0.02	0.33 ± 0.03	1.00
NC12.5%N(60)/NG(40)/GAP(0)	-46	1.03 ± 0.03	0.12 ± 0.02	0.99
	21	1.02 ± 0.02	0.16 ± 0.02	0.99
	63	0.99 ± 0.03	0.20 ± 0.03	0.99
NC12.5%N(90)/NG(0)/GAP(10)	-46	0.89 ± 0.01	0.09 ± 0.00	1.00
	21	0.86 ± 0.00	0.11 ± 0.00	1.00
	63	0.83 ± 0.00	0.14 ± 0.00	1.00
NC12.5%N(80)/NG(0)/GAP(20)	-46	0.84 ± 0.01	0.13 ± 0.00	1.00
	21	0.82 ± 0.01	0.15 ± 0.01	1.00
	63	0.77 ± 0.02	0.21 ± 0.02	1.00
NC12.5%N(70)/NG(0)/GAP(30)	-46	0.84 ± 0.01	0.14 ± 0.00	1.00
	21	0.80 ± 0.01	0.19 ± 0.01	1.00
	63	0.77 ± 0.01	0.24 ± 0.01	1.00
NC12.5%N(60)/NG(0)/GAP(40)	-46	0.82 ± 0.01	0.18 ± 0.01	1.00
	21	0.79 ± 0.01	0.23 ± 0.01	1.00
	63	0.77 ± 0.01	0.30 ± 0.01	1.00
NC12.5%N(80)/NG(10)/GAP(10)	-46	0.81 ± 0.01	0.20 ± 0.01	1.00
	21	0.78 ± 0.01	0.25 ± 0.02	1.00
	63	0.79 ± 0.02	0.27 ± 0.02	1.00
NC12.5%N(60)/NG(10)/GAP(30)	-46	0.83 ± 0.02	0.20 ± 0.02	1.00
	21	0.81 ± 0.01	0.25 ± 0.02	1.00
	63	0.79 ± 0.01	0.30 ± 0.02	1.00
NC12.5%N(60)/NG(20)/GAP(20)	-46	0.85 ± 0.01	0.20 ± 0.01	1.00
	21	0.83 ± 0.01	0.25 ± 0.01	1.00
	63	0.81 ± 0.02	0.30 ± 0.02	1.00
NC12.5%N(60)/NG(30)/GAP(10)	-46	0.88 ± 0.01	0.23 ± 0.02	1.00
	21	0.93 ± 0.01	0.20 ± 0.01	1.00
	63	0.86 ± 0.02	0.31 ± 0.03	1.00

	T [ºC]	α	β	R^2
NC11%N(60)/NG(0)/GAP(40)	-46	0.69 ± 0.01	0.40 ± 0.01	1.00
	21	0.62 ± 0.01	0.62 ± 0.02	1.00
	63	0.64 ± 0.01	0.62 ± 0.04	1.00
NC13.4%N(0)/NG(0)/GAP(40)	-46	0.75 ± 0.01	0.16 ± 0.00	1.00
	21	0.75 ± 0.00	0.18 ± 0.00	1.00
	63	0.78 ± 0.00	0.18 ± 0.00	1.00

Table S 3 Solubility results for NCs, GAPs and AC (PB400-N3) in various solvents. 0 indicate that the polymer is not soluble and 1 that a clear solution is obtained.

	GAP 5527	**GAP 0700**	**PB400 N3**	**13.4%N HV**	**12.6%N HV**	**11%N HV**	**11%N LV**
1,4-Dioxane	1	1	1	0	0	0	1
1-Nitropropane	1	1	0	1	1	1	1
1-Pentanol	0	0	0	0	0	0	0
1-Propanol	0	0	0	0	0	0	0
2-Butanol	1	0	0	0	0	0	0
2-Propanol	0	0	0	0	0	0	0
Acetic Acid	0	1	0	0	1	1	1
Acetone	1	1	1	1	1	1	1
Acetonitrile	1	1	0	0	1	1	1
Carbon Disulfide	0	0	0	0	0	0	0
Chloroform	1	1	0	0	0	0	0
Cyclohexanol	-	0	0	0	0	0	0
Diacetone Alcohol	1	1	-	1	1	1	1
Diethyl Phthalate	1	1	0	1	1	1	1
Diethylene Glycol	0	0	1	1	1	1	1
2-(2-ethoxyethoxy)ethyl acetate	1	1	-	1	1	1	1
Dimethyl Amine	1	1	-	1	1	1	1
Dimethyl Formamide	1	1	1	1	1	1	1
Ethanol	0	0	0	0	0	0	0
Ethanolamine	0	0	1	1	1	1	1
Ethyl Acetate	1	1	1	1	1	1	1
Ethylene Dichloride	0	1	0	0	0	0	0
2-Ethoxyethyl acetate	0	1	0	1	1	1	1
Hexane	0	0	0	0	0	0	0
Isobutyl Alcohol	0	0	0	0	0	0	0
Mesityl Oxide	1	1	0	1	1	1	1
Methanol	0	1	0	0	1	1	1
Methyl Acetate	1	1	0	0	1	1	1
Methyl Ethyl Ketone (MEK)	1	1	0	1	1	1	1
Methyl Isobutyl Carbinol	0	0	0	0	0	1	0
Methylene Dichloride	1	1	0	0	0	0	0
Morpholine	1	1	-	1	1	1	1
N,N-Dimethyl Acetamide	1	1	1	1	1	1	1
n-Butyl Acetate	1	1	0	1	1	1	1
Nitrobenzene	1	1	1	1	1	1	1
o-Xylene	0	1	0	0	0	0	0
Propylene Carbonate	1	1	1	1	1	1	1
Pyridine	1	1	1	1	1	1	1
Tetrahydrofuran	1	1	1	1	1	1	1

	GAP 5527	**GAP 0700**	**PB400 N3**	**13.4%N HV**	**12.6%N HV**	**11%N HV**	**11%N LV**
Toluene	1	1	0	0	0	0	0
Water	0	0	0	0	0	0	0